Theoretical Investigation of Relativistic Effects in Heavy Atoms and Polar Molecules

A thesis submitted
for the degree of

Doctor of Philosophy

in the Faculty of Science

by

Malaya Kumar Nayak

Department of Physics
Indian Institute of Science
Bangalore - 560 012. INDIA

March 2006

Declaration

I hereby declare that the work reported in this thesis entitled ***"Theoretical Investigation of Relativistic Effects in Heavy Atoms and Polar Molecules"*** is entirely original. I have carried out this work at the Non Accelerated Particle Physics Group, *Indian Institute of Astrophysics (IIA)*, Bangalore under the guidance of Dr. Rajat K. Chaudhuri, *IIA*, Bangalore under the *Joint Astronomy Programme*.

I further declare that this thesis has not formed the basis for award of any degree, diploma, fellowship, associateship or similar title of any University or Institution.

Dr. Rajat K. Chaudhuri
(Thesis Supervisor)
NAPP Group, IIA
II Block, Koramangala
Bangalore - 560 034, India

Malaya Kumar Nayak
(Ph.D. Candidate)
Department of Physics
Indian Institute of Science
Bangalore - 560 012, India
&
NAPP Group, IIA
II Block, Koramangala
Bangalore - 560 034, India

To, My Teachers & Parents . . .

Acknowledgments

This thesis is an outcome of five and half years of valuable research work. During these years many people have provided professional and personal help without which, it would have been difficult to reach at this stage. It's my pleasure to acknowledge my institute IIA, and people here who have directly or indirectly encouraged me in pursuing my research work.

First of all, I would like to thank my thesis advisor Dr. Rajat K. Chaudhuri, for his valuable guidance throughout my Ph.D. career. His proper co-operation consistent encouragement, positive criticism and suggestions have helped me in improving my overall performance and self-confidence during the thesis work. I am also thankful to him for giving me enough space for independent thinking as well as advice whenever necessary that have played a crucial role in my work.

I wish to thank my IISc co-guide and co-ordinator of Joint Astronomy Programme Prof. Arnab R. Choudhuri, who has been kind enough to provide me a hassle-free environment, in crucial matters of administrative relevance.

It's my pleasure to express my sincere gratitude to Prof. B. P. Das, for his kind help and support at the time of my need. I have never seen such a person like him, whose door is always open for students. His constant support for my academic as well as non-academic matter has helped me a lot to carry out this research work.

I express my sincere thanks to Prof. D. Mukherjee, Director of IACS, Kolkata, India, for his valuable suggestions for this work. The fruitful discussions I had with him were of immense help for my work.

I express my gratitude to the Director of IIA, for extending the facilities to pursue my research work at IIA. I express my thanks to the Chair-person and the Members of the Board of Graduate Studies, for providing me a comfortable space as well as research environment, during my entire tenure at IIA.

It's my pleasure to remember my M.Sc. teachers and class-mates and express my thanks to them. My heartfelt thanks to Dr. K. C. Panda, Department of Physics, Sambalpur University, Orissa, India, supervisor of my M.Phil. dis-

sertation and a well wisher, whose consistent inspiration opened the door of research career in my life, without which I would not have stepped into the field of research.

I am pleased to thank all my friends at IISc and IIA. I wish to thank all my JAP batch-mates Vikram, Poonam, Anand, Ravi, Latha and Shalima, for making my course work at IISc enjoyable and full of fun. I still remember going together to attend first year classes at RRI and IIA, celebrating each other's birthday, doing assignments and having nice time altogether throughout the year. I also wish to thank my room-mates and office-mates Nagaraj, Maithi, Baliga, Nataraj, Viresh and Reji, for providing me a nice friendly environment here at IIA.

I express my special thanks to Ramesh, Chandra, Hemanta, Kshama, Ashish, Mr.& Mrs. Pitamber and Mr.& Mrs. Gagan da, for making my stay in Bagalore cheerful as well as memorable with fun and pleasure.

At last, but not least, I would like to thank my parents, brother-in-laws and sisters for providing their constant encouragement throughout the Ph.D. period. The love and blessing of my parents as well as their care and support during my Ph.D. career are not expressible with pen and paper, only it can be realized. Words are not just enough to describe support of my wife who was always there with me during my tough time for providing her help and support whenever I was needed. In addition to her own school duty, she beautifully manage to take care of all the house-hold responsibilities to make sure that, I can spent maximum time with my research. Our little son, Shashwat, brought happiness and joy in our life with his innocent smile.

Abstract

Extensive theoretical studies on the ground and excited state properties of systems containing heavy atoms have shown that accurate prediction of transition energies and related properties requires the incorporation of both relativistic and higher order correlation and relaxation effects as these effects are strongly interwined. The relativistic and dynamical electron correlation effects can be incorporated in many-electron systems through a variety of many-body methods like configuration interaction (CI), coupled cluster method (CCM) etc. which are very powerful and effective tool for high precision description of electron correlation in many-electron systems. In this thesis, we investigate the relativistic and correlation effects in heavy atomic and molecular systems using these two highly correlated many-body methods.

It is well recognized that, heavy polar diatomic molecules such as BaF, YbF, TlF, PbO, etc. are the leading experimental candidates for the search of violation of Parity (P) and Time-reversal (T) symmetry. The experimental detection of such P, T-odd effects in atoms and molecules has important consequences for the theory of fundamental interactions or for physics beyond the standard model (SM). For instance, a series of experiments on TlF have already been reported which provide the tightest limit available on the tensor coupling constant C_T, proton electric dipole moment (EDM) d_p, etc. Experiments on YbF and BaF molecules are also of fundamental significance to the study of symmetry violation in nature,

as these experiments have the potential to detect effects due to the electron EDM d_e. It is therefore imperative that high precession calculations are necessary to interpret these ongoing (and perhaps forthcoming) experimental outcome. For example, the knowledge of the effective electric field E (characterized by W_{d}) at the unpaired electron is required to link the experimentally determined P,T-odd frequency shift with the electron EDM d_e.

We begin with a brief review of P,T-odd effects in heavy atoms and polar diatomics and the possible mechanisms which can give rise to such effects, in particular, the one arises due to the intrinsic electron EDM d_e. The P,T-odd interaction constant W_{d} is computed for the ground ($^2\Sigma$) state of YbF and BaF molecules using all-electron DF orbitals at the restricted active space (RAS) CI level. The RASCI space used for both systems in this calculation is sufficiently large to incorporate important core-core, core-valence, and valence-valence electron correlation effects. In addition to W_{d}, we also report the dipole moment (μ_e) for these systems to assess the reliability of the method. The basis set dependency of W_{d} is also analyzed.

The single reference coupled cluster (SRCC) method, developed by the cluster expansion of a single determinant reference function, is one of the most sophisticated method for treating dynamical correlation effects in a size-extensive manner. The non-uniqueness of the exponential nature of the wave operator diversifies the methods in multi-reference context. The multi-reference coupled cluster (MRCC) strategies fall within two broad classes: (a) State-Universal (SU), a Hilbert-space approach and (b) Valence-Universal (VU), a Fock-space approach. In this thesis, we shall be mainly concerned with the VU-MRCC which unlike SU-MRCC uses a single wave operator that not only correlates the reference functions, but also all the lower valence (or the so called *subdued*) sectors, obtained by deleting the occupancies systematically. The linear response theory (LRT) or equation of motion (EOM) method is another possible alternative which is nowadays extensively used to compute the atomic and molecular properties. Although, the CCLRT or EOM-CC

method is not fully extensive in nature, this method has some distinct advantages over the traditional VU-MRCC theory. Further, for one-valence problem like ionization processes, the CCLRT/EOM-CC is formally equivalent to VU-MRCC, and hence, size-extensive.

In this thesis, the core-extensive CCLRT and core-valence extensive (all electron) VU-MRCC methods are applied to compute the ground and excited state properties of various atomic and molecular systems (HCl, CuH, Ag, Sr, Yb and Hg) using non-relativistic and relativistic (for heavy atoms) spinors. The similarities and differences in the structure of these two formalisms are also addressed.

We also investigate the ground and excited state properties of HCN which is a system of astrophysical importance. This system has raised interest among the astrophysicists due to its detection in the atmosphere of Titan and Carbon stars. HCN has also been identified via radio-techniques in both comets and interstellar atmosphere.

In the flash-photolysis of oxazole, iso-oxazole, and thiozole a transient band system was observed in the region 2500-3050 Å. This band system was attributed to a meta-stable form of HCN, i.e, either HNC or triplet HCN. We carry out detailed theoretical investigations using CCLRT and complete active space self-consistent field (CASSCF) method to characterize this unidentified band and other experimentally observed transitions.

Contents

List of Figures

List of Tables

Chapter 1

Survey of P, T-odd effects in Heavy atoms and Polar molecules

1.1 Introduction

It was believed for a long time that the fundamental laws of nature were invariant under space inversion, and hence the conservation of space inversion symmetry (P) was an universally accepted principle. However, non-conservation of this symmetry was discovered experimentally by Wu and co-workers in the β decay of ^{60}Co in 1957 [1]. After the discovery of P violation, the combined operation of charge conjugation C and space inversion P (CP) was thought to be a good symmetry. In 1964, the experiment of Christenson *et al.* [2] provided the evidence of a small violation of CP symmetry in the decay of neutral K_L^0 meson. This, in conjunction with the so called CPT-theorem [3, 4], implies the violation of time reversal symmetry (T). Apart from this indirect evidence of the T violation, there is no other instance where, such an effect has been observed. Lee and Yang [5] as well as Landau [6] showed that a non-zero permanent electric dipole moment (EDM) of any non-degenerate quantum mechanical system will be a signature of the non-conservation of space inversion and time reversal symmetries. Thus the experimental observation of a permanent EDM of an elementary particle, an atom

or a molecule will be a direct evidence of the violation of time reversal symmetry (T).

On the other hand, since the permanent EDM of an elementary particle vanishes unless the discrete symmetries space inversion (P) and time reversal (T) are both violated. This naturally makes the EDM small in fundamental particles of ordinary matter. For instance, in the Standard Model (SM) of elementary particle physics, the expected value of the electron EDM d_e is less than $10^{-38} e.cm.$ [7] (which is effectively zero), but some extensions of the SM, predict the value of the electron EDM in the range $10^{-26} - 10^{-28} e.cm.$ (see [8] for details). The search for a non-zero electron EDM is, therefore, a search for physics beyond the SM and particularly it is a search for T violation. This is an important and active field at present, because the prospects of discovering new physics seems possible.

It is well recognized that heavy atoms and heavy-polar diatomic are very promising candidates for the experimental search of permanent EDMs arising from violation of P and T. The search of non-zero P,T-odd effects in these systems with the presently accessible (expected) level of experimental sensitivity would indicate the presence of so-called "new physics" beyond the SM of electroweak and strong interaction (see [9] and references therein) which is certainly of fundamental importance. Despite the well known drawbacks and unresolved problems of SM there are no experimental data available which would be in direct contradiction with this theory. In turn, some popular extensions of the SM, which allow one to overcome it's disadvantages, are not yet confirmed experimentally (see [8, 10] for details).

A crucial feature of search for P,T-odd effects in atoms and molecules is that in order to interpret the measured data in terms of fundamental constants of these interaction, one must calculate those properties of the systems, which establish a connection between the measured data and and studied fundamental constants. These properties are described by operators that are prominent in the nuclear region; they cannot be measured and their theoretical study is a non trivial task.

During the last several years the significance of (and requirement for) ab-initio calculation of electronic structure providing a high level of reliability and accuracy in accounting for both relativistic and correlation effects associated with these properties has gained in importance. In this thesis, we will compute one of the P,T-odd interaction constants, the so-called $W_{\rm d}$, which is a measure of the effective electric field at the unpaired electron, for the ground state of YbF and BaF molecule with reliable accuracy of the method. In addition to $W_{\rm d}$, we also compute some other atomic and molecular properties for various systems in the later part of this thesis

1.2 Summary of Search for EDMs of Heavy atoms and Polar molecules arising from P,T-odd interactions

After the discovery of the combined charge and space parity violation, or CP-violation, in the decay of neutral K_L^0-meson [2], the search for the electric dipole moments (EDMs) of elementary particles has become one of the fundamental problems in physics. A permanent EDM is induced by the super-weak interaction that violates both the space inversion symmetry and time-reversal invariance [11]. Considerable experimental effort has been invested in probing for atomic EDMs induced by EDMs of proton, neutron and electron, and by the P,T-odd interactions between them. The best available limit for the electron EDM, d_e was obtained from atomic Tl experiment [12], which established an upper limit of $|d_e| < 1.6 \times 10^{-27} e \cdot cm$, where e is the charge of the electron. The benchmark upper limit on a nuclear EDM is obtained in the atomic EDM experiment on ^{199}Hg [13], $|d_{Hg}| < 2.1 \times 10^{-28} e \cdot cm$, from which the best restriction on the proton EDM, $|d_p| < 5.4 \times 10^{-24} e \cdot cm$, was also obtained by Dmitriev and Sen'kov recently [14]. The previous upper limit on the proton EDM was obtained from the molecular TlF experiment [15].

Since 1967, when Sandars suggested the use of polar heavy-atom molecules

in the experimental search for the proton EDM [16], molecules have been considered the most promising candidates for such experiments. Sandars also noticed earlier [17] that the P-odd and P,T-odd effects are strongly enhanced in heavy atoms due to relativistic and other effects. For example, in paramagnetic atoms the enhancement factor for an electron EDM, d_a/d_e, is roughly proportional to $\alpha^2 Z^3 \alpha_D$ where $\alpha \approx 1/137$ is the fine structure constant, Z is the nuclear charge and α_D is the atomic polarisability. It can be of the order of 100 or greater for highly polarizable heavy atoms ($Z \geq 50$). Furthermore, the effective intermolecular electric field acting on electrons in polar molecules can be five or more orders of magnitude greater than the maximal electric field accessible in a laboratory. The first molecular EDM experiment was performed on TlF by Sandars *et al.* [15] (Oxford, UK); it was interpreted as a search for the proton EDM and other nuclear P,T-odd effects. In 1991, in the last series of the ^{205}TlF experiments by Hinds *at al.* [18] (Yale,USA), the restriction on proton EDM, $d_p = (-4 \pm 6) \times 10^{-23} e \cdot cm$ was obtained. In 2002, this was recalculated by Petrov *et al.* [19] and obtained the restriction as $d_p = (-1.7 \pm 2.8) \times 10^{-23} e \cdot cm$.

In 1978, the experimental investigation of the electron EDM, d_e and other parity non conservation (PNC) effects was further stimulated by Labzowsky *et al.* [20, 21] and Sushkov and Flambaum [22] who clarified the possibilities of additional enhancement of these effects in diatomic radicals like BiS and PbF due to the closeness of levels of opposite parity in Ω-doublets having a $^2\Pi_{1/2}$ ground state. Then Sushkov *et al.* [23] and Flambaum and Khriplovich [24] suggested the use of Ω-doubling in diatomic radicals with a $^2\Sigma_{1/2}$ ground state for such experiments and the HgF, HgH and BaF molecules were first studied semi-empirically by Kozlov [25]. At the same time, the first two-step ab-initio calculation of PNC effects in PbF initiated by labzowsky was completed by Titov *at al.* [26]. A few years later, Hinds started an experimental search for the electron EDM in the YbF molecule, on which the first result was obtained by his group in 2002 (Sussex, UK) [27], $d_e = (-0.2 \pm 3.2) \times 10^{-26} e \cdot cm$. Though that restriction is worse than the best

current d_e datum (from the Tl atom experiment), nevertheless, it is only counting statistics, as Hinds *et al.* [27] pointed out later.

A new series of electron EDM experiments on YbF by Hinds' group (Imperial College, UK) are in progress and a new generation of electron EDM experiments using a vapors cell, on the metastable a(1) state of PbO, is being prepared by the group of DeMille (Yale, USA), The unique suitability of PbO for searching for the elusive d_e is demonstrated by the very high projected statistical sensitivity of the Yale experiment to the electron EDM. In prospect, it allows one to detect d_e of order of $10^{-29} - 10^{-31} e \cdot cm$ [28], two-four orders of magnitude lower than the current limit quoted above. Some other candidates for the EDM experiments, in particular, HgH, HgF, TeO*, and HI^+ are being discussed and an experiment on PbF is planned (Oklahoma Univ. USA)

1.3 Particle physics implications for the existence of an electron EDM

As mentioned in the introduction, the observation of a non-zero EDM of an electron would be a signature of "new physics" beyond the Standard Model (see [9] and references therein). It would be a more sensitive probe of the SM than the neutron EDM which could have non-zero EDM due to CP violation in the QCD sector of the SM.

In Table 1.1, we give estimates of the electron EDM predicted by different particle physics models [8, 9]. It can be seen from this table that the value of the electron EDM in the SM is 10-12 orders of magnitude smaller than in the other models. This is due to the fact that the first non vanishing contribution to this quantity arises from three-loop diagrams [29]. There are strong cancellations between diagrams at the one-loop as well as two-loop levels. It is indeed significant that the electron EDM sensitive to a variety of extensions of the SM: super-symmetry

Table 1.1: *Prediction for the electron EDM, $|d_e|$ in popular theoretical models.*

Model	$\lvert d_e\rvert$ (in $e \cdot cm$)
Standard Model	$< 10^{-38}$
Left-right symmetry	$10^{-28} - 10^{-26}$
Lepton flavor-changing	$10^{-29} - 10^{-26}$
Multi-Higgs	$10^{-28} - 10^{-27}$
Super-symmetric	$\leq 10^{-25}$
Experimental limit [12]	$< 1.6 \times 10^{-27}$

(SUSY), multi-Higgs, left-right symmetry, lepton flavor-changing, etc. [10]. This is particularly true for the minimal ("naive") SUSY model, which predicts an electron EDM already at the level of $10^{-25} e \cdot cm$. However, the best experimental estimate on the electron EDM, $1.6 \times 10^{-27} e \cdot cm$, obtained in the experiment on the Tl atom [12], is almost two orders of magnitude smaller. More sophisticated SUSY models have many desirable features such as their ability to explain the "gauge hierarchy problem" and solve the problem of dark matter in astrophysics etc. Interestingly they predict the electron EDM at the level of $10^{-27} e \cdot cm$ or somewhat smaller. It is certainly remarkable that studies of the electron EDM can shed light on super-symmetry which is one of the most profound ideas in contemporary physics.

1.4 General principle for the measurement of EDMs

The basic physics governing the measurement of the EDM of all types of electrically neutral system is almost the same as we are going to discuss in this section. If the system under consideration has a magnetic moment $\boldsymbol{\mu}$ and is exposed to a magnetic field $\mathbf{B}$, the interaction Hamiltonian is

$$H_{mag} = -\boldsymbol{\mu} \cdot \mathbf{B}. \tag{1.1}$$

From a classical point of view, the magnetic field exerts a torque on the system so that the magnetic moment $\boldsymbol{\mu}$ and hence the angular momentum **J** begin to precess about the magnetic field **B**. The precession frequency for a system having $J = \frac{1}{2}$ like the neutron corresponds to the energy separation of $2\mu B$ between $m = +\frac{1}{2}$ and $m = -\frac{1}{2}$ states, is given by

$$\delta\omega = \frac{2\mu B}{\hbar} \tag{1.2}$$

If the system under consideration also possesses an electric dipole moment **d** and is exposed to an electric field **E**, the interaction Hamiltonian is

$$H_{ele} = -\mathbf{d} \cdot \mathbf{E} \tag{1.3}$$

As a result of the so-called projection theorem [30], we know that the expectation value of the EDM operator **d**, which is a vector operator, will be proportional to the expectation value of **J**, in the eigenstate of angular momentum. This, in conjunction with the previous equation above, implies that the electric field will modify the precession frequency of the system because of the additional torque experienced by the system due to the interaction between the electric field and the EDM. If the applied electric field **E** is parallel to the magnetic field **B**, the modified precession frequency will be

$$\Delta\omega_+ = \frac{2\mu B + 2dE}{\hbar}, \tag{1.4}$$

and if **E** is anti-parallel to **B**, the precession frequency will be

$$\delta\omega_- = \frac{2\mu B - 2dE}{\hbar}. \tag{1.5}$$

The aim of the experiment is to measure the change in the precession frequency, $\Delta\omega_+ - \Delta\omega_-$, as a result of flipping the **E**-field with respect to the **B**-field. From the

above two expression, it is obvious that this change is

$$\Delta\omega_+ - \Delta\omega_- = \frac{4dE}{\hbar}. \tag{1.6}$$

Thus the above equation can be served to obtain the value of d, the permanent EDM of the system. The most recent and the best limit available so far on the intrinsic EDM of the electron was set to be $|d_e| = 1.6 \times 10^{-27} e \cdot cm$ by Regan *et al.* [12], obtained from the atomic EDM experiment on Tl atom. The basis idea of the experiment was based on the principle as we discussed above.

1.5 Mechanisms giving rise to permanent EDMs of atoms and molecules

A permanent EDM of a stable atomic or molecular state can arise only when both P and T invariance are broken. However, it is often said that molecules known as polar molecules have a large "permanent" EDMs. However, this kind of EDM of a polar molecule is not an indication of P and T violation [10]. If the measurements of Stark shift were carried out with an infinitesimally weak electric field **E** at zero temperature, the energy shift resulting from the interaction of this EDM with the electric field has no linear dependence on **E** (see [10] for more details), and hence is not an indication of P and T violation. What we interested is not an EDM of this kind, but a permanent EDM which causes a linear Stark effect even for an infinitesimally weak **E**. Such an EDM is a genuine signature of P and T violation or CP violation in conjunction with the CPT theorem.

In this section, we will discuss about the possible sources of such P and T violating P, T-odd terms in the Hamiltonian, which can produce permanent EDMs of atoms and molecules. There are several mechanisms that can give rise to such P, T-odd effects and as a result, the permanent EDMs of atoms and molecules.

Some of them are:

(1) intrinsic electric dipole moments of electrons;
(2) intrinsic electric dipole moments of nucleons;
(3) P and T violating electron-nucleon interaction;
(4) P and T violating electron-electron interaction;
(5) P and T violating nucleon-nucleon interaction;

The second chapter of this thesis is concerned with the calculation of the P,T-odd effects in the ground state of YbF and BaF molecules arising due to mechanism (1) mentioned above. We have considered these effects especially for the YbF molecule because this is one of the leading candidates for the search of effects due to the electron EDM as a result of it's high internal effective electric field at the unpaired electron.

1.5.1 Intrinsic EDMs of electrons

Let us first consider the effects of the intrinsic EDM of an electron on an atom or a molecule from the non-relativistic point of view. Let us suppose that the value of the intrinsic EDM of an electron is d_e. The EDM operator corresponding to the ith electron in the atom/molecule is given by

$$\mathbf{d}_i = d_e \boldsymbol{\sigma}_i \tag{1.7}$$

where $\boldsymbol{\sigma}_i$ are the Pauli spin matrices for the ith electron.

Therefore, in the presence of an external electric field of strength E_z in the z-direction, the non-relativistic molecular many-body Hamiltonian is

$$H = H_0 + H_I + H_{ext}, \tag{1.8}$$

where

$$\begin{aligned} H_0 &= \sum_i \left(p_i^2/2m + \sum_n V_n(r_i) \right) + \sum_{j \neq i} \frac{e^2}{r_{ij}}, \\ H_I &= -d_e \sum_i \boldsymbol{\sigma}_i \cdot \mathbf{E}_i^{int}, \end{aligned}$$

and

$$H_{ext} = -eE_z \sum_i \left(z_i + \frac{d_e}{e} \sigma_{zi} \right).$$

$\mathbf{E}_i^{int}$ is the internal electric field which the ith electron sees due to the other electrons and the nuclei of the molecule, where the subscript n denotes the nth nucleus. Clearly, we can write

$$e\mathbf{E}_i^{int} = -\nabla_i \left(\sum_n V_n(r_i) + \sum_{j \neq i} \frac{e^2}{r_{ij}} \right), \tag{1.9}$$

so that we get

$$H_I = \frac{d_e}{e} \sum_i \boldsymbol{\sigma}_i \cdot \nabla_i \left(\sum_n V_n(r_i) + \sum_{j \neq i} \frac{e^2}{r_{ij}} \right).$$

But it turns out that the above Hamiltonian leads to a vanishing value of the atomic or molecular EDM due to the Schiff's theorem [31]. This result is most surprising because it implies that even though the individual electrons in the molecule have nonzero EDMs, the molecular EDM is still zero. However, Sandars [32] showed that if the electrons in the molecule are treated relativistically, the intrinsic EDM of the electrons leads to a nonzero EDM of the whole atom or molecule. Now we will discuss this relativistic approach to the molecular EDM.

If we consider the intrinsic EDM of the electron relativistically then the interaction Hamiltonian in presence of an electric and a magnetic field can be written

like

$$h_{edm} = -d_e\beta(\boldsymbol{\sigma}\cdot\mathbf{E} + i\boldsymbol{\alpha}\cdot\mathbf{H}) \tag{1.10}$$

where $\mathbf{E}$ and $\mathbf{H}$ are the electric and magnetic fields experienced by the electron and $\boldsymbol{\alpha}$, $\boldsymbol{\sigma}$, β are the Dirac matrices.

For the case of many-electron molecular system, this can be easily generalized to the form

$$H_0 = \sum_i \left(c\boldsymbol{\alpha}_i\cdot\mathbf{p}_i + \beta mc^2 + \sum_n V_n(r_i)\right) + \sum_{j\neq i}\frac{e^2}{r_{ij}} \tag{1.11}$$

and

$$H_{edm} = -d_e\sum_i \beta_i(\boldsymbol{\sigma}_i\cdot\mathbf{E}_i + i\boldsymbol{\alpha}_i\cdot\mathbf{H}_i)$$

However, the second term of above expression is of the order of $O(v^2/c^2)$ compared to the first term because of the presence of the $\boldsymbol{\alpha}$ matrix and the magnetic field $\mathbf{H}$. Therefore we will neglect it and consider the molecular EDM due to the first term only, i.e.,

$$H_{edm} \approx -d_e\sum_i \beta_i\boldsymbol{\sigma}_i\cdot\mathbf{E}_i \tag{1.12}$$

If the atom as a whole is also exposed to an external electric field E_z in the z-direction, the total perturbation Hamiltonian will be

$$H' = -d_e\sum_i \beta_i\boldsymbol{\sigma}_i\cdot\mathbf{E}_i^{int} - eE_z\sum_i\left(z_i + \frac{d_e}{e}\beta_i\sigma_{zi}\right). \tag{1.13}$$

Using the previous expression for $e\mathbf{E}_i^{int}$ in the above equation for H', we get the total relativistic molecular many-body Hamiltonian to be

$$H = H_0 + H' \tag{1.14}$$

or

$$H = \sum_i \left(c\boldsymbol{\alpha}_i \cdot \mathbf{p}_i + \beta mc^2 + \sum_n V_n(r_i) \right) + \sum_{j \neq i} \frac{e^2}{r_{ij}} - eE_z \sum_i \left(z_i + \frac{d_e}{e} \beta_i \sigma_{zi} \right) + \frac{d_e}{e} \sum_i \beta_i \boldsymbol{\sigma}_i \cdot \nabla_i \left(\sum_n V_n(r_i) + \sum_{j \neq i} \frac{e^2}{r_{ij}} \right).$$

Since we know that, in the non-relativistic limit ($\beta = 1$) and this leads to a vanishing value of the molecular EDM according to Schiff's theorem, so we can replace β by $(\beta - 1)$ in the expression for H'. In this case the residual EDM interaction of an electron with internal electric field looks like [33]

$$H_d = -d_e(\beta - 1)\boldsymbol{\Sigma} \cdot \mathbf{E}^{int} \tag{1.15}$$

where $\boldsymbol{\Sigma}$ is the 4-component Dirac matrix (defined later) and the corresponding linear Stark splitting is

$$\Delta E = -2d_e eE_z \sum_{n \neq 0} \frac{\langle \psi_0 | z | \psi_n \rangle \langle \psi_n | (\beta - 1)\boldsymbol{\Sigma} \cdot \mathbf{E}^{int} | \psi_0 \rangle}{E_0 - E_n} - d_e E_z \langle \psi_0 | (\beta - 1)\Sigma_z | \psi_0 \rangle. \tag{1.16}$$

where ψ_0 and ψ_n are eigenfunction of H_0 corresponding to the energy eigenvalues E_0 and E_n, respectively (see [8, 33] for details).

The high value of the electron density at the nucleus leads to the enhancement of the electron EDM in heavy atom. The second term in the right hand side of the above equation does not contain this enhancement and for this reason is much smaller. The other possible source of the enhancement is the presence of small energy denominators in the sum over n state in the first term. In particular, this takes place in diatomic, where $(E_0 - E_n)$ may be of the order of the molecular rotational constant. Moreover, in this case the Stark matrix element $(eE_z\langle \psi_0 | z | \psi_n \rangle)$ may be comparable with the energy denominator $(E_0 - E_n)$ and hence the non-perturbation treatment of the Stark effect is required [33]. Then

the above equation reduces to the form (see [8, 27] for details).

$$\Delta E = \langle\psi_0|H_d|\psi_0\rangle = -d_e\langle\psi_0|(\beta-1)\mathbf{\Sigma}\cdot\mathbf{E}^{int}|\psi_0\rangle. \tag{1.17}$$

We have used this expression in our calculation of the P,T-odd interaction constant $W_{\rm d}$ for the ground $^2\Sigma_{1/2}$ states of YbF and BaF molecules. The expression for $W_{\rm d}$ is given by [34]

$$W_{\rm d} = \frac{2}{d_e}\langle^2\Sigma_{1/2}|H_d|^2\Sigma_{1/2}\rangle. \tag{1.18}$$

It can be clearly understood from this expression that, $W_{\rm d}$ is a measure of the effective electric field at the unpaired electrons of YbF and BaF molecules.

1.6 Some details of Computational procedure

1.6.1 Internal electric field of a diatomic molecule MF

In case of a molecule, the internal electric field experienced by an electron can be written like

$$\mathbf{E}^{int} = \mathbf{E}_i^{mol} = \sum_m \mathbf{E}_i^m + \sum_{j\neq i}\mathbf{E}_{i,j} \tag{1.19}$$

where $\mathbf{E}_i^m$ is the field due to the mth nucleus at the site of the ith electron and $\sum_{j\neq i}\mathbf{E}_{i,j}$ is the electric field due to the jth electron at the site of ith electron. For the case of a diatomic molecule like MF (in general), the above equation reduces to

$$\mathbf{E}_i^{mol} = \mathbf{E}_i^M + \mathbf{E}_i^F + \sum_{j\neq i}\mathbf{E}_{i,j} \tag{1.20}$$

In the next section we will discuss about, how to evaluate the nuclear electric fields $\mathbf{E}_i^M$ and $\mathbf{E}_i^F$ for the spherically symmetric charge distributions.

1.6.2 Spherically symmetric charge distribution and the electric field

If the nuclear charge distribution is spherically symmetric such as "Gaussian nucleus", "Fermi nucleus" or the nucleus is assumed to be a uniformly charged spherical ball, the electric field at a point $\mathbf{r}$ outside the nucleus can be evaluated using Gauss law (in SI unit) as

$$E(\mathbf{r}) = \frac{1}{4\pi\epsilon_0}\frac{Q}{r^2}\hat{\mathbf{r}} \tag{1.21}$$

where Q is the total charge inside the nucleus (proportional to the atomic number Z of the atom) and $\mathbf{r}$ is the position vector of a point under consideration relative to the center of the nucleus. [Note that, though the electric field outside the nucleus is same for all the above mentioned charge distributions, however, the electric field inside the nucleus may be different for different charge distributions]

If we consider the system like MF molecule, the combined nuclear electric field at the point $\mathbf{r}$ which is located at $\mathbf{r}_M$ and $\mathbf{r}_F$ from the center of M and F nucleus, respectively, will be

$$\mathbf{E}(\mathbf{r}) = \frac{1}{4\pi\epsilon_0}\frac{Z_M}{r_M^2}\hat{\mathbf{r}}_M + \frac{1}{4\pi\epsilon_0}\frac{Z_F}{r_F^2}\hat{\mathbf{r}}_F \tag{1.22}$$

So, the total molecular electric field at the site of i^{th} electron is,

$$\mathbf{E}_i^{mol} = \frac{1}{4\pi\epsilon_0}\frac{Z_M}{r_M^2}\hat{\mathbf{r}}_M + \frac{1}{4\pi\epsilon_0}\frac{Z_F}{r_F^2}\hat{\mathbf{r}}_F + \sum_{j\neq i}\mathbf{E}_{i,j} \tag{1.23}$$

The last term of the above equation is quite small as compared to the other two terms and can be neglected (as an approximation). So, neglecting the last term, we get

$$\mathbf{E}_i^{mol} = \frac{1}{4\pi\epsilon_0}\frac{Z_M}{r_M^2}\hat{\mathbf{r}}_M + \frac{1}{4\pi\epsilon_0}\frac{Z_F}{r_F^2}\hat{\mathbf{r}}_F \tag{1.24}$$

We have used this expression of the molecular electric field in our calculation of the P,T-odd interaction constant W_{d} for the ground state of YbF and BaF molecules.

1.6.3 Molecular orbitals of a diatomic molecule like MF

In general, using spherical Gaussian basic functions, all relativistic orbitals are assumed to be of the form

$$\frac{1}{r}\begin{pmatrix} P_{nk}(r)\Omega_{km}(\hat{\mathbf{r}}) \\ iQ_{nk}(r)\Omega_{-km}(\hat{\mathbf{r}}) \end{pmatrix} \tag{1.25}$$

where $P_{nk}(r)$ and $Q_{nk}(r)$ are the radial parts of the large and small component basis functions, respectively. Ω_{km} are the corresponding angular parts 'spinor spherical harmonics' of the basis functions. Molecular orbitals can be obtained by the straightforward generalization of the 'linear combination of atomic orbitals' (LCAO) method, which are of the form [35].

$$\phi_I(\mathbf{r}) = \sum_{p=1}^{n}\begin{pmatrix} X_{Ip}^{P}\chi_p^P(\mathbf{r}_p) \\ iX_{Ip}^{Q}\chi_p^Q(\mathbf{r}_p) \end{pmatrix} \tag{1.26}$$

where $\phi_I(r)$ is I-th four-component molecular orbital, X_{Ip}^P and X_{Ip}^Q are complex numbers (so called MO coefficients), and $\chi_p^P(\mathbf{r}_p)$ and $\chi_p^Q(\mathbf{r}_p)$ are, respectively, the 'large' and 'small' two-component basis spinors, $r_p = r - C_p$, and C_p is the 'center' of the basis function p (see [35, 36] for details).

The magnitude of the nuclear electric field (defined earlier) is determined principally by contribution from the regions in and around the nuclei; here both the electric field and the small component (relativistic effect) of the wave functions are largest. In the absence of screen ($\mathbf{E}_{i,j}$), the nuclear electric field diminishes with the square of the distance from the center of a nucleus; screen further accelerates the decline of the electric field with distance. The electrons of each 'constituent atom' have completely screened 'their' nuclei at the location of any other nucleus, for which reason, and to a very good approximation, the problem is 'uncoupled' for the various nuclear regions.

The single particle molecular orbital which has components at each of the two

centers of MF molecule can be written as

$$\begin{aligned}\phi_I(\mathbf{r}) &= \sum_{k_M,m_M} \frac{1}{r_M} \begin{pmatrix} f^p_{I\,k_M,m_M}(r_M)\Omega_{k_M,m_M}(\hat{\mathbf{r}}_M) \\ i f^q_{I\,k_M,m_M}(r_M)\Omega_{-k_M,m_M}(\hat{\mathbf{r}}_M) \end{pmatrix} \\ &+ \sum_{k_F,m_F} \frac{1}{r_F} \begin{pmatrix} f^p_{I\,k_F,m_F}(r_F)\Omega_{k_F,m_F}(\hat{\mathbf{r}}_F) \\ i f^q_{I\,k_F,m_F}(r_F)\Omega_{-k_F,m_F}(\hat{\mathbf{r}}_F) \end{pmatrix} \end{aligned} \tag{1.27}$$

In this above expression of I-th molecular orbital, we have omitted the MO coefficients for our convenience. Based on the approximation mentioned above, we will use these molecular orbitals to evaluate the matrix element of the residual P,T-odd interaction operator H_d in the next section.

1.6.4 Matrix elements of the P,T-odd interaction operator H_d

Let us first re-write the residual P,T-odd interaction operator H_d (defined in the previous section), using the standard representation of Dirac matrices β and $\mathbf{\Sigma}$. According to this representation, we can write

$$\beta = \begin{pmatrix} I & 0 \\ 0 & -I \end{pmatrix}, \tag{1.28}$$

and

$$\mathbf{\Sigma} = \begin{pmatrix} \hat{\boldsymbol{\sigma}} & 0 \\ 0 & \hat{\boldsymbol{\sigma}} \end{pmatrix}. \tag{1.29}$$

So, the residual P,T-odd interaction operator H_d can be written as

$$H_d = 2d_e \begin{pmatrix} 0 & 0 \\ 0 & \hat{\boldsymbol{\sigma}} \end{pmatrix} \cdot \mathbf{E}^{\mathsf{int}}. \tag{1.30}$$

Neglecting the electric field due to electrons and replacing $\mathbf{E}^{\text{int}}$ by $\mathbf{E}_i^{mol}$ (defined earlier), we can express the P,T-odd interaction operator H_d as

$$H_d^I = 2d_e \begin{pmatrix} 0 & 0 \\ 0 & \hat{\boldsymbol{\sigma}} \cdot \hat{\mathbf{r}}_M \end{pmatrix} \frac{1}{4\pi\epsilon_0} \frac{Z_M}{r_M^2} + 2d_e \begin{pmatrix} 0 & 0 \\ 0 & \hat{\boldsymbol{\sigma}} \cdot \hat{\mathbf{r}}_F \end{pmatrix} \frac{1}{4\pi\epsilon_0} \frac{Z_F}{r_F^2} \tag{1.31}$$

We can see clearly that this operator couples only the small components of the relativistic molecular wave functions. Since the small components as well as the nuclear electric fields are prominent in and around the nuclear regions, the dominant contribution to the matrix elements of H_d comes from that region. It should be noted that, neglecting the screening term $\mathbf{E}_{i,j}$ is likely to yield overestimate the value of the matrix element of H_d. However, the amount of overestimation should be small.

Further, it can be realized that the evaluation of the integrals using the spherical polar coordinates is relatively simpler. With a slight mathematical manipulation, the matrix element of the operator H_d can be written as

$$\begin{aligned} \langle \phi_I | H_d^I | \phi_I \rangle \;=\; & -2d_e \sum_{\substack{k_M,\, m_M \\ k'_M,\, m'_M}} \delta_{-k_M,k'_M} \delta_{m_M,m'_M} \int_r f^Q_{I,k_M,m_M}(r) E_M(r) f^Q_{I,k'_M,m'_M}(r) \mathrm{dr} \\ & -2d_e \sum_{\substack{k_F,\, m_F \\ k'_F,\, m'_F}} \delta_{-k_F,k'_F} \delta_{m_F,m'_F} \int_r f^Q_{I,k_F,m_F}(r) E_F(r) f^Q_{I,k'_F,m'_F}(r) \mathrm{dr} \end{aligned} \tag{1.32}$$

Here we have removed the factor $1/4\pi\epsilon_0$ because in atomic unit (a.u.) it's value is unity. We have also used the short hand notations $E_M(r) = Z_M/r_M^2$ and $E_F(r) = Z_F/r_F^2$ for the nuclear electric field. Furthermore, we have made use of the following two identities to get the above expression.

$$(\hat{\boldsymbol{\sigma}} \cdot \hat{\mathbf{r}}) \Omega_{km} = -\Omega_{-km} \tag{1.33}$$

and

$$\int \Omega^{\dagger}_{km}\Omega_{k'm'}d\Omega = \delta_{k,k'}\delta_{m,m'} \tag{1.34}$$

The approximate molecular wave-function Ψ is the slater determinant of the single particle orbitals ϕ_I.

$$|\Psi\rangle = \frac{1}{\sqrt{N!}}\mathrm{Det}|\phi_1\phi_2\cdots\phi_N| \tag{1.35}$$

The expectation value of the operator H_d in a specific molecular state Ψ can be expressed as

$$\langle\Psi|H_d^N|\Psi\rangle = \sum_I \langle\phi_I|H_d^I|\phi_I\rangle \tag{1.36}$$

where

$$H_d^N = \sum_I H_d^I \tag{1.37}$$

Which means, to calculate the expectation value of this operator, we have to first evaluate the matrix element $\langle\phi_I|H_d^I|\phi_I\rangle$ at the single particle level and then sum over all $I's$ to get the expectation value $\langle\Psi|H_d^N|\Psi\rangle$.

Some molecular codes such as DIRAC04 [37], which we have used in our calculations of the P,T-odd interaction constant W_{d} for the ground $^2\Sigma$ state of YbF and BaF molecules, uses “Cartecian Gaussian spinors”. The procedure for evaluating the matrix elements of the P,T-odd interaction operator H_d using Cartesian Gaussian spinors is little bit complicated and somehow different from the case of using Spherical Gaussian spinors. Some details of the procedure for evaluating the matrix elements of H_d using Cartesian Gaussian spinor are given in Appendix-A.

Bibliography

[1] C. S. Wu, E. Ambler, R. W. Hayward and R. P. Hudson, Phys. Rev **105**, 1413 (1957).

[2] J. H. Christenson, J. W. Cronin, V. L. Fitch and R. Turlay, Phys. Rev. Lett. **13**, 138 (1964).

[3] W. Pauli, *Neils Bohr and the Development of Physics* (Mc Graw-Hill, New York, 1955).

[4] G. Luders, Ann. Phys. **2**, 1 (1957).

[5] T. D. Lee and C. N. Yang, Brookhaven National Lab, Report No. **BNL443**, 791 (1957).

[6] L. D. Landau, Nucl. Phys. **3**, 127 (1957).

[7] M. Pospelov and I. B. Khriplovich, Sov. J. Nucl. Phys. **53**, 638 (1991).

[8] E. D. Commins, Adv. At. Mol. Opt. Phys. **40**, 1 (1999).

[9] A. V. Titov, N. S. Mosyagin, T. A. Isaev and D. DeMille, Eprint http://arXiv:physics/0506038, Jun (2005).

[10] W. Bernreuther and Mahiko Suzuki, Rev. Mod. Phys. **63**, 313 (1991).

[11] L. D. Landau, Sov. Phys.-JETP **5**, 336 (1957).

[12] B. C. Regan, E. D. Commins, C. J. Schmidt and D. DeMille, Phys. Rev. Lett. **88**, 1 (2002).

[13] M. V. Romalis, W. C. Griffith and E. N. Fortson, Phys. Rev. Lett. **86**, 2505 (2001).

[14] V. F. Dimitriv and R. A. Sen'kov, Phys. Rev. Lett. **91**, 1 (2003).

[15] E. A. Hinds, C. E. Loving and P. G. H Sandars, Phys. Lett. B **62**, 97 (1976).

[16] P. G. H. Sandars, Phys. Rev. Lett. **19**, 1396 (1967).

[17] P. G. H. Sandars, Phys. Lett. **14**, 194 (1965).

[18] D. Cho, K. Sangster and E. A. Hinds, Phys. Rev. A **44**, 2783 (1991).

[19] A. N. Petrov, N. S. Mosyagin, T. A. Isaev, A. V. Titov, V. F. Ezov, E. Eliva and U. Kaldor, Phys. Rev. Lett. **88**, 1 (2002).

[20] L. N. Labzowsky, Sov. Phys.-JETP **48**, 434 (1978).

[21] V. G. Gorshkow, L. N. Labzowsky and A. N. Moskalyov, Sov. Phys.-JETP **49**, 209 (1979).

[22] O. P. Sushkov and V. V. Flambaum, Sov. Phys.-JETP **48**, 608 (1978).

[23] O. P. Sushkov, V. V. Flambaum and I. B. Khriplovich, Sov. Phys.-JETP **87**, 1521 (1984).

[24] V. V. Flambaum and I. B. Khriplovich, Phys. Lett. A **110**, 121 (1985).

[25] M. G. Kozlov, Sov. Phys.-JETP **62**, 1114 (1985).

[26] M. G. Kozlov, V. I. Fomichev, Y. Y. Dmitriev, L. N. Labzowsky and A. V. Titov, J. Phys. B **20**, 4939 (1987).

[27] J. J. Hudson, B. E. Sauer, M. R. Tarbutt and E. A. Hinds, Phys. Rev. Lett. **89**, 1 (2002).

[28] D. DeMille, F. Bay, S. Bickman, D. Kawall, Jr. D. Krause, S. E. Maxwell, and L. R. Hunter, Phys. Rev. A **61**, 1 (2000).

[29] F. Hoogeveen, Nucl. Phys. B **341**, 322 (1990)

[30] J. J. Sakurai, *Modern Quantum Mechanics* (Addison Wesley Publishing Company Inc., New York, 1985), p. 241.

[31] L. I. Schiff, Phys. Rev. **132**, 2194 (1963).

[32] P. G. H. Sandars, Phys. Lett. **14**, 194 (1965).

[33] M. G. Kozlov and L. N. Labzowsky, J. Phys. B **28**, 1933 (1961).

[34] N. S. Mosyagin, M. G. Kozlov and A. V. Titov, J. Phys. B **31**, L763 (1998).

[35] F. A. Parpia, J. Phys. B **31**, 1409 (1998).

[36] F. A. Parpia and A. K. Mohanty, Phys. Rev. A **52**, 962 (1995).

[37] (see http://dirac.chem.sdu.dk/obtain/Dirac-site-license.shtml): *Dirac, a relativistic ab-initio electronic structure program, Release DIARC04 (2004)*, written by H. J. Aa. Jensen, T. Saue and L. Visscher with contributions from V. Bakken, E. Eliav, T. Enevoldsen, T. Fleig, O. Fossgaard, T. Helgaker, J. Laerdahl, C. V. Larsen, P. Norman, J. Olsen, M. Pernpointner, J. K. Pedersen, K. Ruud, P. Salek, J. N. P. Van Stralen, J. Thyssen, O. Visser, and T. Winther (http://dirac.chem.sdu.dk)

Chapter 2

Ab-initio calculation of P, T-odd effects in YbF and BaF molecules

2.1 Introduction

As mentioned in the previous chapter, heavy polar diatomic molecules such as BaF, YbF, TlF, PbO, etc. are the prime experimental probes for the search of violation of inversion symmetry (P) and time-reversal invariance (T). The experimental detection of such effects has important consequences [1, 2] for the theory of fundamental interactions or for physics beyond the standard model [3, 4]. For instance, a series of experiments on TlF [5] have already been reported which provide the tightest limit available on the tensor coupling constant C_T, proton electric dipole moment (EDM) d_p, etc. Experiments on YbF, BaF molecules are also of fundamental significance to the study of symmetry violation in nature, as these experiments have the potential to detect effects due to the electron EDM d_e. It is imperative that accurate theoretical calculations are also necessary to interpret these ongoing (and perhaps forthcoming) experimental outcome. For example, in the ground ($^2\Sigma$) state of YbF and BaF, knowledge of the effective electric field E (characterized by W_{d}) on the unpaired electron is required to link the experimentally determined P, T-odd frequency shift with electron EDM d_e.

The twin facts that heavy atom compounds like BaF, TlF, YbF, etc. contain many electrons and that the behavior of these electrons must be treated relativistically introduce severe impediments to theoretical treatments, i.e., to the inclusion of sufficient electron correlation in this kind of molecules. Due to this computational complexity, calculations of P,T-odd interaction constants were carried out with "relativistic matching" of non-relativistic wave functions (approximate relativistic spinors) [6], the relativistic effective core potential (RECP) [7, 8], or the all-electron Dirac-Fock (DF) level [9, 10]. For example, the first calculation of P,T-odd interactions on TlF was carried out in 1980 by Hinds and Sandars [6] using approximate relativistic wave functions generated from non-relativistic single particle orbitals.

The P,T-odd interaction constant $W_{\rm d}$, in YbF was first calculated by Titov *et al.* [7] using generalized RECP (GRECP) as this procedure provides reasonable accuracy with small computational cost. Titov and co-workers have also reported $W_{\rm d}$ computed using a restricted active space self-consistent field (RASSCF) scheme [7, 8] with GRECP orbitals. Assuming that the valence-valence electron correlation effect is negligible, Parpia [9] estimated $W_{\rm d}$ from the all-electron unrestricted DF method (UDF) in 1998. In the same year Quiney *et al.* [10] reported the P,T-odd interaction constant $W_{\rm d}$ computed at the core-polarization level with all-electron DF orbitals. Though the effect of pair correlation and higher order effects to $W_{\rm d}$ are non-negligible, these terms were not included in Quiney *et al.*'s calculations. The calculations cited above predict the value of the P,T-odd interaction constant in a rather large range: [-0.62,-1.5]$\times 10^{25}$ Hz/e-cm. Therefore, more precise estimation of $W_{\rm d}$ is necessary to set narrower limits on d_e.

For the BaF molecule, the first calculation of the P,T-odd interaction constant $W_{\rm d}$ was carried out by Kozlov *et al.* [11] using the generalized relativistic effective core potential (GRECP) at the level of self-consistent field (SCF) and a restricted active space SCF (RASSCF). They have also reported $W_{\rm d}$ computed using the effective-operator (EO) technique at SCF-EO and RASSCF-EO level. The result

of $W_{\rm d}$ computed by Kozlov *et al.* [11] is quite consistent with the semi-empirical result of Kozlov and Labzowsky [12] estimated from experimental hyperfine structure constants measured by Knight *et al.* [13]. Though the RASSCF-EO result [11] is close to the semi-empirical result of Kozlov and Labzowsky, it is worthwhile to compute this constant more accurately using correlated many-body methods like the configuration interaction (CI).

In this chapter, we estimate the P,T-odd interaction constant $W_{\rm d}$ for the ground ($^2\Sigma$) state of YbF and BaF molecule using all-electron DF orbitals at the restricted active space (RAS) configuration interaction (CI) level. The RASCI space used for both systems in this calculation is sufficiently large to incorporate important core-core, core-valence, and valence-valence electron correlation effects, and hence, should be capable of providing a reliable estimate of $W_{\rm d}$. In addition to the P,T-odd interaction constant $W_{\rm d}$, we also compute ground to excited state transition energies, ionization potential, dipole moment (μ_e), ground state equilibrium bond length ($\rm R_e$), and vibrational frequency (ω_e), for YbF molecule. Similarly, for BaF molecule we have computed the ground state dipole moment μ_e along with $W_{\rm d}$.

2.2 Configuration Interaction (CI) method

In this section, we will describe the method of configuration interaction (CI) for obtaining the exact energy of a many-electron state and the corresponding wave function of the state. This also involves the method of obtaining the correlation energy of the many-electron state. Among all the approaches developed so far, CI method is conceptually simplest but computationally challenging. The basic idea in this method is to diagonalize the N-electron Hamiltonian in a basis of N-electron functions (Slater determinants). In other words, we represent the exact wave function of any state as a linear combination of N-electron trial functions and use the variational method to optimize the energy of the state. If the basis were complete, we would obtain the exact energies of ground as well as

of all excited states of the system. In principle, CI provides an exact solution of the many-electron system. In practice, however, we can handle only a finite set of N-electron trail function; consequently, CI provides only upper bounds to the exact energies.

The starting point of CI method is the ground state Dirac-Fock (DF) wave function $|\Phi_0\rangle$. Suppose we have solved Roothan's equation in a finite basis set and obtained a set of $2K$ molecular spin orbitals $\{\chi_i\}$. The determinant formed from the N lowest energy spin orbitals is $|\Phi_0\rangle$. Other than $|\Phi_0\rangle$, we can form a large number of N-electron determinants from the $2K$ spin orbitals. It might be convenient to describe these other determinants by stating how they differ from $|\Phi_0\rangle$. Thus the set of all possible determinants include $|\Phi_0\rangle$, the singly excited determinants $|\Phi_a^r\rangle$ (which differ from $|\Phi_0\rangle$, in having the spin orbital χ_a replaced by χ_r), the doubly excited determinant $|\Phi_{ab}^{rs}\rangle$ (differing from $|\Phi_0\rangle$ by replacing χ_a with χ_r and χ_b with χ_s), etc., up to and including N-truply excited determinants. We can use these many-electron wave functions as a basis to expand the exact many-electron wave function $|\Psi_0\rangle$. If $|\Phi_0\rangle$ is a reasonable approximation to $|\Psi_0\rangle$, then a better approximation according to variation principle (which becomes exact as the basis becomes complete) is

$$
\begin{aligned}
|\Psi_0\rangle \;=\; & c_0|\Phi_0\rangle + \sum_{ar} c_a^r|\Phi_a^r\rangle + \sum_{\substack{a<b\\ r<s}} c_{ab}^{rs}|\Phi_{ab}^{rs}\rangle \\
& + \sum_{\substack{a<b<c\\ r<s<t}} c_{abc}^{rst}|\phi_{abc}^{rst}\rangle + \sum_{\substack{a<b<c<d\\ r<s<t<u}} c_{abcd}^{rstu}|\Phi_{abcd}^{rstu}\rangle + \cdots
\end{aligned}
\tag{2.1}
$$

This is the form of full CI wave function. The restriction on the summation indices (i.e. $a < b$, $r < s$, ets.) is to avoid multiple counting of a given excited

determinant. The above expression can be simplified as

$$
\begin{aligned}
|\Psi_0\rangle &= c_0|\Phi_0\rangle + \left(\frac{1}{1!}\right)^2 \sum_{ar} c_a^r |\Phi_a^r\rangle + \left(\frac{1}{2!}\right)^2 \sum_{abrs} c_{ab}^{rs} |\Phi_{ab}^{rs}\rangle \\
&\quad + \left(\frac{1}{3!}\right)^2 \sum_{\substack{abc \\ rst}} c_{abc}^{rst} |\phi_{abc}^{rst}\rangle + \left(\frac{1}{4!}\right)^2 \sum_{\substack{rstu \\ abcd}} c_{abcd}^{rstu} |\Phi_{abcd}^{rstu}\rangle + \cdots
\end{aligned} \tag{2.2}
$$

where a factor of $(1/n!)^2$ is included in front of the summation to avoid multiple counting in the case of unrestricted summation indices.

Now, let us analyze how many n-tuples excited determinants can arise. If we have $2K$ spin orbitals and N are occupied in $|\Phi_0\rangle$, then $2K - N$ will be unoccupied. We can choose n spin orbitals from those occupied in $|\Phi_0\rangle$ in $\binom{N}{n}$ ways. Similarly, we can choose n orbitals from the $2K - N$ number of virtual orbitals in $\binom{2K-N}{n}$ ways. Thus the total number of n-truply determinants is $\binom{N}{n}\binom{2K-N}{n}$. Even for small molecules and moderate size one-electron basis sets, the number of n-truply excited determinants is extremely large for all n except 0 and 1. Therefore, doing full CI calculation even for a moderately heavy molecule is practically impossible.

Once we have the trial functions of the above equation, we can find the corresponding energies by using the linear variational method. This consists of forming the matrix representation of the Hamiltonian in the basis of N-electron functions which we have used to expand the above equation. Then we have to find the eigenvalues of this matrix by diagonalizing the Hamiltonian matrix. This is called the full CI matrix, and the method is referred as full CI. The lowest eigenvalue will be an upper bound to the ground state energy of the system and the higher eigenvalues will be upper bounds to exited states. The difference between the

lowest eigenvalue ($\mathcal{E}_0$) and the Dirac-Fock energy (E_0) obtained within the same one-electron basis is called the *basis set correlation energy*. As the one-electron basis set approaches completeness, this basis set correlation energy approaches the exact correlation energy. However, the basis set correlation energy obtained by performing a full CI is exact within the subspace spanned by the one-electron basis.

Next, let us construct the full CI matrix and examine it's properties. It is convenient to re-write the previous full CI wave function in a symbolic form

$$|\Psi_0\rangle = c_0|\Phi_0\rangle + c_S|\Phi_S\rangle + c_D|\Phi_D\rangle + c_T|\Phi_T\rangle + c_Q|\Phi_Q\rangle + \cdots \tag{2.3}$$

where $|\Phi_S\rangle$ represents the terms involving single excitations, $|\Phi_D\rangle$ represents terms involving double excitations, and so on. Similarly, c_S and c_D are coefficients corresponding to terms involving single and double excitations, respectively. Using this notation, the full CI matrix has the following form.

$$\begin{array}{c} \\ \\ \langle\Phi_0| \\ \langle S| \\ \langle D| \\ \langle T| \\ \langle Q| \\ \vdots \end{array}
\begin{array}{c}
\begin{array}{ccccccc} & & |\Phi_a^r\rangle & |\Phi_{ab}^{rs}\rangle & |\Phi_{abc}^{rst}\rangle & |\Phi_{abcd}^{rstu}\rangle & \cdots \end{array} \\
\begin{array}{ccccccc} & |\Phi_0\rangle & |S\rangle & |D\rangle & |T\rangle & |Q\rangle & \cdots \end{array} \\
\left[\begin{array}{ccccccc}
\langle\Phi_0|\mathcal{H}|\Phi_0\rangle & 0 & \langle\Phi_0|\mathcal{H}|D\rangle & 0 & 0 & \cdots \\
\langle S|\mathcal{H}|S\rangle & \langle S|\mathcal{H}|D\rangle & \langle S|\mathcal{H}|T\rangle & 0 & \cdots \\
 & \langle D|\mathcal{H}|D\rangle & \langle D|\mathcal{H}|T\rangle & \langle D|\mathcal{H}|Q\rangle & \cdots \\
 & & \langle T|\mathcal{H}|T\rangle & \langle T|\mathcal{H}|Q\rangle & \cdots \\
 & & & \langle Q|\mathcal{H}|Q\rangle & \cdots \\
 & & & & \vdots
\end{array}\right]
\end{array}$$

Since the matrix is Hermitian, hence the lower triangle will be same as the upper triangle. As mentioned earlier, we have to diagonalize this full CI matrix to get the eigenvalues and the corresponding eigenvectors, but the following observation of the full CI matrix are important

1. There is no coupling between DF ground state and single excitations (i.e., $\langle\Phi_0|\mathcal{H}|S\rangle = 0$). This is a consequence of Brillouin's theorem which states that all matrix element of the form $\langle\Phi_0|\mathcal{H}|\Phi_a^r\rangle$ are zero.

2. There is no coupling between $|\Phi_0\rangle$ and triples or quadruples. Similarly, there is no mixing between singles and quadruples. This is a consequence of the fact that all matrix element of the Hamiltonian between Slater determinants which differ by more than two spin orbitals are zero. This also indicates that the blocks which are not zero are sparse. For instance, the matrix element $\langle D|\mathcal{H}|Q\rangle$ represents

$$\langle D|\mathcal{H}|Q\rangle \leftrightarrow \langle\Phi_{ab}^{rs}|\mathcal{H}|\Phi_{cdef}^{tuvw}\rangle$$

For a matrix element of this type to be non-zero, the indices a and b must be included in the set $\{c, d, e, f\}$ and also the indices r and s must be included in the set $\{t, u, v, w\}$.

3. Since there is no mixing of single excitations with $|\Phi_0\rangle$ directly, they can be expected to have a very small influence on the ground state energy. There effect is not zero because they do mix indirectly, i.e, they interact with doubles which in turn interact with $|\Phi_0\rangle$. Although they have almost negligible effect on the ground state energy, still they can influence one-electron properties like dipole moment, significantly.

4. Because the double excitations mix directly with $|\Phi_0\rangle$, it may be expected that, they have important contribution. In fact for small systems they have dominant contribution in determining the correlation energy. Moreover, it turns out that quadruple excitations are more important than triple or single, if one concerned solely with the ground state energy.

As we have mentioned earlier, the number of determinants in extremely large even for a small system and it becomes practically impossible to do full CI calculation. One of the ultimate approximation is to truncate the full CI matrix or equivalently the CI expansion for the exact many-electron wave function at certain excitation level. If one include only single excitations in the trial function for the CI expansion, this scheme is called singly excited CI (SCI). Similarly, including single and double excitation in the CI expansion is called singly and doubly excited CI (SDCI), and so on.

For heavier system, doing SDCI calculation is also quite impossible. In such kind of heavier system, a better approximation is restricted active space (RAS) configuration interaction (CI). In RASCI method, one would consider a limited number of occupied orbitals in $|\Phi_0\rangle$ and limited number of virtual (un-occupied) orbitals with respect to $|\Phi_0\rangle$. These orbitals are called active orbitals in RASCI method. Within these active orbitals one could do a truncated CI calculation at certain excitation level.

Further more, in the RASCI method, the total active orbitals are divided into three active subspaces: (a) RAS1 with a restricted number of holes allowed, (b) RAS2 where all possible configuration are permitted, and (c) RAS3 with an upper limit on the number of electrons allowed. We have used this RASCI method in our calculation to compute the P,T-odd interaction constant $W_{\rm d}$ for the ground ($^2\Sigma$) state of YbF and BaF molecule. In addition to $W_{\rm d}$ we have also computed some other molecular properties of these systems.

2.3 Working equation for $W_{\rm d}$

We have already discussed in detail about the expression for the P,T-odd interaction constant $W_{\rm d}$ in the previous chapter. Here, we will re-cast few relevant equations for our convenience and discuss some of the essential features.

As given in the previous chapter, the expression for the non-vanishing part of the P,T-odd interaction operator H_d is defined as

$$H_d = 2d_e \begin{pmatrix} 0 & 0 \\ 0 & \hat{\boldsymbol{\sigma}} \end{pmatrix} \cdot \mathbf{E}_i^{mol}. \tag{2.4}$$

For a molecule like MF, the molecular electric field $\mathbf{E}_i^{mol}$ is of the form

$$\mathbf{E}_i^{mol} = \mathbf{E}_i^M + \mathbf{E}_i^F + \sum_{j \neq i} \mathbf{E}_{i,j}. \tag{2.5}$$

For our calculation of W_d we have neglected the last term of the above equation because it is quite small compared to the first two terms. We have also assumed that, both M and F nuclei are uniformly charged spherical balls of negligible dimensions. In this case we can evaluate the nuclear electric field at $\mathbf{r}$ (out side the nucleus) using the Gauss law (in atomic unit) as

$$\mathbf{E}(\mathbf{r}) = \frac{Q}{r^2}\hat{\mathbf{r}}, \tag{2.6}$$

where, Q is the total charge inside the nucleus and $\hat{\mathbf{r}}$ is a unit vector relative to the center of the nucleus under consideration. Using these approximations the molecular electric field at the unpaired electron reduces to one-body form as

$$\mathbf{E}^{mol} = \frac{Z_M}{r_M^2}\hat{\mathbf{r}}_M + \frac{Z_F}{r_F^2}\hat{\mathbf{r}}_F \tag{2.7}$$

where M will be replaced by Yb and Ba in the case of YbF and BaF, respectively.

The P,T-odd constant W_d is evaluated from the following expression given by Mosyagin *et al.* [8]

$$W_\mathrm{d} = \frac{2}{d_e}\langle {}^2\Sigma_{1/2}|H_d|{}^2\Sigma_{1/2}\rangle \tag{2.8}$$

where ${}^2\Sigma_{1/2}$ represents the ground states of YbF and BaF molecules in the calculations of Nayak *et al* [16, 19].

It should be noted that the expression for the nuclear electric field $E \propto \frac{1}{r^2}$ is reasonable if the dimensions of the nuclei are assumed to be negligible (i.e., point charge approximation). Since it is well known that nuclei are of finite dimensions, the given expression will over estimate the electric field inside the nuclear region, which can affects the accuracy of W_{d}. In case of a uniformly charged spherical nucleus of finite dimension, the appropriate expression for the electric field inside(outside) the nuclear region $E \propto r (E \propto \frac{1}{r^2})$ should be used. Some other form of the nuclear charge distribution such as, "Gaussian nucleus" or "Fermi nucleus" can also be used.

2.4 Results and discussion of YbF molecule

The ground and excited state properties of YbF are calculated at the optimized geometry using the restricted active space (RAS) configuration interaction (CI) method. We employ $27s27p12d8f$ and $15s10p$ uncontracted Gaussian functions for Yb and F, respectively. The basis employed here is almost same as that used by Parpia [9] in his YbF calculation. The RASCI space employed in this calculation comprised 31 electrons and 56 active orbitals.

The W_{d} estimated from RASCI is compared with other theoretical calculations [7, 8, 9, 10] in Table 2.1. As can be seen in Table 2.1 the present DF estimate of W_{d} is in agreement with the Dirac-Fock (DF) value reported by Parpia [9] but $\sim 7\%$ off from Titov *et al.*'s [7] estimate of W_{d}. At this juncture we emphasize that the DF estimate of W_{d} reported by Quiney *et al.* differs by factor of *three* from ours (as well as from those of Parpia [9] and Titov *et al.* [7]) because a single combination of symmetry type is considered in their [10] calculations. While the deviation in the estimated P,T-odd interaction constant is negligible (among these calculations) at the Dirac-Fock level, the deviation is quite significant at the post Dirac-Fock level. For example, Quiney *et al.* show that the contribution of first order *core-polarization* is almost 100%. On the other hand, Parpia's unre-

Table 2.1: *P,T-odd interaction constant W_d and dipole moment μ_e for the ground $^2\Sigma$ state of YbF molecule.*

Methods or Experiment	$W_{\rm d}$ (10^{25} Hz/e-cm)	μ_e (Debye)
Experiment [2]		3.91(4)
Semi-empirical [14]	-1.50	
GRECP/RASSCF [7]	-0.91	
Semi-empirical [15]	-1.26	
DHF [10]	-0.31	
DHF+CP [10]	-0.61	
UDF (unpaired electron) [9]	-0.962	
UDF (all electrons) [9]	-1.203	4.00
GRECP/RASSCF-EO [8]	-1.206	
DF (Nayak *at al.*) [16]	-0.963	3.98
RASCI (Nayak *et al.*) [16]	-1.088	3.91
MRCI (pseudo-potential) [17]		3.55

stricted Dirac-Fock (UDF) calculation indicates that the correlation contribution is $\sim 25\%$. Note that though the core polarization contribution is most important, the effect of pair correlation and higher order terms are non-negligible. We also emphasize that the inclusion of electron correlation through the UDF is *generally* not recommended as the UDF theory suffers from spin-contamination.

As we have mentioned in the previous section, inclusion of electron correlation to $W_{\rm d}$ via configuration interaction (CI) is straightforward but computationally challenging as a large number of electrons and orbitals need to be included in the RASCI space. In this calculation, we analyze the effect of electron correlation using the RASCI method. There are 39 doubly and one singly occupied orbitals in YbF of which the 25th occupied orbital of YbF corresponds to the $5s$ occupied spin orbitals of Yb. As the contribution of the $5s$ and $5p$ orbitals of Yb to $W_{\rm d}$ is quite significant [7, 15, 14], these orbitals are included in the RASCI space. The occupied orbitals above the 25th are also included in the RASCI space from energy consideration. [Note that the $4f$ orbitals of Yb and the $2p$ orbitals of F in YbF are

Table 2.2: *Vertical ionization potential and transition energies of YbF molecule (in cm^{-1}), computed using RASCI method.*

State	RASCI [16]	Expt. [18]
IP	48537	
$X^2\Sigma$	0	0
$A^2\Pi(1/2)$	18509	18090
$A^2\Pi(3/2)$	19838	19460
$B^2\Sigma(1/2)$	21505	21067

energetically quite close (see Table 12 of Ref. [9])]. Thus, altogether 31 active electrons (16α and 15β) are included in the CI space. In the present calculations for $W_{\rm d}$ and μ_e, we consider six sets of RASCI space which are constructed from 31 active electrons and 19, 26, 36, 46, 51, and 56 active orbitals to analyze the convergence of $W_{\rm d}$ and μ_e.

In Figs. 2.1 and 2.2 we plot $W_{\rm d}$ and μ_e, respectively, against the size of the CI space used in these calculations (summarized in the preceding paragraph). With the exception of a very small increase between the final two calculations, the parameter $W_{\rm d}$ has essentially stabilized. Figs. 2.1 and 2.2 indicate that contribution to $W_{\rm d}$ and μ_e from orbitals 60-75 (CSFs 2-3$\times 10^6$) is most significant compared to other unoccupied (at DF level) active orbitals.

The first ionization potential and low lying ground ($^2\Sigma$) to excited ($^2\Sigma$ and $^2\Pi$) state transition energies of YbF are compared with experiment [18] in Table 2.2. The transition energies from our largest model are quite accurate: departures from experiment are 419 cm^{-1}, 2.3%, for the $A^2\Pi(1/2)$ level; 378 cm^{-1}, 1.9%, for the $A^2\Pi(3/2)$ level; 438 cm^{-1}, 2.1%, for the $B^2\Sigma(1/2)$ level; further, the $A^2\Pi(1/2)$ - $A^2\Pi(3/2)$ gap is accurate to 97%.

The equilibrium bond length (R_e), and ground state vibrational frequencies (ω_e) computed at the DF and RASCI level are compared with experiment and with other calculations in Table 2.3. It is evident from Table 2.3 that the RASCI offers a more accurate estimate of R_e than DF while the later method yields a more

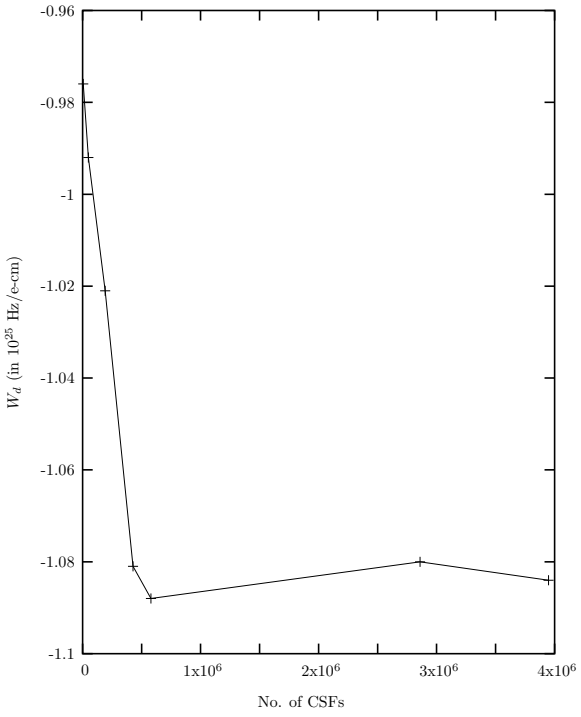

Figure 2.1: *Plot of the P,T-odd interaction constant W_d vs. No. of CSFs for YbF molecule.*

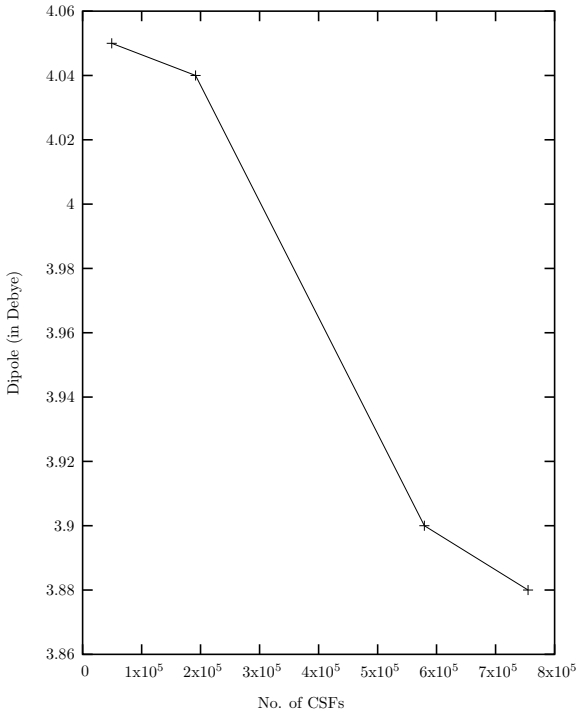

Figure 2.2: *Plot of the molecular dipole moment μ_e vs. No. of CSFs for YbF molecule.*

Table 2.3: *Ground state spectroscopic constants R_e and ω_e of YbF molecule.*

Spectroscopic constant	Nayak *et al.* [16] DF	RASCI	Others	Expt. [18]
R_e (in Å)	2.073	2.051	2.074 [9] 2.045 [17]	2.016
ω_e (in cm^{-1})	504	529	492 [17]	502

accurate estimate of the vibrational frequency ω_e. However, the minuscule error in ω_e (at DF level) is perhaps fortuitous given the larger R_e error of 2.8%.

2.5 Results and discussion of BaF molecule

The P,T-odd constant $W_{\rm d}$ and dipole moment μ_e for the ground state of BaF molecule are calculated using the restricted active space (RAS) configuration interaction (CI) method at the experimental geometry $R_e = 2.16\mathring{A}$ [18]. We employ $27s27p12d8f$ and $15s10p$ uncontracted Gaussian functions for Ba and F, respectively. The RASCI space employed for BaF molecule is composed of 17 electrons and 76 active orbitals.

The $W_{\rm d}$ estimated from the RASCI is compared with other theoretical calculations [12, 11] in Table 2.4. As can be seen in Table 2.4 the present DF estimate of $W_{\rm d}$ is $\sim 21(29)\%$ off from the SCF(RASSCF) result of Kozlov *et al.* [11] and $\sim 17\%$ off from the semi-empirical result of Kozlov and Labzowsky [12] while our RASCI result is $\sim 6(3)\%$ off from the SCF-EO(RASSCF-EO) of Kozlov *et al.* [11] and is in good agreement with the semi-empirical result of Kozlov and Labzowsky. At this juncture, we emphasize that our computed ground state dipole moment of BaF ($\mu_e = 3.203$ Debye) is also reasonably close to experiment $\mu_e = 3.2$ Debye (see Table 5 of Ref. [2]).

In this calculation also, we analyze the effect of electron correlation using the RASCI method. There are 32 doubly and one singly occupied orbitals in BaF of

Table 2.4: *P,T-odd interaction constant W_d for the ground $^2\Sigma$ state of BaF molecule.*

Methods	$W_{\rm d}$ (10^{25} Hz/e-cm)
SCF [11]	-0.230
RASSCF [11]	-0.224
SCF-EO [11]	-0.375
RASSCF-EO [11]	-0.364
Semi-empirical [12]	-0.35
DF (Nayak *et al.*) [19]	-0.293
RASCI (Nayak *et al.*) [19]	-0.352

which the 25th occupied orbital of BaF corresponds to the $5s$ occupied spin orbitals of Ba. As the contribution of the $5s$ and $5p$ orbitals of Yb to $W_{\rm d}$ is quite significant [7] in case of YbF molecule, in this case also we have included the $5s$ and $5p$ orbitals of Ba in our CI space for the calculation of $W_{\rm d}$ and μ_e for the ground state of BaF molecule. The occupied orbitals above the 25th are also included in the RASCI space from energy consideration. Thus, altogether 17 active electrons (9α and 8β) are included in the CI space. In the present calculations for $W_{\rm d}$ we consider nine sets of RASCI space which are constructed from 17 active electrons and 16, 21, 26, 31, 36, 46, 56, 66 and 76 active orbitals to analyze the convergence of $W_{\rm d}$.

In Fig. 2.3 we plot $W_{\rm d}$ against the size of CI space used in the calculations summarized in the preceding paragraph. Fig. 2.3 demonstrates that the $W_{\rm d}$ decreases with increasing size of the CI space till it reaches -0.352$\times 10^{25}$ Hz/e-cm. With the exception of a very small increase at the final calculation, the parameter has essentially stabilized. Fig. 2.3 further indicate that contribution to $W_{\rm d}$ from orbitals 70-100 (CSFs 1-6$\times 10^5$) is most significant compared to other unoccupied (at DF level) active orbitals.

The present calculation shows that inclusion of $2g(2g+1h)$ functions on Ba yields $W_{\rm d} = -0.356(-0.351) \times 10^{25}$ Hz/e-cm. Our calculation (with more ac-

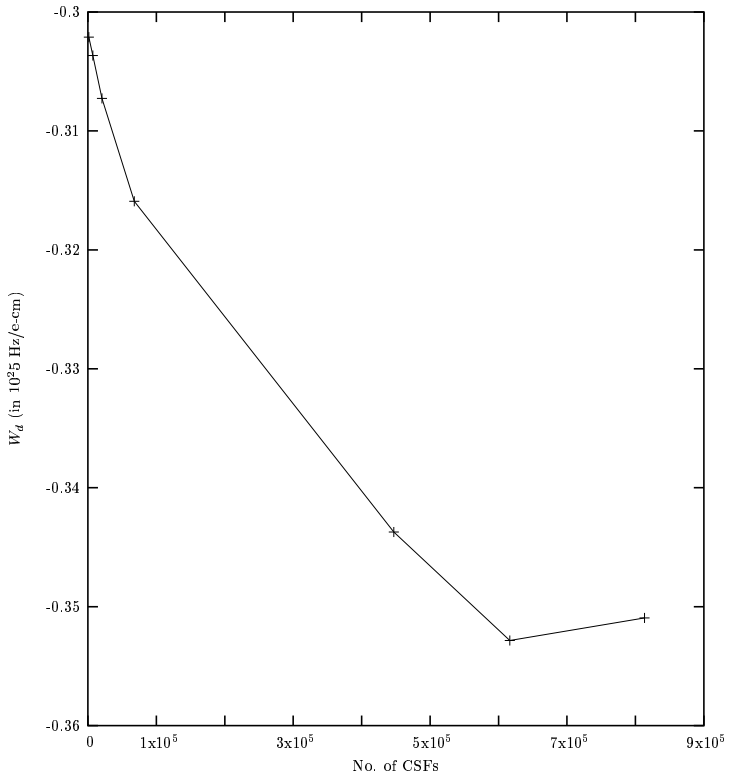

Figure 2.3: *Plot of the P,T-odd interaction constant W_d vs. No. of CSFs for BaF molecule.*

tive orbitals/determinants in the CI space) further shows some minor oscillatory behavior of $W_{\rm d}$, where the variation of $W_{\rm d}$ is roughly $\pm 1.2\%$.

At this juncture, we emphasize that the ground $^2\Sigma_{(1/2)}$ state of BaF can mix strongly with the low-lying $^2\Pi_{(1/2)}$ state in presence of an electric field because of the small energy gap between them, which can influence the result obtained for $W_{\rm d}$. To analyze the influence of this mixing on $W_{\rm d}$, one has to consider the perturbative expression for the linear Stark shift given by Kozlov and Labzowsky [11] as well as by Commins [20] (also given in chapter one), which is of the form

$$\begin{aligned} \triangle E &= -2d_e eE_z \sum_{n\neq 0} \frac{\langle\psi_0|z|\psi_n\rangle\langle\psi_n|(\beta-1)\mathbf{\Sigma}\cdot\mathbf{E}_{int}|\psi_0\rangle}{E_0-E_n} \\ &\quad -d_e E_z\langle\psi_0|(\beta-1)\Sigma_z|\psi_0\rangle. \end{aligned} \tag{2.9}$$

where $\mathbf{E}_{int}$ is the internal electric field and E_z is an applied electric field along the z-direction. The second term in this expression is quite small as compared to the first term and can be neglected. The ratio between the Stark matrix element ($eE_z\langle\psi_0|z|\psi_n\rangle$) and the energy denominator ($E_0 - E_n$) determines the strength of mixing between the ground state ψ_0 ($^2\Sigma_{(1/2)}$ here) and excited states ψ_n ($^2\Pi_{(1/2)}$ here) of the system (see [11, 20] for more details). The same situation may arise in the case of YbF molecule and hence these possibilities should be taken care for more precise calculations.

Finally, we would like to point that, experiments on BaF molecule for the detection of P,T-symmetry violation has not yet been performed, but are being planned. So, the present estimated result of $W_{\rm d}$ as well as all the previous calculations [11, 12] will be useful for experimentalists to start experiments on this system. As the experiments progress, calculations with much higher accuracies will be performed by including the effects which are neglected/omitted in the present calculation. Therefore, the accuracy of the present calculation is sufficient at this moment.

Bibliography

[1] B. E. Sauer, J. Wang, and E. A. Hinds, Phys. Rev. Lett. **74**, 1554 (1995).

[2] B. E. Sauer, J. Wang, and E. A. Hinds, J. Chem. Phys. **105**, 7412 (1996).

[3] S. M. Barr, Phys. Rev. D **45**, 4148 (1992).

[4] S. M. Barr, Int. J. Mod. Phys. **8**, 209 (1993).

[5] B. N. Ashkinadzi, Petersburg Nuclear Physics Institute, St.-Petersburg, Report No. **1801**, (1992).

[6] E. A. Hinds and P. G. H. Sandars, Phys. Rev. A **21**, 471 (1980).

[7] A. V. Titov, N. S. Mosyagin, and V. F. Ezhov, Phys. Rev. Lett. **77**, 5346 (1996).

[8] N. S. Mosyagin, M. G. Kozlov, and A. V. Titov, J. Phys. B **31**, L763 (1998).

[9] F. A. Parpia, J. Phys. B **31**, 1409 (1998).

[10] H. M. Quiney, H. Skaane, and I. P. Grant, J. Phys. B **31**, L85 (1998).

[11] M. G. Kozlov, A. V. Titov, N. S. Mosyagin and P. V. Souchkov, Phys. Rev. A **56**, R3326 (1997).

[12] M. G. Kozlov and L. N. Labzowsky, J. Phys. B **28**, 1933 (1995).

[13] L. B. Knight, W. C. Easley, and W. Weltner, J. Chem. Phys. **54**, 322 (1971).

[14] M. G. Kozlov, J. Phys. B **30**, L607 (1997).

[15] M. G. Kozlov and V. F. Ezhov, Phys. Rev. A **49**, 4502 (1994).

[16] M. K. Nayak and R. K. Chaudhuri, Chem. Phys. Lett. **419**, 191 (2006).

[17] M. Dolg, H. Stoll and H. Preuss, Chem. Phys. **165**, 21 (1992).

[18] K. P. Huber and G. Herzberg, *Molecular Spectra and Molecular Structure,Constants of Diatomic Molecules* (Van Nostrand, New York, 1979), Vol. 4.

[19] M. K. Nayak and R. K. Chaudhuri, J. Phys. B **39**, 1231 (2006).

[20] E. D. Commins, Adv. At. Mol. Opt. Phys. **40**, 1 (1999).

Chapter 3

Application of Coupled Cluster method for one-valence problems: Ionization potential and electron affinity

3.1 Introduction

Emergence of the high resolution probes, viz. photo-electron spectroscopy, synchrotron radiation spectroscopy (SRS) [1] and the non-coplanar electron transmission spectroscopy (ETS) [2] have lead to a wealth of accurate physico-chemical data pertaining to ionization and electron attachment processes. The accurate analysis and interpretation of ionization spectra have been a major challenge to experimentalists and theoreticians. Prior to the development of post Hartree-Fock methodologies, the independent particle model (IPM) [3] provided the theoretical rationale for understanding the electron binding energies for electron attachment and detachment processes. The IPM scheme usually provides a reasonable description of the spectrum for the outer valence region, but for inner valence region, this simple model completely breaks-down. The photo-electron spectrum for the inner valence region is most often very complicated and one encounters a number of peaks -called *satellites* -rather than only one *main* peak as predicted by the IPM.

Beside this, the IPM sometimes also predicts the *wrong* ordering of the main ionization potential peaks, e.g. in the N_2 and F_2 [4] molecules. The failure of the IPM strongly suggests that electron correlation has to be treated as accurate as possible to interpret and explain these highly complex phenomena even qualitatively, and this requires theories of matching sophistication far transcending the simple IPM.

Extensive studies have shown that for an accurate prediction of the ionization potentials, electron affinities, etc. requires the incorporation of both electron correlation and orbital relaxation effects as these effects are strongly inter-wined. The single reference coupled cluster (SRCC) [5] method, developed by the cluster expansion of a single determinant reference function, is now considered as one of the most sophisticated, elegant and well established methods among the vast plethora of correlated many-body theories for treating dynamical correlation effects in a size-extensive manner in situations where the non-dynamical correlation effects can be sidelined, for example, the closed-shell states around the equilibrium internuclear configurations. The incorporation of the singly and doubly excited cluster operators (SD) only within the SRCC framework provides an accurate and reliable description of the electron correlation for non-degenerate states, and is one of the most extensively used class of SRCC approaches.

Motivated by the initial success of the SRCC method, several endeavors have come on to force during the past couple of decades to generalize the SRCC method and make it suitable to encompass open-shell and/or quasi-degenerate states. The non-uniqueness of the exponential nature of the wave operator diversifies the methods to a host of multi-reference CC (MRCC) strategies. The traditional MRCC methods hinge on the effective Hamiltonian approach and work within the complete model spaces (CMS), though they are rather more varied in their scope of applications [6]. The effective Hamiltonian based MRCC strategies fall within two broad classes: (i) State-Universal (SU), a Hilbert-space approach [7] and (ii) Valence-Universal (VU), a Fock-space approach [8, 9, 10, 11, 12, 13, 14, 15]. The SU-MRCC method highlights on only one valence sector at a time, with the cluster

operator being defined with respect to each reference function. The VU-MRCC approach, on the contrary, uses a single wave operator that not only correlates the reference functions of interest, but also all the lower valence (or the so called *subdued*) sectors, obtained by deleting the occupancies systematically. At this juncture, we recall that the cluster amplitudes in Fock-space VU-MRCC are generated hierarchically through the *subsystem embedding condition* (SEC) [10, 12] which is equivalent to the *valence universality* condition used by Lindgren [11] in his formulation.

The linear response theory (LRT) or the equation of motion (EOM) methods [16, 17, 18, 19, 20] are other possible alternatives which are used to compute the spectroscopic energies. EOM-CC and SR-CCLRT are identical for the excited states energies, but the approximations in the two methods differ for transition properties. The underlying physics is the same, in particular, state properties defined as energy derivatives are clearly identical since the state energies themselves are identical. Several models, iterative and non-iterative, have also been developed which partially include the effects of triple excitations [21]. Recently, Nooijen and Bartlett have developed a new method for calculating excited state energies and properties, the similarity transformed EOM-CC (STEOM-CC) method [22]. For singly excited states, STEOM-CC is closely related to the Fock space CC method [22], but conceptually they are very different. In STEOM-CC, the ground state CC calculation describes the ground state dynamic correlation very well, whereas the differential correlation is handled through the second similarity transformation, which is built from an active space of ionized and electron-attached states.

The main advantage of the VU-MRCC theory is that its working equation is fully connected and hence size-extensive in nature in contrast to the LRT or EOM method which are core extensive and *not* core-valence extensive due to the presence of the disconnected diagrams while considering the charge-transfer excitations. Although, the LRT or EOM method is not fully extensive in nature, the method is *intruder free* [23] in contrast to the traditional VU-MRCC theory due

to the CI-like structure of the working equation of the former. It should be noted that for the same truncation scheme of the operator manifold, VU-MRCC is equivalent to the LR-based CC methods [16, 17, 18, 19, 20] in the case of one-valence problem.

3.2 Methodology

3.2.1 Valence universal multi-reference coupled cluster theory: A core-valence extensive theory

The basic formalism of VU-MRCC theory for energy difference is available elsewhere [8, 9]. Here, we provide a brief overview of this method for general model space. We choose the Hartree-Fock (HF) (Dirac-HF in relativistic regime) solution for the closed-shell N-electron ground state Φ_{HF} as the vacuum to define holes and particles with respect to the Φ_{HF}. The holes and particles orbitals are further subdivided to introduce multi-reference aspect. We define a *model* space (P) which has all possible electron occupancies in the active orbitals to be *complete*, while others are said to be *incomplete*. In general, any second-quantized operator has k-hole and l-particle destruction operators for the active holes and particles and m particle and n hole excitation operators involving both active and inactive holes and particles. We define an operator A of valence rank (k,l) by $\text{A}^{(k,l)}$ where A contains exactly k-hole and l-particle destruction operators.

Using the "valence-universal" [8, 9, 11, 12, 13, 14, 15] ansatz for the wave operator Ω, the Fock-space Bloch equation for the CC-theory may be written as

$$\text{H}\Omega\text{P}^{(k,l)} = \Omega\text{P}^{(k,l)}\text{H}_{\text{eff}}\text{P}^{(k,l)} \quad \forall(k,l) \tag{3.1}$$

where the superscripts (k,l) represents the k-hole, l-particle valence sector, H is

the N-electron Hamiltonian and

$$\mathrm{H}_{\mathrm{eff}} = \mathrm{P}^{(k,l)}\mathrm{H}\Omega\mathrm{P}^{(k,l)}. \tag{3.2}$$

Here, the equation is taken to be valid for all (k,l), starting from $k = l = 0$, the *core* problem to some desired *parent* model space, with $k = m, l = n$, say. We express Ω in *normal* order as

$$\Omega = \{\exp(\tilde{\mathrm{S}})\} \tag{3.3}$$

with $\tilde{\mathrm{S}}$ contains only *external* operators (operators that connects the model space with the complementary space Q) of various valence ranks

$$\tilde{\mathrm{S}} = \sum_{k,l=0,0}^{m,n} \mathrm{S}^{(k,l)}. \tag{3.4}$$

In second quantized notation, operator S for (0,0), (0,1) and (1,0) valence rank can written as

$$\mathrm{S}^{(0,0)} = \sum_{p}^{unocc}\sum_{\alpha}^{occ}\langle p|s_1^{(0,0)}|\alpha\rangle\{a_p^\dagger a_\alpha\} + \frac{1}{4}\sum_{p,q}^{uocc}\sum_{\alpha,\beta}^{occ}\langle pq|s_2^{(0,0)}|\alpha\beta\rangle\{a_p^\dagger a_q^\dagger a_\beta a_\alpha\} + \cdots, \tag{3.5}$$

$$\mathrm{S}^{(0,1)} = \frac{1}{2}\sum_{p,q,r}^{uocc}\sum_{\alpha}^{occ}\langle pr|s_2^{(0,1)}|q\alpha\rangle\{a_p^\dagger a_r^\dagger a_\alpha a_q\} + \cdots \tag{3.6}$$

for all active particles, and

$$\mathrm{S}^{(1,0)} = \frac{1}{2}\sum_{p}^{uocc}\sum_{\beta,\gamma,\alpha}^{occ}\langle p\alpha|s_2^{(1,0)}|\gamma\beta\rangle\{a_p^\dagger a_\alpha^\dagger a_\beta a_\gamma\} + \cdots \tag{3.7}$$

for all active holes, respectively. At this juncture, it is convenient to single out the core-cluster amplitudes $\mathrm{S}^{(0,0)}$ and call them T. The rest of the cluster amplitudes will henceforth be called S. Since Ω is in normal order, we can rewrite eq.(3.3) as

$$\Omega = \exp(\mathrm{T})\{\exp(\mathrm{S})\} \tag{3.8}$$

Premultiplying eq.(3.1) by exp(-T) and using eq.(3.8), we get as [24]

$$\bar{\mathrm{H}}\Omega_v \mathrm{P}^{(k,l)} = \Omega_v \mathrm{P}^{(k,l)} \bar{\mathrm{H}}_{\mathrm{eff}} \mathrm{P}^{(k,l)} \quad \forall (k,l) \neq (0,0) \tag{3.9}$$

where

$$\bar{\mathrm{H}} = \exp(\text{-T})\, \mathrm{H} \exp(\mathrm{T}) \tag{3.10}$$

and

$$\Omega_v = \{\exp(\mathrm{S})\} \tag{3.11}$$

Here, the core-cluster amplitudes T are assumed as solved at the lowest level of hierarchy of $(k,l) \equiv (0,0)$. Since $\bar{\mathrm{H}}$ can be split into an operator part $\tilde{\mathrm{H}}$ and the ground state energy E_{gr}, we likewise define $\tilde{\mathrm{H}}_{\mathrm{eff}}$, generating the energy differences, and write

$$\bar{\mathrm{H}}_{\mathrm{eff}} = \tilde{\mathrm{H}}_{\mathrm{eff}} + \mathrm{E}_{\mathrm{gr}} \tag{3.12}$$

and thus get the Fock-space Bloch equation for energy differences as

$$\tilde{\mathrm{H}}\Omega_v \mathrm{P}^{(k,l)} = \Omega_v \mathrm{P}^{(k,l)} \tilde{\mathrm{H}}_{\mathrm{eff}} \mathrm{P}^{(k,l)} \quad \forall (k,l) \neq (0,0) \tag{3.13}$$

Proceeding hierarchically from the lowest nontrivial valence ranks (1,0) and (0,1), we get

$$\tilde{\mathrm{H}}\Omega_v \mathrm{P}^{(1,0)} = \Omega_v \mathrm{P}^{(1,0)} \tilde{\mathrm{H}}_{\mathrm{eff}} \mathrm{P}^{(1,0)} \tag{3.14}$$

and

$$\tilde{\mathrm{H}}\Omega_v \mathrm{P}^{(0,1)} = \Omega_v \mathrm{P}^{(0,1)} \tilde{\mathrm{H}}_{\mathrm{eff}} \mathrm{P}^{(0,1)} \tag{3.15}$$

for the one-hole and one-particle model space, which correspond to the IP and EA problem.

The scheme of generating the elementary excitations (IP, EA, EE, etc.) proceed hierarchically. We first solve the ground state problem to determine the T amplitudes. The $\mathrm{S}^{(1,0)}$and $\mathrm{S}^{(0,1)}$ are solved in the next level of hierarchy which are

decoupled from each other.

3.2.2 Single-reference coupled cluster based linear response theory: A core extensive theory

In CC based LRT method the ground state CC operator is used to perform a similarity transformation of the Hamiltonian, which is then diagonalized within the space of excited determinants. SR-CCLRT is nowadays routinely used for the investigation of excited states of closed-shell molecules. A major theoretical advantage of the response based method lies in the representation of the excited state in terms of the ground state. This description thus automatically includes the components of the correlation contribution from the ground state that remains more or less unchanged and which largely dominates in the low-lying excited state correlation. The additional differential correlations accompanying excitation can then be incorporated in a systematic manner in the dynamic linear response function. As a consequence, the response approach offers the flexibility for including the differential correlation and the additional correlation effects on top of the ground state correlation components. The common correlation terms then drop out in the energy differences, and the excitation energies obtained are thus described in a more balanced manner. It is thus not surprising that the pre-eminent success of the SRCC theory for the ground state has produced in turn a very successful linear response theory based on the SRCC wave function, and widely accepted as a major method of choice for the excited states whose ground state is predominantly SR in character.

The CCLRT method for energy difference was first put forward by Mukherjee *et al.* [17]. In their formulation, the atom/molecule in its ground state is subjected to a photon field and the linear response of the the ground state function described CC-ansatz is computed where the poles of the response functions are the elementary excitations. Depending on the nature of perturbation one may obtain

IP, EA, EE, DIP etc. of the ground state. Mukherjee and co-workers [25] have also shown that an equivalent but simpler derivation of this scheme (called coupled cluster based linear response theory or CCLRT) is possible.

In CCLRT approach, the wave operator Ω in eq.3.8 is expressed as

$$\Omega = \exp(\mathrm{T}) W_k^\dagger \tag{3.16}$$

where the cluster operator $W_k^\dagger$ are expressed as

$$W_k^\dagger = \sum_{\alpha}^{occ} x_\alpha \{a_\alpha\} + \sum_{\alpha,\beta}^{occ} \sum_{p=1}^{unocc} x_{\alpha\beta}^p \{a_p^\dagger a_\beta a_\alpha\} + \cdots \quad \text{(for IP)}, \tag{3.17}$$

$$W_k^\dagger = \sum_{p}^{unocc} x_p \{a_p^\dagger\} + \sum_{p,q}^{uocc} \sum_{\alpha}^{occ} x_\alpha^{pq} \{a_p^\dagger a_q^\dagger a_\alpha\} + \cdots \quad \text{(for EA)}, \tag{3.18}$$

and

$$W_k^\dagger = \sum_{p}^{unocc} \sum_{\alpha}^{occ} x_\alpha^p \{a_p^\dagger a_\alpha\} + \frac{1}{2} \sum_{p,q}^{uocc} \sum_{\alpha,\beta}^{occ} x_{\alpha\beta}^{pq} \{a_p^\dagger a_q^\dagger a_\beta a_\alpha\} + \cdots \quad \text{(for EE)}. \tag{3.19}$$

The ionized/excited states Ψ_k are generated from the ground state by the action of ionization/excitation operators $W_k^\dagger$ and the corresponding state energies E_k are obtained from an equation of the form [17, 25, 26, 27, 28, 29]:

$$[\mathrm{H}, W_k^\dagger] |\Psi_0\rangle = \mathrm{E}_k W_k^\dagger |\Psi_0\rangle \tag{3.20}$$

Since T and $W_k^\dagger$ commute, premultiplying eq.(3.20) by exp(-T) we get the following equation of motion:

$$[\tilde{\mathrm{H}}, W_k^\dagger] |\phi_0\rangle = (\mathrm{E}_k - \mathrm{E}_{\mathrm{gr}}) W_k^\dagger |\phi_0\rangle \equiv \omega_k W_k^\dagger |\phi_0\rangle \tag{3.21}$$

where $\bar{\mathrm{H}} = \tilde{\mathrm{H}} + \mathrm{E}_{\mathrm{gr}}$ and ω_k is the difference energy. Projecting eq.(3.21) on to the

bi-orthogonal space, we get an eigenvalue value equation of the form

$$AX_k = \Lambda X_k. \tag{3.22}$$

It is clear from above that CCLRT has altogether a much simpler structure compared to core-valence extensive CC-theory. There is no hierarchical generation of the cluster amplitudes except for the ground state (which is common to both), neither there is any special consideration for the appropriate choice of normalization. From the very mode of derivation it is quite clear that the energies computed via CCLRT method is core-extensive in nature, for remaining part (valence) its behave like a truncated CI. Thus the method is not core-valence extensive in nature. At this juncture, we emphasize that the CCLRT not only yields the *main* (valence) but also the *satellite* (shake-up) state energies.

3.2.3 The Fock space eigenvalue independent partitioning technique

In spite of formal rigor, the VU-MRCC equations are often plagued by the *intruder state problem* [23]. This was circumvented in an elegant way by Mukherjee *et al.* [30] via "eigenvalue independent partitioning technique" (EIP). The EIP technique converts the non-linear VU-MRCC equations for any model space into a set of non-hermitian eigenvalue equations. Since the details of EIP scheme are documented elsewhere [30, 31], we will only outline the essential features of this scheme here.

Let us assume a real non-symmetric matrix H of dimension $M \times M$. We intend to determine selected M_p ($M_p \ll M$) roots (λ_i) and associated eigenvectors $\{C_i\}$ of this $M \times M$ matrix. Denoting the components of the subspace P and the rest by Q, the associated eigenvalue problem can be written as

$$\begin{bmatrix} \mathrm{H_{PP}} & \mathrm{H_{PQ}} \\ \mathrm{H_{QP}} & \mathrm{H_{QQ}} \end{bmatrix} \begin{bmatrix} \mathrm{X_{PP}} \\ \mathrm{X_{QP}} \end{bmatrix} = \begin{bmatrix} \mathrm{X_{PP}} \\ \mathrm{X_{QP}} \end{bmatrix} \begin{bmatrix} \Lambda_{\mathrm{P}} \end{bmatrix} \tag{3.23}$$

where Λ_P is a diagonal $M_P \times M_P$ matrix of eigenvalues and X_{PP} and X_{QP} are the matrix components of the eigenvector C in the P and Q spaces, respectively. Let us introduce a "partitioning matrix" Σ and an "effective" Hamiltonian matrix H_{eff} defined by

$$\Sigma = X_{QP}X_{PP}^{-1} \;\; ; \quad H_{eff} = X_{PP}\Lambda_P X_{PP}^{-1}. \tag{3.24}$$

Σ exists whenever X_{PP} is non-singular. Using Eq.(3.24), Eq.(3.23) can be expressed as

$$H_{PP} + H_{PQ}\Sigma = H_{eff}, \tag{3.25}$$

$$H_{QP} + H_{QQ}\Sigma = \Sigma H_{eff} \tag{3.26}$$

While Eq.(3.26) yields a set of coupled quadratic equations for the components Σ, Eq.(3.25) furnishes selected M_P roots upon diagonalization of H_{eff}

$$\Lambda_P = X_{PP}^{-1}H_{eff}X_{PP} \tag{3.27}$$

Since H_{eff} does not depend parametrically on the eigenvalue $\{\lambda_i\}$, the reduction of Eq.(3.23) to Eqs.(3.25) and (3.26) is called an "eigenvalue independent partitioning" technique (EIP). EIP allows us to cast Eq. (3.23) for M_P selected roots from $M \times M$ matrix into an M_P dimensional matrix involving H_{eff}. Conversely, any two sets of equations of the form of Eqs.(3.25) and (3.26) can be cast into a single eigenvalue problem as in Eq.(3.23).

3.3 Applications of CCLRT

3.3.1 Direct determination of ionization potentials of HCl via CCLRT: one electron detachment process

The valence and satellite lines of HCl [32, 33, 34, 35, 36] have been studied experimentally by Adam [34, 35] and by Svensson *et al.* [36] who have

recorded the HCl valence ionization spectrum up to 52 eV using XPS and SRPS [36]. So far, eleven satellite lines have been observed of which seven peaks are found to lie below the continuum for doubly ionized states. The HCl satellite peaks have been studied theoretically [37] by the Green's function (GF) method, ADC(3) (algebraic diagrammatic construction accurate to 3rd order), approximate ADC(4) (algebraic diagrammatic construction accurate to 4th order) [38, 39], symmetry-adapted-cluster configuration interaction general-R (SAC-CI-general-R) [40, 41, 42, 43, 44], and the SAC-CI-SD-R (single double-R) methods. While the previous theoretical studies are quite successful in assigning some satellite peaks, the computed first valence ionization potentials for the $^2\Pi$ state deviates significantly (by 0.3-0.4 eV) from experiment.

An aug-CC-PVTZ basis comprised 84 GTOs is employed for the CC computations. The Cl basis is constructed from the (15s9p2d1f)/[5s4p2d1f] GTOs of Woon and Dunning [45] augmented with one $s(\zeta_s = 0.0591)$, one $p(\zeta_p = 0.0419)$, one $d(\zeta_d = 0.135)$, and one $f(\zeta_f = 0.312)$ diffuse function. For the H atom, the (5s2p1d)/[3s2p1d] GTO basis of Dunning [46] is augmented by one $s(\zeta_s = 0.02526)$, one $p(\zeta_p = 0.102)$, and one $d(\zeta_d = 0.247)$ diffuse function. The ADC [37] and SAC-CI calculations [47] employ a smaller basis of 67 GTOs constructed from a (14s11p4d/5s2p)/[10s8p4d/3s2p] set.

The vertical ionization potentials (valence as well as satellite) of HCl obtained from CCLRT are compared with experiment [36] and with other correlated calculations [37, 47] in Table 3.1. The two main peaks $^2\Pi$ and $^2\Sigma$ at 12.8 and 16.6 eV, respectively, in the experimental ionization spectrum are more accurately reproduced in our calculation than the other theoretical approaches. The CCLRT estimates the $(2\pi)^{-1}$ and $(5\sigma)^{-1}$ states to be at 12.54 and 16.61 eV while they are predicted to lie at 12.50 and 16.56 eV by the SAC-CI-SD-R method. The shake-up states are mainly described as two-electron processes (often called 2h-1p process). Theoretical investigations suggest that the 4σ orbital plays a quite significant role in characterizing the shake-up states. On the other hand, the contribution of the

Table 3.1: *Comparison main peaks and shake-up ionization potentials (in eV) of HCl obtained from CCLRT, with experiment and other correlated calculations. All these theoretical calculations are performed at* $R_{HCl} = 1.2746\mathring{A}$.

State	ADC [37]	SAC-CI [47]	CCLRT [48]	Expt. [36]
$^2\Sigma$				
	16.45	16.46	16.61	16.60
	25.88	26.38	25.60	25.85
	27.94	28.78	28.64	28.50
	31.91	32.43	32.21	32.00
	34.90	34.65	34.60	34.65
	36.61		36.44	35.5-41.0
$^2\Pi$				
	12.43	12.41	12.54	12.80

4σ orbital to $^2\Pi$ valence ionization potentials (VIP) is not so important.

3.4 Overview of Relativistic spinors

The relativistic VU-MRCC method is applied to compute the ionization and excitation energies of Ag and Hg atoms, in the next section. Here, we employ the straight forward extension of non-relativistic coupled cluster theory to the relativistic regime by adopting the no-virtual-pair approximation (NVPA) along with appropriate modification of the orbitals form and potential terms [49]. The problem of "continuum dissolution" is formally avoided by introducing projection operators to select the positive energy states or, in other words, by excluding all summations over negative energy states [50].

The Dirac-Coulomb Hamiltonian for the many-electron system is written as

$$H = \sum_{i=1}^{N} [c\vec{\alpha}_i.\vec{p}_i + (\beta_i - 1)mc^2 + V_{nuc}(r_i)] + \frac{1}{2}\sum_{i\neq j}\frac{e^2}{|\vec{r}_i - \vec{r}_j|} \tag{3.28}$$

in terms of the customary Dirac operators $\vec{\alpha}$ and β that are represented by the

matrices,

$$\vec{\alpha} = \begin{pmatrix} 0 & \vec{\sigma} \\ \vec{\sigma} & 0 \end{pmatrix} \qquad \beta = \begin{pmatrix} I & 0 \\ 0 & -I \end{pmatrix} \quad , \tag{3.29}$$

where $\bar{\sigma}$ denotes the Pauli matrices and I is the 2x2 unit matrix. The simplest choice for $V_{nuc}(r)$ is a point source of electric field with a Coulomb potential of the form,

$$V_{nuc}(r) = -\frac{Z}{r}. \tag{3.30}$$

where Z is the atomic number. However, this nuclear model introduces a non-physical singularity which is known to influence the convergence properties of the finite basis set expansion, particularly if a Gaussian type basis set is employed [51]. Further, the nuclear volume isotope shift, observed in heavy atoms, reflects the finite size of the nucleus with the nuclear charge distribution depending upon the mass number A. Among the various nuclear models, the "Fermi nucleus" is a popular choice for nuclear model without a sharp cutoff. Experimental studies suggest that the nuclear charge distribution posses a "skin" of finite thickness across which the nuclear charge density falls to zero as in the "Fermi nucleus" model. The present work uses the "Fermi nucleus" model in which the charge density inside the nucleus varies as,

$$\rho(r) = \rho_0[1 + \exp\{(r-b)/a\}]^{-1}, \tag{3.31}$$

where ρ_0 is a constant (depending on Z) [52] and b is the cut-off radius (also called "half-density radius"), at which the charge density $\rho(b) = \rho_0/2$. The parameter a is related to the nuclear skin thickness (t) by

$$a = t/(4 \ln 3), \tag{3.32}$$

where $t = 2.30$ fm for the "Fermi nucleus" model [53]. The relativistic orbitals are

expressed in the form,

$$\begin{pmatrix} r^{-1}P_{n\kappa}(r)\chi_{\kappa m}(\theta,\phi) \\ ir^{-1}Q_{n\kappa}(r)\chi_{-\kappa m}(\theta,\phi) \end{pmatrix} \tag{3.33}$$

where $r^{-1}P_{n\kappa}(r)$ and $r^{-1}Q_{n\kappa}(r)$ are the large and small components of the radial wave functions, respectively, that satisfy the orthogonality condition,

$$\int_0^\infty dr[P_{n\kappa}(r)^* P_{m\kappa}(r) + Q_{n\kappa}(r)^* Q_{m\kappa}(r)] = \delta_{mn}. \tag{3.34}$$

The quantum number κ classifies the orbital according to symmetry and is given by,

$$\kappa = \mp(j \pm \frac{1}{2}), \tag{3.35}$$

where l is the orbital quantum number and $j = l \pm \frac{1}{2}$ is the total angular quantum number. The spinors $\chi_{\kappa m}(\theta,\phi)$ are written as,

$$\chi_{\kappa m}(\theta,\phi) = \sum_{\sigma=\pm\frac{1}{2}} C^{j,m}_{l,m-\sigma;\frac{1}{2},\sigma} Y_{l,m-\sigma}(\theta,\phi)\eta_\sigma, \tag{3.36}$$

where $C^{j,m}_{l,m-\sigma;\frac{1}{2},\sigma}$ and $Y_{l,m-\sigma}(\theta,\phi)$ represent the Clebsch-Gordon coefficients and the normalized spherical harmonics, respectively, and η_σ is a two-component spinor.

The large and small component radial wave functions are expressed as linear combinations of basis functions,

$$P_{n\kappa}(r) = \sum_{p=1}^{N} C^L_{\kappa p} g^L_{\kappa p}(r) \quad ; \quad Q_{n\kappa}(r) = \sum_{p=1}^{N} C^S_{\kappa p} g^S_{\kappa p}(r), \tag{3.37}$$

where the summation index p runs over the number of basis functions N and $g^L_{\kappa p}$ ($g^S_{\kappa p}$) and $C^L_{\kappa p}$ ($C^S_{\kappa p}$) are the basis functions and expansion coefficients for the large (small) components, respectively. The basis functions employed in these calculations are Gaussian type orbitals (GTOs) of the form,

$$g^L_{\kappa p}(r) = N^L_p r^{n_\kappa} e^{-\alpha_p r^2}, \tag{3.38}$$

with

$$\alpha_p = \alpha_0 \beta^{p-1}, \tag{3.39}$$

where α_0 and β are user defined constants, n_κ specifies the orbital symmetries (1 for s, 2 for p, etc.) and constant N_p^L is the normalization factor for the large component defined as [53]

$$N_p^L = \sqrt{\frac{2^{n_\kappa+3/2}\alpha_p^{n_\kappa+1/2}}{(2n_\kappa-1)!!\sqrt{\pi}}} \tag{3.40}$$

The small component normalization factor N_p^S is obtained by imposing the *kinetic balance* condition,

$$g_{\kappa p}^S(r) = N_p^S(\frac{d}{dr} + \frac{\kappa}{r}) g_{\kappa p}^L(r), \tag{3.41}$$

where

$$N_p^S = \sqrt{\frac{2n_\kappa - 1}{\alpha_p[4(\kappa^2+\kappa+n_\kappa)-1]}}. \tag{3.42}$$

We will also use these relavistic spinors discussed above, for the computation of ionization potential and excitation energies of Sr and Yb atom using (0h-2p) relativistic VU-MRCC method in the next chapter.

3.5 Applications of VU-MRCC

3.5.1 Computation of valence electron removal energy of Ag via (0h-1p) VU-MRCC: one electron attachment process

We employ a $36s30p28d15f$ GTOs basis to compute the ionization potential and excition energies of Ag using VU-MRCC method. The ground state configuration of Ag is [Kr]$4d^{10}5s^1$ ($^2S_{1/2}$). Because of its high Z value, Ag must be treated relativistically. As because the ground state of Ag is open-shell doublet, we begin with Ag^+ which defines the (0h,0p) valence sector. The ground and excited state energies of Ag are computed through (0h,1p) VU-MRCC method.

$$Ag^{+} + e \rightarrow Ag$$

The ionization potential (IP) and excitation energies (EE) of Ag are compared with other correlated calculations [54, 55] and with recommended data from National Institute of Standards and Technology (NIST) database [56] in Table 3.2. The IP of Ag was computed by Neogrady *et al.* [54] using CCSD(T) method with spin-free Douglas-Kroll [57] (DK) orbitals whereas Safronova *et al.* [55] employed relativistic spinors in their IP and EE calculations using third order MBPT method. As can be seen in Table 3.2, the ionization potential computed using the CCSD(T) method with DK orbitals is more accurate (off by 683 cm^{-1}) than that obtained from third order MBPT calculations with relativistic spinors (off by 2737 cm^{-1}). This effectively indicates that higher order correlation contribution is quite significant in IP calculations for this system. It is also evident from Table 3.2 that the relativistic effect is non-negligible for Ag. The IP computed using (0h,1p) VU-MRCC with Dirac-Fock orbitals is off by only 283 cm^{-1} (or 0.4%) and is in much better agreement with experiment than the other two calculations mentioned above. The present calculations also provide reasonably accurate estimate of the EEs and fine-structure splittings (FSs) for Ag than the MBPT(3) estimates.

The errors in our estimated excitation energies are 227 cm^{-1} (or 0.5%) for the $^2S_{1/2}$ state, 205 cm^{-1} (or 0.7%) for the $^2P_{1/2}$ state, 167 cm^{-1} (or 0.5%) for the $^2P_{3/2}$ state, 232 cm^{-1} for the $^2D_{3/2}$ state, and 231 cm^{-1} (or 0.5%) for the $^2D_{5/2}$ state. The oscillator strengths (f) for $5s \rightarrow 5p$ transitions are also displayed in Table 3.2. Since our estimated transitions energies are quite accurate, we believe that our predicted oscillator strengths will be in good agreement with experiment.

Table 3.2: *Ionization potential (IP) and excitation energies (EE) of Ag (in cm^{-1}), computed using VU-MRCC method. Entrees within parentheses are oscillator strengths.*

Property	State	VU-MRCC [48]	MBPT(3) [55]	CCSD(T) [54]	Expt. [56]
IP	$5s_{1/2}(^2S_{1/2})$	60823	58369	60423	61106
EE	$6s_{1/2}(^2S_{1/2})$	42329			42556
	$6p_{1/2}(^2P_{1/2})$	29757	28073		29552
		(0.2467)	(0.2497)		
	$6p_{3/2}(^2P_{3/2})$	30639	28946		30472
		(0.5024)	(0.5134)		
Interval		882	873		920
	$5d_{3/2}(^2D_{3/2})$	48512	46082		48744
	$5d_{5/2}(^2D_{5/2})$	48533	46104		48764
Interval		21	22		20

3.5.2 Computation of ionization potentials of Hg via (1h-0p) VU-MRCC: one electron detachment process

In this section, we will present the ground and excited state properties of Hg using VU-MRCC method with four component Dirac-Fock orbitals. The accurate estimation of electric quadrupole moment Θ of Hg^+ is important as it can be used as possible frequency standards to test the stability of fundamental constants. In fact, the transition frequency $\nu_{\rm Hg}$ at 282 nm of $^{199}Hg^+$, arising from the $5d^{10}6s(^2S_{1/2}, F = 0, m_F = 0) \leftrightarrow 5d^96s^2(^2D_{5/2}, F = 2, m_F = 0)$ electric quadrupole transitions, is now being compared [58] with the frequency $\nu_{\rm Cs}$ arising from the hyperfine transition $[Xe]6s(^2S_{1/2}, F = 3, m_F = 0) \leftrightarrow [Xe]6s(^2S_{1/2}, F = 4, m_F = 0)$ in the ground state of neutral Cs, to test the stability of the product of fundamental constants $g_{\rm Cs}(m_e/m_p)\alpha$, where g is the nuclear g-factor, (m_e/m_p) the electron-to-proton mass ratio and α is the fine-structure constant.

Here, we employ (1h-0p) VU-MRCC method to compute the electric quadrupole moment of Hg^+. Since the electric quadrupole shift is zero in the $5d^{10}6s(^2S_{1/2})$ state, the electric quadrupole shift of the $5d^96s^2(^2D_{5/2})$ state alone determines the

shift of the Hg^+ optical clock transition. To our knowledge, only two theoretical calculations on quadrupole moment of Hg^+ are available in the literature. The first one is the single reference Hartree-Fock (HF) calculation of Itano [60] and the other is multi-configuration Dirac Hartree-Fock (MCDHF) calculation of Oskay *et al.* [61]. The HF calculation estimates the quadrupole moment for the ($^2D_{5/2}$) state of Hg^+ to be Θ=-0.664 ea_0^2, whereas the MCDHF calculation predict Θ=-0.544 ea_0^2 (a_0 is the Bohr radius). Though MCDHF estimates Θ better than HF, it is still $\sim$ 7% larger than experimental value (Θ=-0.510 ea_0^2) [61]. The accurate estimation of magnetic dipole hyperfine matrix element A for the $5d^96s^2(^2D_{5/2})$ state of Hg^+ is also a non-trivial problem. For instance, using MCDHF with limited configuration state functions, Brage *et al.* [62] obtain A to be 1315 MHz for this state. On the other hand, employing larger configuration space, Oskay *et al.* [61] obtain a value for A to be 963.5 MHz which is 22.5 MHz lower than experimental value (986.19 MHz) [60].

The ground and excited state properties of Hg and its positive ion are computed with two sets of basis functions to investigate the convergence of the computed properties. The first basis set (Basis I) is constructed from $34s32p30d20f15g$ GTOs. To this set $10h$ GTOs are added to construct the second basis set (Basis II). Since the contribution from high lying unoccupied are not significant [63, 64], these orbitals kept frozen in CC calculations.

The IPs of Hg computed using VU-MRCC method with Dirac-Coulomb Hamiltonian are compared with experimental results in Table 3.3. It is worth mentioning that the Breit interaction is not included in the present calculations. We have also quoted the results of Eliav *et al.* [65] where they have used the same method with Dirac-Coulomb-Breit Hamiltonian. As can be seen in Table 3.3, the IPs computed for $5d^{10}6s$ and $5d^96s^2$ states by Eliav *et al.* [65] are closer to experimental values than those obtained by us. Since the basic formalism and working equations of Eliav *et al.* [65] and ours are same, we feel that the difference in the estimated IPs may arise due to the absence of Breit interaction in our calculations. Although

Table 3.3: *Ionization potential (IP) of ^{199}Hg and excitation energies (EE) of its positive ion. All entrees are in cm^{-1}.*

Property	Config.	State	VU-MRCC [48] Basis I	VU-MRCC [48] Basis II	AERCC [65]	Expt. [59]
IP						
	$5d^{10}6s$	$^2S_{1/2}$	83895	83894	84237	84184
EE						
	$5d^{10}6s$	$^2S_{1/2}$	0	0		0
	$5d^96s^2$	$^2D_{5/2}$	33506	33506	35437	35514
		$^2D_{3/2}$	48622	48622	50785	50552
Interval			15116	15116	15348	15038
	$5d^{10}6p$	$^2P_{1/2}$	52792	52780	52030	51485
		$^2P_{3/2}$	61607	61594	61269	60608
Interval			8814	8814	9239	9123

Table 3.4: *Electric quadrupole moment Θ (in ea_0^2) and magnetic hyperfine matrix elements A (in MHz) for the $5d^96s^2(^2D_{5/2})$ state of $^{199}Hg^+$.*

Constant	VU-MRCC [48] Basis I	VU-MRCC [48] Basis II	HF [60]	MCDHF [61]	Experiment
Θ	-0.527	-0.527	-0.664	-0.544	-0.510 [61]
$A^s_{1/2}$	40440	40464			40507 [58]
$A^d_{3/2}$	2713	2720			
$A^d_{5/2}$	972	972		963.5	986.19 [60]

the ^2P fine structure splitting is better reproduced in their [65] calculations, our present calculation represents a more accurate estimate of the ^2D fine structure splitting.

We now discuss the quadrupole moment results for $^2D_{5/2}$ state, displayed in Table 3.4. The large deviation in Itano's predicted Θ value for Hg^+ primarily arises due to the neglect of electron correlation in the calculation. The importance of electron correlation is also evident from the MCDHF calculation of Oskay *et al.* [61] which shows that the electron correlation contribution to Θ is $\sim 25\%$. Such a huge correlation effect is, however, difficult to incorporate via MCDHF scheme

or even through finite order many-body perturbation theory (MBPT) [66]. In fact, CC is the most suitable scheme for such problem. Being an all-order approach, it can incorporate higher order electron correlation and relaxation effects more efficiently than the finite order MBPT method. Our calculation estimates the quadrupole moment for the $^2D_{5/2}$ state of Hg^+ to be Θ=-0.527 ea_0^2 which is the most accurate estimate of Θ for the $^2D_{5/2}$ state of Hg^+, to our knowledge. The magnetic hyperfine matrix elements A reported for Hg^+ are also in agreement with experiment. The present calculations further show that contribution of h orbitals to IP, A and Θ of Hg and its positive ion is negligible.

Bibliography

[1] G. Dujardin, S. Leach, O. Dutvit, P. M. Guyan and M. Richard-Viard, Chem. Phys. **88**, 339 (1984); P. Pianetta and I. Lindau, J. Elect. Spect. Rel. Phenom. **11**, 13 (1977); T. Sagawa, R. Kato, S. Sato, M. Watanbe, T. Ishi, I. Nagakura, S. Kono and S. Sujuki, J. Elect. Spect. Rel. Phenom. **5**, 551 (1974); K. Thimn, J. Elect. Spect. Rel. Phenom. **5**, 755 (1974).

[2] K. D. Jordon and P. D. Burrow, Chem. rev. **87**, 557 (1987).

[3] J. C. Slater, *in Quantum Theory of Matter*, (McGraw Hill N.Y. 1968); J. A. Pople and M. D. Newton, Radom L *in Modern Theoretical Chemistry*, edited by H. Schaeffer III, Vol. 4, (Plenum Press N. Y. 1977).

[4] J. Schirmer, L. S. Cederbaum, W. Domcke and W. von Niessen, Chem. Phys. Lett. **26**, 149 (1977).

[5] F. Coester, Nucl. Phys. **7**, 421 (1958); F. Coester and H. Kümmel, Nucl. Phys. **17**, 477 (1960); J. $\check{C}\acute{i}\check{z}$ek, J. Chem. Phys. **45**, 4256 (1966); Adv. Chem. Phys. **14**, (1969) 35; J. $\check{C}\acute{i}\check{z}$ek and J. Paldus, Adv. Chem. Phys. **9**, 105 (1975); R. J. Bartlett and W. D. Silver, Int. J. Quantum Chem. **S9**, 183 (1975); R. J. Bartlett, Ann. Rev. Phys. Chem. **32**, 359 (1981); R. J. Bartlett, J. Phys. Chem. **93**, 1697 (1989); in *Modern Electronic Structure Theory* (1995), edited by D. R. Yarkony, (World Scientific, Singapore).

[6] G. Hose and U. Kaldor, J. Phys. Chem. **86**, 2133 (1982).

[7] B. Jeziorski and H. J. Monkhorst, Phys. Rev. A **24**, 1668 (1981); B. Jeziorski and J. Paldus, J. Chem. Phys. **88**, 5673 (1988); J. Paldus, J. Pylypow and B. Jeziorski, in *Quantum Chemistry, Lecture Notes in Chemistry*, (1989), edited by U. Kaldor, Springer, Berlin, Vol. 52; A. Balkova, S. A. Kucharski, L. Meissner and R. J. Bartlett, Theor. Chim. Acta. **80**, 335 (1991); S. A. Kucharski, A. Balkova, P. G. Szalay and R. J. Bartlett, J. Chem. Phys. **97**, 4289 (1992).

[8] D. Mukherjee, R. K. Moitra and A. Mukhopadhyay, Mol. Phys. **30**, 1861 (1975); **33**, 955 (1977); Pramana **12**, 203 (1979).

[9] I. Lindgren and D. Mukherjee, Phys. Rep. **151**, 93 (1987); D. Mukherjee and S. Pal, Adv. Quantum Chem. **20**, 561 (1989).

[10] D. Mukherjee, Pramana **12**, 203 (1979).

[11] I. Lindgren, Int. J. Quantum Chem. **S12**, 33 (1978).

[12] A. Haque and D. Mukherjee, J. Chem. Phys. **80**, 5058 (1984).

[13] W. Kutzelnig, J. Chem. Phys. **77**, 3081 (1982); **80**, 822 (1984).

[14] D. Sinha, S. K. Mukhopadhyay and D. Mukherjee, Chem. Phys. Lett. **129**, 369 (1986); S. Pal, M. Rittby, R. J. Bartlett, D. Sinha and D. Mukherjee, Chem. Phys. Lett. **137**, 273 (1987); J. Chem. Phys. **88**, 4357 (1988); S. K. Mukhopadhyay, R. K. Chaudhuri, D. Mukhopadhyay and D. Mukherjee, Chem. Phys. Lett. **173**, 181 (1990); M. Musial and R. J. Bartlett, J. Chem. Phys. **121**, 1670 (2004).

[15] A. Haque and U. Kaldor, Chem. Phys. Lett. **120**, 261 (1989); S. Pal, M. Rottby and R. J. Bartlett, Chem. Phys. Lett. **160**, 212 (1989).

[16] H. J. Monkhorst, Int. J. Quantum Chem. **S11**, 421 (1977).

[17] D. Mukherjee and P. K. Mukherjee, Chem. Phys. **39**, 325 (1979); B. Datta, P. Sen and D. Mukherjee, J. Phys. Chem. **99**, 6441 (1995).

[18] H. Nakatsuji and K. Hirao, J. Chem. Phys. **68**, 2053 (1978); H. Nakatsuji, Chem. Phys. Lett. **59**, 362 (1978); **67**, 329 (1979); H. Nakatsuji, Computational Chemistry-Review of Current Trends (World Scientific, Singapore, 1997).

[19] H. Sekino and R. J. Bartlett, Int. J. Quantum Chem. **S18**, 255 (1984); J. F. Stanton and R. J. Bartlett, J. Chem. Phys. **98**, 7029 (1993).

[20] D. Mukhopadhyay, S. Mukhopadhyay, R. K. Chaudhuri and D. Mukherjee, Theor. Chim. Acta. **80**, 441 (1991).

[21] J. D. Watts and R. J. Bartlett, Chem. Phys. Lett. **233**, 81 (1995); **258**, 581 (1996).

[22] M. Nooijen and R. J. Bartlett, J. Chem. Phys. **106**, 6441 (1997); M. Nooijen and R. J. Bartlett, J. Chem. Phys. **107**, 6812 (1997).

[23] T. H. Schucan and H. A. Weidenmüller, Ann. Phys. **73**, 108 (1972); G. Hose and U. Kaldor, J. Phys. B **12**, 3827 (1979).

[24] D. Sinha, S. K. Mukhopadhyay and D. Mukherjee, Chem. Phys. Lett. **129**, 369 (1986).

[25] S. Ghosh, D. Mukherjee and S. N. Bhattacharyya, Chem. Phys. **72**, 1611 (1982); Mol. Phys. **43**, 173 (1981).

[26] S. S. Adnan, S. N. Bhattacharyya and D. Mukherjee, Mol. Phys. **39**, 519 (1982); Chem. Phys. Letts **85**, 204 (1982).

[27] S. Mukhopadhyay, D. Sinha, M. D. Prasad and D. Mukherjee, Chem. Phys. Lett. **117**, 437 (1985).

[28] D. Mukhopadhyay and D. Mukherjee, Chem. Phys. Lett. **163**, 171 (1989); *ibid.* **177**, 441 (1991).

[29] R. K. Chaudhuri, B. Kundu, K. Das and D. Mukherjee, Int. J. Quantum Chem. **60**, 347 (1996).

[30] D. Sinha, S. Mukhopadhyay, R. K. Chaudhuri and D. Mukherjee, Chem. Phys. Lett. **154**, 544 (1989).

[31] B. Datta, R. K. Chaudhuri and D. Mukherjee, J. Mol. Structure (Theochem), **361**, 21 (1996).

[32] C. E. Brion, S. T. Hood, I. H. Suzuki, E. Weigold and G. R. Williams, J. Electron Spectroscopy **21**, 71 (1980).

[33] S. Daviel, Y. Iida, F. Carnovale and C. E. Brion, Chem. Phys. **83**, 391 (1984).

[34] M. Y. Adam, Chem. Phys. Lett. **128**, 280 (1986).

[35] M. Y. Adam, Phys. Scr. **35**, 477 (1987).

[36] S. Svensson, L. Karlsson, P. Baltzer, B. Wannberg, U. Gelius and M. Y. Adam, J. Chem. Phys. **89**, 7193 (1988).

[37] W. von Niessen, P. Tomasello, J. Schirmer, L. S. Cederbaum, R. Cambi, F. Tarantelli and A. Sgamellotti, J. Chem. Phys. **89**, 7193 (1988).

[38] W. von Niessen, P. Tomasello, J. Schirmer and L. S. Cederbaum, Aust. J. Phys. **39**, 687 (1986).

[39] P. Tomasello, J. Chem. Phys. **87**, 7148 (1987); P. Tomasello and W. von Niessen, Mol. Phys. **69**, 1043 (1990).

[40] H. Nakatsuji and K. Hirao, J. Chem. Phys. **68**, 2053 (1978).

[41] H. Nakatsuji, Chem. Phys. Lett. **59**, 362 (1978); *ibid.* **67**, 329 (1979), *ibid.* **67**, 334 (1979).

[42] H. Nakatsuji, *Computational Chemsitry, Reveiw of Current Trends*, Vol. 2, (World Scientific, Singapore, 1997), p. 62.

[43] H. Nakatsuji, Chem. Phys. Lett **177**, 331 (1991).

[44] H. Nakatsuji, J. Chem. Phys. **83**, 731 (1985); **83**, 5743 (1985); **94**, 6716 (1991).

[45] D. E. Woon and T. H. Dunning, J. Chem. Phys. **98**, 1358 (1993).

[46] T. H. Dunning, J. Chem. Phys. **53**, 2823 (1970); T. H. Dunning and P. J. Hay, in *Modern Theoretical Chemistry*, Vol. 3, edited by H. F. Schaefer Ed.; (Plenum Press, New York, 1976).

[47] M. Ehra, P. Tomasello, J. Hasegawa and H. Nakatsuji, Theor. Chem. Acta. **102**, 161 (1999).

[48] M. K. Nayak, R. K. Chaudhuri, S. Chattopadhyay and U. S. Mahapatra, Theochem, (submitted).

[49] E. Eliav and U. Kaldor, Phys. Rev. A **53**, 3050 (1996).

[50] J. Sucher, Int. J. Quantum Chem. **24**, 3 (1984).

[51] J. D. Morgan, *New Methods in Quantum Theory*, Vol. 8, edited by C. A. Tsipis, V. S. Popov, D. R. Herschback and J. S. Avery *High Technology NATO ASI Series, Vol. 3*, (Dordrecht, Kluwer), p. 311.

[52] K. G. Dyall and K. Faegri, Chem. Phys. Lett. **201**, 27 (1993).

[53] F. A. Paripa, J. Phys. B **31**, 1409 (1998).

[54] P. Neogrady, V. Kellö, M. Urban and A. J. Sadlej, Int. J. Quantum Chem. **63**, 557 (1997).

[55] U. L. Safronova, I. M. Savukov, M. S. Safronova and W. R. Johnson, Phys. Rev. A **68**, 062505 (2003).

[56] C. E. Moore, in *Atomic Energy Level* (NBS Data Series), U. S. Govt. Printing Office, (Washington, D.C., 1971).

[57] B. Hess, Phys. Rev. A, **33**, 3742 (1986).

[58] S. Bize, S. A. Diddams, U. Tanaka, C. E. Tanner, W. H. Oskay, R. E. Drullinger, T. E. Parkar, T. P. Heavner, S. R. Jefferts, L. Hollberg, W. M. Itano and J. C. Bergquist, Phys. Rev. Lett. **90**, 150802 (2003).

[59] W. C. Martin, R. Zalubas and L. Hagan, in *Atomic Energy Levels-The Rare-Earth Elements*, Natl. Bur. Standards, (Washington, D.C., 1978).

[60] W. M. Itano, J. Res. Natl. Inst. Stand. Technol. **105**, 829 (2000).

[61] W. H. Oskay, W. M. Itano and J. C. Bergquist, (preprint).

[62] T. Brage, C. Proffitt and D. S. Leckrone, Astrophys. J. **513**, 524 (1999).

[63] U. Kaldor, J. Chem. Phys. **87**, 4676 (1987); *ibid.* **87**, 4693 (1987).

[64] R. K. Chaudhuri, B. K. Sahoo, B. P. Das, H. Merlitz, U. S. Mahapatra and D. Mukherjee, J. Chem. Phys. **119**, 10633 (2003).

[65] E. Eliav, U. Kaldor, Phys. Rev. A **52**, 2765 (1995).

[66] R. K. Chaudhuri and K. F. Freed, J. Chem. Phys. **122**, 204111 (2005).

Chapter 4

Application of Coupled Cluster method for two-valence problems

4.1 Introduction

In the previous chapter, we have discussed and applied the core-valence extensive, valence universal multi-reference coupled cluster (VU-MRCC) method [1, 2, 3, 4, 5, 6, 7, 8] and core-extensive, coupled cluster based linear response theory (CCLRT) [9, 10, 11, 12, 13] to the typical one-valence problems such as ionization potential and electron affinity computations. Since for one-valence problem there is no valence-valence interaction, the core-valence extensive and core-extensive theories are formally equivalent. As the valence-valence interaction is nonzero for two-valence and higher-valence problems, the equivalency among these two classes of theories holds good only for one-valence problem. In this chapter, we have selected to study the hole-particle excitation (1h-1p), double ionization (2h-0p) and double electron attachment (0h,2p) processes, which are typical examples of two-valence problems.

Among these two valence processes, the electronic transition phenomenon involved in the excitation process is one of the oldest problems tackled by spectroscopists and still remains one of the most widely studied subject for experimen-

talists and theoreticians. The emergence of high resolution probes such as XAFS, XANES [14] and high resolution laser spectroscopy [15] etc. have also widened the scope and range of applications of electronic transition spectroscopy.

The double ionization or the Auger process has also been a subject of interest to theoretician and experimentalists. The Auger process is a radiation less reorganization process [16] produced by the electron impact, synchrotron radiation, double charge transfer, or charge stripping spectroscopy. In this process, core-hole is created, and the core ionized state eventually reorganizes its electron whereby the core-vacancy is filled by the higher lying electron with a simultaneous ejection of the valence electron. The final state thus becomes a doubly ionized state, and the kinetic energy of the ejected "Auger" electron is a measure of the double IPs of the molecule/atom. Being a property of the system, an estimate of the kinetic energies offers valuable insight about the electronic environment of the system and is a property of chemical interest.

The double electron attachment scheme is primarily developed to study the excited states of the systems whose ground state is open-shell. For instance, Kaldor *et al.* [17] and Nayak *et al.* [18] employed the two electron attachment processes to compute the transition energies of heavy elements. Kaldor *et al.* [19] have also employed this technique to study the stability of negative ions of heavy elements.

We recall that for more than one valence occupancies in the model functions, we have the option of maintaining size-extensive either (a) with respect to the core electrons, whose total number N_c usually far exceeds those in the valence space, N_v; or (b) with respect to N_c and N_v separately. The former choice leads to the core-extensive formalisms while the later leads to core-valence extensive formalisms. Just as in the last chapter, we shall use CCLRT and VU-MRCC to study excitation, double ionization and double electron attachment processes.

4.2 Valence universal multi-reference CC method for two valence problems

In the last chapter, we have presented the general structure of VU-MRCC equations for general model space. In this chapter, we shall derive the VU-MRCC equations for (0h-2p) and (2h-0p) valence space from the generalized Fock-space Bloch equations.

4.2.1 Two-electron detachment process

The reference functions for the two-electron detached states $\Phi_{\text{ref}}^{(2,0)}$ are generated from a appropriate combination of spin-adapted functions $\Phi_{\alpha\beta}$ with $(N_c - 2)$ number of electrons as

$$|\Phi_{\text{ref}}^{(2,0)}\rangle = \sum_{\alpha\beta} C_{\alpha\beta}|\Phi_{\alpha\beta}\rangle \tag{4.1}$$

where

$$|\Phi_{\alpha\beta}\rangle = a_\alpha a_\beta |\Phi_{\text{ref}}^{(0,0)}\rangle. \tag{4.2}$$

Since the excited determinants are absent in the model space, the correlation displayed by the model space determinants is called the "non-dynamical correlation". The dynamical electron correlations are brought in by the cluster expansion induced by the valence universal wave operator Ω. To incorporate the dynamical correlation, we proceed as follows: The exact wave functions $\Psi^{(2,0)}$ are generated by the action of normal ordered valence universal wave operator Ω on the approximate two-hole valence functions $\Phi_{\text{ref}}^{(2,0)}$

$$\Psi^{(2,0)} = \Omega\Phi_{\text{ref}}^{(2,0)} \tag{4.3}$$

where

$$\Omega = \Omega_c\Omega_v \tag{4.4}$$

with

$$\Omega_c = \{\exp(S^{(0,0)})\} \equiv \exp(T) \tag{4.5}$$

and

$$\Omega_v = \{\exp(S_v)\}; \quad S_v = S^{(1,0)} + S^{(2,0)} \tag{4.6}$$

We arrive at the two valence problem hierarchically i.e., starting from (0h-0p) valence sector, we go on through (1h-0p) valence sector to (2h-0p) problem, following the Fock-space strategy depicted in Fig. 4.1. In this procedure, the cluster amplitudes $S^{(0,0)}$ of (0h,0p) valence sector are first solved using the closed shell CC equations. The cluster operator $S^{(1,0)}$ for (1h-0p) valence sector are then introduced to generate the function $\Psi^{(1,0)}$. The corresponding cluster amplitudes $S^{(1,0)}$ are determined by solving the (1h-0p) VU-MRCC equations as discussed in the previous chapter. For the two-hole valence situation, we write

$$S^{[2,0]} = S^{(2,0)} + S^{(1,0)} + ... \tag{4.7}$$

The new cluster amplitudes entering in (2h-0p) valence sector are $S^{(2,0)}$ with the cluster amplitudes $S^{(1,0)}$ frozen at their (1h-0p) valence level. Thus, the amplitudes of $S^{(2,0)}$ are the only new amplitudes in the two-hole valence VU-MRCC equations. We may generally write that for m-valence

$$S^{[m,0]} = S^{(m,0)} + S^{(m-1,0)} + ... \tag{4.8}$$

and for solving the $S^{(k,0)}$ amplitudes, $S^{(l,0)}$ with $l < k$ do not appear. Solutions of the various $(k,0)$ valence sectors are thus decoupled, which is the essence of the subsystem embedding condition (SEC) [3].

In actual applications, the cluster expansion of the reference function $\Phi_{\text{ref}}^{(2,0)}$ has to be truncated and depending upon the physics of the problem, $S^{(2,0)}$ has to be terminated after a certain electron rank. It can be shown that for a *complete model space* (CMS) under the two-body truncation scheme $S^{(2,0)}$ is simply equal to zero,

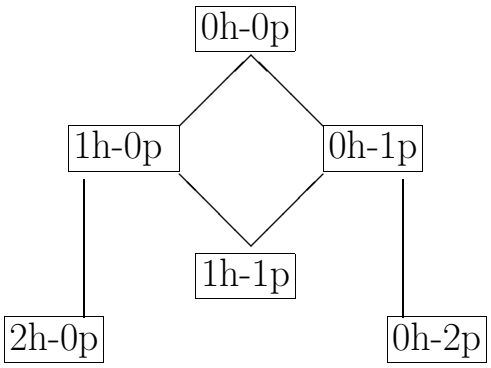

1

Figure 4.1: *Hierarchical generation of CC equations.*

and hence,

$$|\Psi_I^{(2,0)}\rangle = \exp(T)[1 + S^{(1,0)} + \frac{1}{2}S^{(1,0)}S^{(1,0)}]|\Phi_{ref}^{(2,0)}\rangle. \quad (4.9)$$

This implies that under the above approximation, no new cluster amplitudes enter in the VU-MRCC equations for Auger calculations. The general structure of the effective Hamiltonian $H_{eff}^{(2,0)}$ for two-hole model space is given by

$$P^{(2,0)}H_{eff}^{(2,0)}P^{(2,0)} = P^{(2,0)}\bar{H}P^{(2,0)} + P^{(2,0)}\bar{H}S^{(1,0)}P^{(2,0)} + \frac{1}{2}P^{(2,0)}\bar{H}S^{(1,0)}S^{(1,0)}P^{(2,0)} \quad (4.10)$$

with

$$\bar{H} = \tilde{H} + E_{gr} \quad (4.11)$$

and

$$\tilde{H} = \exp(-T)\, H_N \exp(T). \quad (4.12)$$

The normal ordered Hamiltonian H_N is defined as

$$H = H_N + \langle 0|H|0\rangle = H_N + E_{HF} \quad (4.13)$$

where, $|0\rangle$ is the vacuum.

4.2.2 Two-electron attachment process

In this section we present the (0h-2p) VU-MRCC scheme which we will use to compute the excitation energies of closed shell atoms like Sr and Yb. We emphasize that the determination of excitation energies via double electron attachment process is computationally simple provided the M^{+2} ion is closed shell or dominated by single reference function. In our VU-MRCC formulation for (0h-2p) valence sector, we will assume the reference state of M^{+2} ion as the (0-hole,0-particle) sector.

Two-electrons are then added to the correlated reference space state following the Fock-space strategy

$$M^{+2} + e \rightarrow M^{+1}$$

$$M^{+1} + e \rightarrow M$$

The unperturbed function $\Phi_{\text{ref}}^{(0,2)}$ for the double electron attached state can be expressed as

$$|\Phi_{\text{ref}}^{(0,2)}\rangle = \sum_{p,q} C_{pq} a_p^\dagger a_q^\dagger |\Phi_{\text{ref}}^{(0,0)}\rangle. \tag{4.14}$$

Following the same strategy as discussed above, the effective Hamiltonian operator for two-electron attachment process $H_{\text{eff}}^{(0,2)}$ can be written as

$$P^{(0,2)} H_{\text{eff}}^{(0,2)} P^{(0,2)} = P^{(0,2)} \bar{H} P^{(0,2)} + P^{(0,2)} \bar{H} S^{(0,1)} P^{(0,2)} + \frac{1}{2} P^{(0,2)} \bar{H} S^{(0,1)} S^{(0,1)} P^{(0,2)}. \tag{4.15}$$

Thus, for CMS, the excited energies for the neutral species can be determined with aid of $S^{(0,0)}$ and $S^{(0,1)}$ cluster amplitudes. We emphasize that in the procedure, valence electron removal energies are the by-products of this scheme with *no extra* cost. Some typical Goldstone diagrams for effective Hamiltonian $H_{\text{eff}}^{(0,2)}$ and $H_{\text{eff}}^{(0,1)}$ are depicted in Fig. 4.2.

4.3 Applications of CCLRT

4.3.1 Direct calculation of excitation energies of CuH via CCLRT: (1h-1p) valence problem

The ground state properties of CuH have been studied extensively by several research groups. For instance, Hrusak *et al.* [20] have studied the ground state potential energy surface of CuH using various CC scheme with Hartree-Fock orbitals. On the other hand, Marian [21] and Collins [22] employed spin-free Douglas-Kroll transformed Dirac Hamiltonian [23] and its variants in their calculations. Here, we investigate the ground state properties of CuH using CC method with Hartree-Fock orbitals. We also present the excited state energies computed with Hartree-Fock orbitals using CCLRT for EE problem at the singles-doubles level. The basis

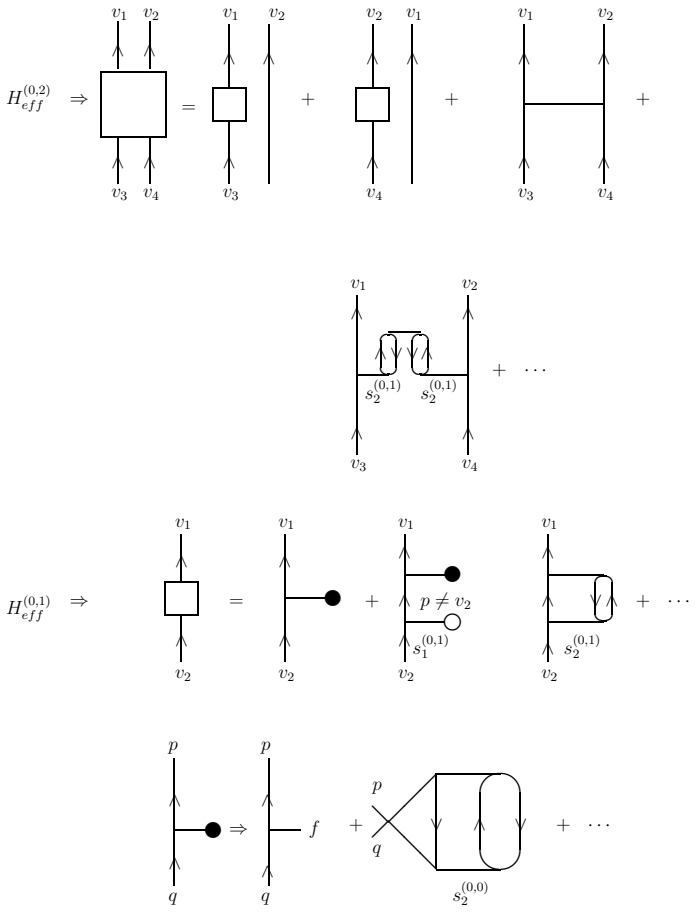

1

Figure 4.2: *Representative H_{eff} diagrams for (0,1) and (0,2) valence sector.*

set employed in this calculation is constructed from Roos's [24] (7s3p)/[3s2p] (for H) and (17s12p9d4f)/[7s7p4d2f] (for Cu) contraction scheme.

Fig. 4.3 depicts the ground and excited states potential energy curves (PECs) of CuH is computed using CC method (CCLRT for excited states). Here, we emphasize that the potential energy estimated from CC with perturbative triples CCSD(T) fails badly upon dissociation (not shown in figure). However, this type of behavior of the CCSD(T) potential curves near the bond breaking region is com-

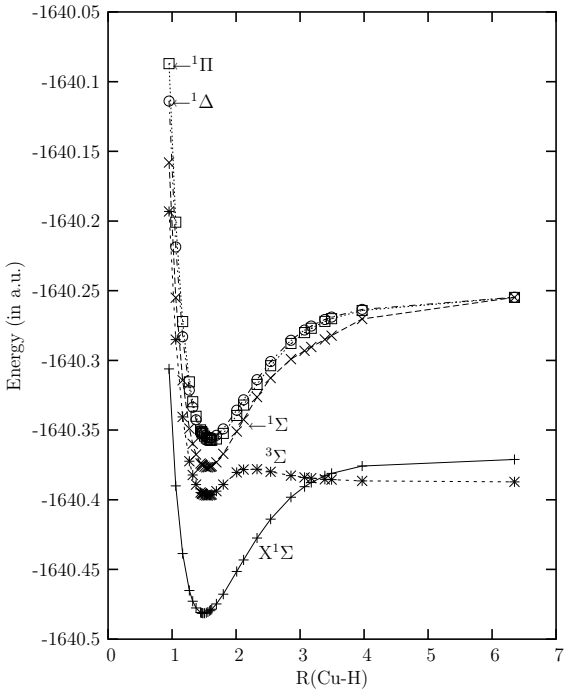

Figure 4.3: *Plot of the ground and excited states potential energy curves vs. inter-nuclear distance of CuH.*

Table 4.1: *Comparison of the equilibrium bond length r_e (in $\mathring{A}$), harmonic vibrational frequency ω (in cm^{-1}) and dissociation energy D_e (in eV) of CuH.*

Method/Experiment	r_e	ω	D_e
Experiment [25]	1.463	1941	2.75
SCF (Collins *et al.*) [22]	1.569	1642	1.42
DHF (Collins *et al.*) [22]	1.541	1699	1.48
DHF (Nakajima *et al.*) [26]	1.540	1715	1.45
DKS (Nakajima *et al.*) [26]	1.460	1928	2.86
HF-CCSD (Hrusak *at al.*) [20]	1.501	1814	2.48
HF-CC (Nayak *et al.*) [27]	1.492	1818	2.64

monly observed and appears even in the bond fragmentation of simple diatomic molecules. The spectroscopic constants for the ground state of CuH computed using the CC method are compared with experiment [25] and with other calculations [22, 26] in Table 4.1. It can be seen from the table that, the spectroscopic constants estimated by Nakajima *et al.* [26] through Douglas-Kohn-Sham approximation [28, 29] matches favorably well with experiment. The present HF-CC calculation produces quite accurate ground state dissociation energy but the equilibrium bond length and harmonic vibrational frequency deviates from experiment by 0.03$\mathring{A}$ and 123 cm^{-1}.

Though the CC calculations overestimate the equilibrium bond length and under estimates the vibrational frequency, it offers excellent estimate of excited state energies, summarized in Table 4.2. The vertical excitation energies of CuH are computed at the experimental geometry using CCLRT for EE problem with HF orbitals. As can be seen from Table 4.2, CCLRT-EE provides reasonable accurate estimate of low lying transition energies. The excitation energies computed using CCLRT-EE are off by 0.007 eV for $^1\Sigma$, 0.042 eV for $^3\Pi$ state. The experimental transition energy for $X^1\Sigma \rightarrow \Delta$ is $\sim$ 3.53 eV. According to the present calculation, the observed Δ state lying at 3.53 eV above the ground $X^1\Sigma$ state is $1^1\Delta$ state.

Table 4.2: *Vertical excitation energies (in eV) of CuH computed using CCLRT and experiment.*

State	CCLRT [27]	Expt. [25]
$1^3\Sigma$	2.338	
$1^1\Sigma$	2.899	2.905
$1^3\Pi$	3.207	3.275
$1^3\Delta$	3.315	
$1^1\Delta$	3.529	3.530
$1^1\Pi$	3.540	
$2^3\Sigma$	4.981	

4.4 Applications of VU-MRCC

4.4.1 Direct calculation of Auger energies of HCl via (2h-0p) VU-MRCC: two-electron detachment process

The Auger spectrum of HCl has been measured by Svensson *et al.* [30] and Aksela *et al.* [31]. Subsequent independent theoretical interpretations of the high kinetic energy region of HCl by Aksela [31] and Kvalheim [32] use direct CI and semi-internal CI. However, the CI (both direct and semi-internal) estimate is not so accurate for the Auger energies relative to the lowest lying doubly ionized $(2\pi)^{-2}(^3\Sigma^-)$ state. Except for the first excited doubly ionized state $(2\pi)^{-2}(^3\Sigma^-)$, the computed CI Auger energies deviate substantially (by 0.3 eV or more) from experiment.

An aug-CC-PVTZ basis comprised 84 GTOs is employed for the double IP and Auger energies computations. The basis used for Cl atom is constructed from the (15s9p2d1f)/[5s4p2d1f] GTOs of Woon and Dunning [33] augmented with one $s(\zeta_s = 0.0591)$, one $p(\zeta_p = 0.0419)$, one $d(\zeta_d = 0.135)$ and one $f(\zeta_f = 0.312)$ diffuse function. Similarly, for the H atom, the (5s2p1d)/[3s2p1d] GTOs basis of Dunning [34] is augmented by one $s(\zeta_s = 0.02526)$, one $p(\zeta_p = 0.102)$ and one $d(\zeta_d = 0.247)$ diffuse function. All the calculations are performed at $R_{HCl} = 1.2746$ Å.

Table 4.3: *Comparison of relative Auger energies with respect to the lowest lying doubly ionized $(2\pi)^{-2}(^3\Sigma^-)$ state (in eV) of HCl, obtained from VU-MRCC calculations, with experiment and other correlated calculations.*

Assignment	SDCI [32]	VU-MRCC[27]	Expt. [30, 31]
$(2\pi)^{-2}(^3\Sigma^-)$	0.0	0.0	0.0
$(2\pi)^{-2}(^1\Delta)$	1.6	1.54	1.48
$(2\pi)^{-2}(^1\Sigma^+)$	3.0	2.53	2.75
$(2\pi 5\sigma)^{-1}(^3\Pi)$	3.9	3.67	3.29
$(2\pi 5\sigma)^{-1}(^1\Pi)$	5.5	5.34	
$(5\sigma)^{-2}(^1\Sigma^+)$	10.6	10.25	9.70

The Auger energies of HCl are computed using VU-MRCC method via eigenvalue independent partitioning (EIP) technique [35]. In this approach, the CCLRT for IP problem is first solved followed by the generation of $S^{(1,0)}$ cluster amplitudes from CCLRT-IP eigenvectors via EIP procedure. The effective Hamiltonian H_{eff} for (2,0) valence sector is then constructed (using the $S^{(1,0)}$ cluster amplitudes) and diagonalized to get the desired roots. The Auger energies of HCl relative to its lowest lying doubly ionized state $(2\pi)^{-2}(^3\Sigma^-)$ state are shown in Table 4.3. The VU-MRCC calculations for the $(5\sigma)^{-2}(^1\Sigma^+)$ transition energy (with respect to the lowest lying $(2\pi)^{-2}(^3\Sigma^-)$ state) is, however, not as accurate as the rest of the states, but this deficiency is also present for semi-internal CI calculations [32].

4.4.2 Computation of excitation energies of Sr and Yb via (0h-2p) VU-MRCC: two-electron attachment process

The accurate estimation of transition energies and nuclear magnetic dipole hyperfine constants for singly ionized metal ions, such as Sr^+ and Yb^+ is important because these atoms can be used in cold traps as possible frequency standards. For instance, an optical frequency standard based on Sr^+ has recently been developed at the National Physical Laboratory [36, 37]. In addition, calculations of the hyperfine coupling constant are relevant to studies of parity non-conservation in

atoms because the electro-weak interaction is also a short range force like those determining the hyperfine coupling constant. However, the theoretical determination of the hyperfine coupling constant is, probably, one of the most non-trivial problems in atomic physics because an accurate prediction requires precise incorporation of the strongly entangled relativistic and higher order correlation and relaxation effects.

The ground and excited state properties of Sr, Yb and their positive ions are computed using $37s33p28d12f5g$ GTOs with $\alpha_0 = 0.00525$ and $\beta = 2.73$. [High lying unoccupied orbitals are kept frozen in VU-MRCC calculations.] Table 4.4 compares our computed first ionization potential (FIP) and low lying excitation energies (EEs) of Sr and Yb atoms with experimental data [38, 39, 40]. As can be seen from Table 4.4, the VU-MRCC ionization potentials for Sr and Yb atoms are in excellent agreement with experiment (off by 28 cm^{-1} for Sr and 111 cm^{-1} for Yb).

The reference space for excitation energy calculations is constructed by allocating $5s$ ($6s$) valence electrons of Sr (Yb) among $5s6s7s5p6p4d5d$ ($6s7s8s6p7p5d6d$) valence orbitals in all possible ways. The computed VU-MRCC excitation energies for the low lying states of Sr atom are in agreement with experiment except for the $^1P_1$ state of Sr. The maximum error in the estimated excitation energy for Sr is only 71 cm^{-1} (or 0.47%) for the $^3P_2(5s5p)$ state. The present calculation using VU-MRCC method also provides a fairly accurate estimates of the $^1S_0(5s^2) \rightarrow {}^3P_0(5s5p)$, $^1S_0(5s^2) \rightarrow {}^3P_1(5s5p)$, $^1S_0(5s^2) \rightarrow {}^1S_0(5s6s)$, and $^1S_0(5s^2) \rightarrow {}^3S_1(5s6s)$ transition energies, which deviates by 6, 31, 60, and 70 cm^{-1}, respectively, from experiment. Compared to S and P states, our computed excitation energies for $^1P_1$ state and $s \rightarrow d$ transitions are not so accurate for Sr atom. The errors in our estimated transition energies for the D states of Sr are off by 1.8%. It is evident from Table 4.4 (also from Tables 3 and 4 of Ref. [41]) that accurate estimate of $s \rightarrow p$ ($^1P_1$) transition energy is quite problematic. Inclusion of low lying f orbitals in the reference space is probably necessary to improve

Table 4.4: *First ionization potential (FIP), low lying excitation energies (EE) and fine structure splittings (FS) of Sr and Yb atoms. All entrees are in* cm^{-1}.

Atom	Propetry	State	VU-MRCC[18]	CC [41]	Expt. [38, 40]
Sr	FIP		45954		45926
	EE				
		$[Kr]5s^2(^1S_0)$	0		0
		$[Kr]5s5p(^3P_0)$	14333		14327
		$[Kr]5s5p(^3P_1)$	14547		14514
	FS		214		187
		$[Kr]5s5p(^3P_2)$	14969		14898
	FS		422		384
		$[Kr]5s4d(^3D_1)$	17839		18159
		$[Kr]5s4d(^3D_2)$	17879		18219
	FS		40		60
		$[Kr]5s4d(^3D_3)$	17957		18319
	FS		78		100
		$[Kr]5s5p(^1P_1)$	22634		21698
		$[Kr]5s6s(^3S_1)$	28978		29038
		$[Kr]5s6s(^1S_1)$	30522		30592
Yb	FIP		50552	51142	50441
	EE				
		$4f^{14}6s^2(^1S_0)$	0		0
		$4f^{14}6s6p(^3P_0)$	17576	17346	17288
		$4f^{14}6s6p(^3P_1)$	18424	18082	17992
	FS		848	736	704
		$4f^{14}6s6p(^3P_2)$	20218	19847	19710
	FS		1794	1765	1718
		$4f^{14}5d6s(^3D_1)$	25865	24981	24489
		$4f^{14}5d6s(^3D_2)$	25966	25229	24751
		$4f^{14}5d6s(^3D_3)$	26125	25735	25270
		$4f^{14}6s7s(^3S_1)$	32967		32695
		$4f^{14}6s7s(^1S_0)$	34932		34351

the accuracy of $^1P_1$ (also D) state energies. However, this is not considered here because of computational complexity.

The ionization and low excitation energies of Yb are also reasonably close to experiment but are not as accurate as those obtained for Sr atom from VU-MRCC method. The earlier CC calculation by Eliav *et al.* [41] estimates the FIP of Yb to be 51142 cm^{-1}, which is off by 732 cm^{-1} from experiment. Like Sr, the transition energies of Yb for ^3S and ^3P states are more accurately reproduced than the D states by VU-MRCC method. At this juncture, we emphasize that similar trend is also observed by Eliav *et al.* in their CC calculations for Yb, Ba and Ra atom [17, 41].

Based on our Sr and Sr$^+$ calculations (see Fig. 4.4), we feel that the correlation contribution to the transition energies from orbitals with $l \geq 5$ will be non-negligible for Yb (l is the orbital angular momentum). Thus, we believe that the inaccuracy in our computed transition energies of Yb mainly arises due to the basis set inadequacy. The absence of Breit interaction in our calculations is also partly responsible for the inaccuracy and efforts are underway to enable including these effects.

Table 4.5 compares the VU-MRCC calculations for low lying valence electron ionization energies of Sr$^+$ and Yb$^+$ with other correlated calculations [42, 43, 41, 44] and with experiment [38]. As can be seen in Table 4.5, the valence electron removal energies and associated fine structure splitting (labeled as FS) for Sr$^+$ and Yb$^+$ are well reproduced in the present calculations. A careful analysis indicates that, for Sr$^+$ ion, only the [Kr]5p valence electron removal energy computed using VU-MRCC method is slightly poor (off by 129 cm^{-1}) compared to the Martensson's [43] estimate (off by 60 cm^{-1}), while the [Kr]5s valence electron removal energy and fine structure splittings (FS) are better reproduced in the present calculations. The FS in the present calculations are off by 4 and 7 cm^{-1} for $^2P_{1/2}(5p) \rightarrow {}^2P_{3/2}(5p)$ and $^2P_{1/2}(6p) \rightarrow {}^2P_{3/2}(6p)$ states of Sr$^+$, respectively.

We now compare the excitation energies of Yb and its positive ion reported by

Table 4.5: *Theoretical and experimental valence electron ionization energies and fine structure splittings (FS) of Sr^+ and Yb^+ ions. All entrees are in cm^{-1}.*

Ion	State	MBPT [42, 44]	CC [43, 41]	VU-MRCC[18]	Expt. [38, 40]
Sr^+					
	$5s(^2S_{1/2})$	89631	89126	88965	88964
	$5p(^2P_{1/2})$	65487	65309	65120	65249
	$5p(^2P_{3/2})$	64663	64499	64315	64448
FS		824	810	805	801
	$6s(^2S_{1/2})$			41079	41228
	$6p(^2P_{1/2})$			33096	33194
	$6p(^2P_{3/2})$			32801	32906
FS				295	288
Yb^+					
	$6s(^2S_{1/2})$	0		0	0
	$5d(^2D_{3/2})$	22888	23770	23179	23285
	$5d(^2D_{5/2})$	23549	25072	24342	24333
FS		661	1302	1163	1048
	$6p(^2P_{1/2})$	26000	27868	27664	27062
	$6p(^2P_{3/2})$	29005	31324	31037	30392
FS		3005	3456	3373	3330

Eliav *et al.* [41] with the present calculations. As can be seen in Tables 4.4 and 4.5 that, the excitation energies (also FS) of Yb are better reproduced than its positive ion state, in the calculations of Eliav *et al.* whereas the positive ion state energies of Yb are in better agreement in our present calculations. The EEs of Yb and Yb^+ in the present calculations are off by $\sim 2.75\%$ and $\sim 1.3\%$, respectively. On the other hand, EEs reported in Ref. [41] are off by $\sim 1.1\%$ (for Yb) and $\sim 3.2\%$ (for Yb^+) from experiment. This is quite interesting but is beyond the scope of the present approach to pinpoint the underlying reason of this trend.

The theoretically determined nuclear magnetic dipole and electric quadrupole hyperfine constants for the excited states of Sr^+ and Yb^+ are presented in Table 4.6. It can be seen from the table that our predicted nuclear magnetic dipole and electric quadrupole hyperfine constants A and B are in general agreement with

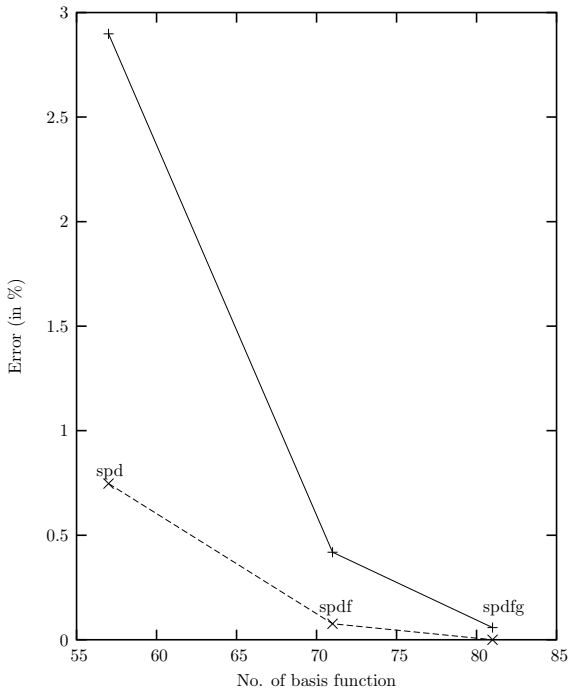

Figure 4.4: *Abs. error (in %) in the computed valence electron removal energy (×) and magnetic dipole hyperfine constant A (+) for the $^2S_{1/2}(5s)$ state of Sr^+ vs. number of basis functions.*

experiments. The nuclear magnetic dipole hyperfine constants reported here for $^2S_{1/2}$, $^2P_{3/2}$ and $^2D_{5/2}$ states of Sr^+ are off by 0.58, 1.20, and 0.5 MHz and are more accurate (on an average) than the previously reported A value [43]. Similar trend is also observed in our predicted B value for $^2D_{5/2}(4d)$ state, which is off by 2.0 MHz from experiment. We emphasize that unlike transition energies, accuracy of one-electron properties such as nuclear magnetic dipole hyperfine constants strongly depends on the choice of the basis set. Fig. 4.4 depicts the accuracy of A_{5s} and $^2S_{1/2}(5s)$ valence electron removal energy of Sr^+ against the size of the basis set. As can be seen in Fig. 4.4, the error in the computed A_{5s} value sharply drops from 3% to 0.5% when f orbitals are included in the basis set. The computed error decreases further (from 0.5% to 0.05%) when g orbitals are also included in the calculations. Since our computed transition energies and related properties (for Sr^+) are quite accurate, we strongly feel that our predicted A constants for

Table 4.6: *Magnetic dipole (A) and electric quadrupole hyperfine (B) constant (in MHz) of the ground and low lying excited states Sr^+ and Yb^+.*

Ion	Constant	State	CC [43]	VU-MRCC [18]	Expt. [45, 46]
Sr^+					
	A_{5s}	$(^2S_{1/2})$	1000.0	999.89	1000.47
	A_{5p}	$(^2P_{1/2})$	177.0	175.12	
	A_{5p}	$(^2P_{3/2})$	35.3	35.60	36.80
	A_{4d}	$(^2D_{5/2})$	1.0	1.87	2.17
	B_{4d}	$(^2D_{5/2})$	52.0	51.12	49.11
Yb^+					
	A_{6s}	$(^2S_{1/2})$		12386.20	
	A_{6p}	$(^2P_{1/2})$		2179.94	
	A_{6p}	$(^2P_{3/2})$		322.60	

Table 4.7: *Electric dipole matrix elements of low lying excited states of Sr^+ and Yb^+. Entrees with parentheses are semi-empirically adjusted values.*

Ion	Transition	Guet *et al.* [42]	Nayak *et al.* [18]
Sr^+			
	$5p_{1/2} \rightarrow 5s_{1/2}$	3.052 (3.060)	3.107
	$5p_{3/2} \rightarrow 5s_{1/2}$	4.313 (4.325)	4.392
Yb^+			
	$6p_{1/2} \rightarrow 6s_{1/2}$		2.781
	$6p_{3/2} \rightarrow 6s_{1/2}$		3.914

Yb^+ will also be in agreement with experiment.

The electric dipole (E1) transition matrix elements for the excited states of Sr^+ and Yb^+ are displayed in Table 4.7. It is evident from the table that, $\eta = \frac{\langle np_{3/2}|E1|ns_{1/2}\rangle}{\langle np_{1/2}|E1|ns_{1/2}\rangle}$ ($n = 5$ for Sr^+ and $n = 6$ for Yb^+) decreases as Z (nuclear charge) increases. [Note that for light atoms, the ratio $\frac{\langle np_{3/2}|E1|ns_{1/2}\rangle}{\langle np_{1/2}|E1|ns_{1/2}\rangle} \approx \sqrt{2}$]. Table 4.7 further shows that our estimated transition matrix elements and η for Sr^+ are reasonably close to those reported by Guet *et al.* [42]. We also belive that, our predicted values of transition matrix elements and η for Yb^+ are also quite reliable.

Bibliography

[1] D. Mukherjee, R. K. Moitra and A. Mukhopadhyay, Mol. Phys. **30**, 1861 (1975); **33**, 955 (1977); Pramana **12**, 203 (1979).

[2] I. Lindgren and D. Mukherjee, Phys. Rep. **151**, 93 (1987); D. Mukherjee and S. Pal, Adv. Quantum Chem. **20**, 561 (1989).

[3] D. Mukherjee, Pramana **12**, 203 (1979).

[4] I. Lindgren, Int. J. Quantum Chem. **S12**, 33 (1978).

[5] A. Haque and D. Mukherjee, J. Chem. Phys. **80**, 5058 (1984).

[6] W. Kutzelnig, J. Chem. Phys. **77**, 3081 (1982); **80**, 822 (1984).

[7] D. Sinha, S. K. Mukhopadhyay and D. Mukherjee, Chem. Phys. Lett. **129**, 369 (1986); S. Pal, M. Rittby, R. J. Bartlett, D. Sinha and D. Mukherjee, Chem. Phys. Lett. **137**, 273 (1987); J. Chem. Phys. **88**, 4357 (1988); S. K. Mukhopadhyay, R. K. Chaudhuri, D. Mukhopadhyay and D. Mukherjee, Chem. Phys. Lett. **173**, 181 (1990); M. Musial and R. J. Bartlett, J. Chem. Phys. **121**, 1670 (2004).

[8] A. Haque and U. Kaldor, Chem. Phys. Lett. **120**, 261 (1989); S. Pal, M. Rottby and R. J. Bartlett, Chem. Phys. Lett. **160**, 212 (1989).

[9] H. J. Monkhorst, Int. J. Quantum Chem. **S11**, 421 (1977); E. Dalgaard and H. J. Monkhorst, Phys. Rev. **A 28**, 1217 (1983).

[10] D. Mukherjee and P. K. Mukherjee, Chem. Phys. **39**, 325 (1979); B. Datta, P. Sen and D. Mukherjee, J. Phys. Chem. **99**, 6441 (1995).

[11] H. Nakatsuji and K. Hirao, J. Chem. Phys. **68**, 2053 (1978); H. Nakatsuji, Chem. Phys. Lett. **59**, 362 (1978); **67**, 329 (1979); H. Nakatsuji, Computational Chemistry-Review of Current Trends (World Scientific, Singapore, 1997).

[12] H. Sekino and R. J. Bartlett, Int. J. Quantum Chem. **S18**, 255 (1984); J. F. Stanton and R. J. Bartlett, J. Chem. Phys. **98**, 7029 (1993).

[13] D. Mukhopadhyay, S. Mukhopadhyay, R. K. Chaudhuri and D. Mukherjee, Theor. Chim. Acta. **80**, 441 (1991).

[14] XAFS and near edge structures: Eds. A. Biancon, L. Incoccia, and R. Stippich, (Springer-Verlag, 1983); Core-level Spectroscopy in condensed Physics: Eds. J. Kanomari and A. Kotani, (Springer-Verlag, 1988).

[15] M. D. Levinson, in *Introduction to non-linear laser spectroscopy*, (Acad. Press, N. Y. 1982); W. Y. Cheung and S. D. Colso, Adv. Laser Spectroscopy **2**, 73 (1983).

[16] E. H. S. Burhop, in *The Auger effect and other radiationless transitions*, (Camb. Univ. Press, London, 1952).

[17] E. Eliav and U. Kaldor, Phys. Rev. A **53**, 3050 (1996).

[18] M. K. Nayak and R. K. Chaudhuri, Eur. Phys. J. D, **37**, 171 (2006).

[19] E. Eliav, U. Kaldor, Ishikwa and P. Pyykko, Phys. Rev. Lett. **77**, 5350 (1996).

[20] J. Hrusak, S. Ten-no and S. Iwata, J. Chem. Phys. **106**, 7185 (1997).

[21] M. Marian, J. Chem. Phys. **94**, 5574 (1991).

[22] C. L. Collins, K. G. Dyall and H. F. Schaefer, J. Chem. Phys. **102**, 2024 (1995).

[23] B. Hess, Phys. Rev. A **33**, 3742 (1986).

[24] K. Pierloot, B. Dumez, B. O. Widmark and B. O. Roos, Theor. Chim. Acta. **90**, 87 (1995).

[25] K. P. Huber and G. Herzberg, *Molecular spectra and molecular structure, Constants of diatomic molecules* (Van Nostrand, Princeton, 1979), Vol. IV.

[26] T. Nakajima, Y. Yanal and K. Hirao, J. Comp. Chem. **23**, 847 (2002).

[27] M. K. Nayak, R. K. Chaudhuri, S. Chattopadhyay and U. S. Mahapatra, Theochem, (submitted).

[28] A. K. Rajagopal, J. Phys. C. **11**, 1943 (1978); Phys. Rev. **50**, 3759 (1966).

[29] A. K. MacDonald and S. H. Vosko, J. Phys. C. **12**, 2977 (1979).

[30] S. Svensson, L. Karlson, P. Baltzer, M. P. Keane and B. Wannberg, Phys. Rev. A **40**, 4369 (1989).

[31] H. Aksela, S. Aksela, M. Hotokka and M. Jaentti, (unpublished).

[32] O. M. Kvalheim, Chem. Phys. Lett. **98**, 457 (1983).

[33] D. E. Woon and T. H. Dunning, J. Chem. Phys. **98**, 1358 (1993).

[34] T. H. Dunning, J. Chem. Phys. **53**, 2823 (1970); T. H. Dunning and P. J. Hay, in *Modern Theoretical Chemistry*, Vol. 3, edited by H. F. Schaefer Ed. (Plenum Press, New York, 1976).

[35] D. Sinha, S. K. Mukhopadhyay, R. Chaudhuri and D. Mukherjee, Chem. Phys. Lett. **154**, 544 (1989).

[36] M. G. Boshier, G. P. Barwood, G. Huang and H. A. Klein, Appl. Phys. B **71**, 51(2000).

[37] G. Barwood *et al*, IEEE Trans. Instrum. Meas. **50**, 543 (2001).

[38] C. E. Moore, Atomic Energy Levels, Natl. Bur. Standard, Ref. Data Ser., Natl. Bur. Stand. (U.S.) Circ. No. 35 (U.S. GPO, Washington, D.C., 1971), Vol. 1.

[39] G. Ferrari, P. Cancio, R. Drullinger, G. Giusfredi, M. Prevedelli, C. Toninelli and G. M. Tino, Phys. Rev. Lett. **91**, 243002 (2003).

[40] W. C. Martin, R. Zalubas, and L. Hagan, in *Atomic Energy Levels-The Rare-Earth Elements*, Natl. Bur. Standards, (Washington, D.C., 1978).

[41] E. Eliav and U. Kaldor, Phys. Rev. A **52**, 291 (1995).

[42] C. Guet and W. R. Johnson, Phys. Rev. A **44**, 1531 (1991).

[43] A. Mårtensson-Pendrill, J. Phys. B **35**, 917 (2002).

[44] V. A. Dzuba, V. V. Flambaum, and M. V. Marchenko, Phys. Rev. A **68**, 022506 (2003).

[45] G. P. Barwood, K. Gao, P. Gill, G. Huang and H. A. Klein, Phys. Rev. A **67**, 013402 (2003).

[46] F. Buchinger *et al.*, Phys. Rev. C **41**, 2883 (1990); *ibid.* **42**, 2754 (1990).

Chapter 5

Theoretical study on the excited states of HCN: A system of astrophysical interest

5.1 Introduction

The hydrogen cyanide (HCN) molecule has been a subject of several experimental and theoretical investigations over several years. Being a small polyatomic molecule, HCN is an ideal system for the development and testing models aimed to calculate its electronic and ro-vibrational states and other related properties. The possibility of intra-molecular isomerization HCN-HNC has also made this an important system for the study of unimolecular reactions. In recent years, HCN has raised interest among the astrophysicists due to its detection in the atmosphere of Titan [1] and Carbon stars [2]. HCN has also been identified via radio-techniques in both comets [3] and interstellar atmosphere [4].

The excited singlet states of HCN were first experimentally studied by Herzberg and Innes [5] who established the existence of three bent excited states of HCN. The lowest excited state lying 6.438 eV above the ground state was assigned as $\tilde{A}^1A''$ with bond angle 125^0 and electronic configuration $5a'^26a'^21a''7a'$. Herzberg and Innes assigned the electronic configuration of second $\tilde{B}^1A''$ ($T_0 = 6.77$ eV) and third $\tilde{C}^1A'$($T_0 = 8.14$ eV) excited singlet states of HCN to be $5a'^26a'1a''^22a''$ with

bond angle 114.5^0 and $5a'6a'^21a''^27a'$ with bond angle 141^0, respectively. While the assignment of first excited singlet state is consistent with Walsh's [6] prediction, there are some serious discrepancies between the theoretical and experimental molecular structures for the $\tilde{B}^1A''$ and $\tilde{C}^1A'$ state of HCN. According to Walsh, there is only one significantly bent $^1A'$ state and the other two $^1A'$ states are either linear or nearly linear. Herzberg and Innes' assignment of $\tilde{C}^1A'$ state of HCN is also not in accord with Walsh's prediction. According to Walsh, this state should be strongly bent and not one with bond angle 141^0. However, subsequent theoretical studies [7, 8] clarified the breakdown of Walsh's rule which was based on one electron energy diagram.

Krishnamachari and Venkatsubrahmanian [9] have observed a transient (300μs half life) absorption system with its origin at 32844.1 cm^{-1} in the flash-photolysis of oxazole, iso-oxazole and thiazole. The band system consists of a long progression involving CN stretching frequency of 1005 cm^{-1} in the upper electronic state. The spectrum was attributed to a meta-stable form of HCN, i.e, either HNC or triplet HCN. For HNC, Laidig and Schaefer [10] predicted the electronic transition to occur at 46830 cm^{-1}, with a CN stretching frequency of 1100 cm^{-1} in the excited electronic state and a bent excited state compared to the linear ground state. The observed spectrum, though nearly agrees with respect to CN stretching frequency, differs considerably with respect to transition energy by about 14000 cm^{-1}. The absence of a progression involving the bending frequency is also not in agreement with the theoretical expectation. Thus the assignment of the HNC is not tenable and the alternative assignment, i.e., to triplet HCN is to be preferred.

The main aim of the present calculation is to characterize the higher triplet states of HCN and assign the transient absorption spectrum. As shown below, the observed spectrum could be assigned to the transition $4^3A' \leftarrow 1^3A'$; the observed value of the transition energy and the CN stretching frequency agree well with the calculated value; the occurrence of a long progression of the CN stretching frequency and the absence of the bands involving the bending frequency are in

conformity with calculated change in the geometry in these two states.

We also computed relevant spectroscopic data, such as ionization potentials, vibrational frequencies, dissociation energies and dipole moments of HCN, some of which to our knowledge have not been reported before.

5.2 Computational details

Two sets of basis functions are employed to compute the excitation energies, ionization potentials and related molecular properties of HCN. The basis set chosen for the geometry optimization consists of (4s,1p)/[2s,1p] contracted Dunning's basis [11] augmented with a s ($\zeta_s = 0.029740$) and p($\zeta_p = 0.141$) function for H atom. For C and N, we employ Dunning's [11, 12] (9s,4p,1d)/[3s,2p,1d] contractions augmented with two s, two p and one d functions. The exponents for the augmented s, p and d functions for C (N) atom are 4.53 (6.233), 0.0469 (0.06124), 14.557 (19.977), 0.04041 (0.05611), and 0.151 (0.23), respectively. The transition energies, ionization potentials, dissociation energies and dipole moment (for the ground state) are computed with a basis comprised of 59a' and 28a'' basis functions. Here, the H atom basis is constructed from Dunning's (5s,2p)/ [3s,2p] aug-cc-pVTZ contraction scheme. On the other hand, Dunning's (11s,6p,3d,1f)/[5s,4p,3d,1f] aug-cc-pVTZ basis is used for C and N atom. While the geometry optimization is performed at the complete active space (CASSCF) level [13], transition energies, ionization potentials and the related properties are computed using the coupled cluster based linear response theory (CCLRT) [14, 15, 16, 17], which is also known as equation of motion CC (EOMCC).

5.2.1 Geometries and Transition energies of HCN

The adiabatic transition energies (T_e) for the singlet and triplet states of HCN are compared with experiment and with other correlated calculations in Table 5.1. The computed transition energies T_e of Schwenzer *et al.* [8] are actually 2.18 eV

higher than their reported value. The motivation of this adjustment was based on the position of the $\tilde{A}^1A''$ state. In their calculations, this excited state was estimated to be 8.22 eV above the ground state, i.e., 2.18 eV higher than the experimental value. Therefore, all the T_e values reported by Schwenzer *et al.* were obtained by subtracting the 2.18 eV from the computed T_e values. This large error in the estimated energy is partly due to predisposition of the calculations in favor of closed shell ground state though the choice of basis function plays a significant role. We emphasize that the semi-empirically adjusted T_e value of Schwenzer *et al.* agrees favorably well with the experiment for $3^1A'(\tilde{C})$ and $3^1A''(\tilde{D})$ electronic states though their predicted T_e value for $3^1A'(\tilde{C})$ is slightly off from the experiment. We also adjust the position of $\tilde{A}^1A''$ state but in our calculation the $\tilde{A}^1A''$ excited singlet state is only off by 0.5 eV (for both CASSCF and CC) compared to 2.18 eV of Schwenzer *et al.*.

Regarding the second excited state, Herzberg and Innes originally assigned a state at 6.78 eV as $\tilde{B}(^1A'')$ [5]. However, it was later shown to be an extension of $1^1A'(\tilde{A})$ state [20]. The present as well as Schwenzer *et al.* calculations predict excited singlet state $1^1A'$ to be at 6.8 eV; though this state has not been directly observed, the existence of this state has been inferred through perturbation in the $\tilde{A}$ state [5]. The observed $\tilde{C}(3^1A')$ and $\tilde{D}(3^1A'')$ electronic state energies are well reproduced in the present calculations.

We now proceed to compare the theoretical and experimental predictions of the excited triplet states of HCN. Excited triplet states are of special interest to the experimentalists as these metastable states can initiate/exhibit many interesting chemical phenomena [21]. To the best of our knowledge, nothing is known experimentally about triplet states of HCN except the one reported by Krishnamachari *et al.* [9]. In their flash-photolysis experiments on oxazole, iso-oxazole, and thiozole, Krishnamachari *et al.* observed a transient spectrum in 2500-3050Å region with a long progression involving CN stretching frequency of 1005 cm^{-1}. This band system was attributed to an excited metastable state of HCN, i.e., either triplet HCN

Table 5.1: *Adiabatic excitation energies (in eV) of HCN.*

State	Dominant configuration(s)	CASSCF [13]	CCLRT [18]	Schwenzer *et al.* [7]	Expt. [19]
$X^1\Sigma^+$	$5\sigma^2 1\pi^4$ ($C_{\infty v}$)	0.0	0.0	0.0	0.0
$1^1A''$	$7a'1a''$	6.48	6.48	6.48	6.48
$2^1A'$	$6a'7a'$	6.70	6.93	6.78	6.77[a]
	$1a''2a''$				
$2^1A''$	$6a'2a''$	7.66	7.79	7.52	
	$8a'1a''$				
	$6a'3a''$				
$3^1A'$	$1a''2a''$	8.23	8.10	7.85	8.14
	$1a''3a''$				
	$6a'8a'$				
	$5a'8a'$				
$3^1A''$	$7a'1a''$	8.99	8.64	8.97	8.88
$1^3A'$	$6a'8a'$	4.46	4.44	4.42	
$1^3A''$	$8a'1a''$	5.42	5.47	5.46	
$2^3A'$	$1a''2a''$	6.28	6.13	5.91	
$2^3A''$	$6a'2a''$	7.08	7.00	6.85	
$3^3A'$	$1a''2a''$	7.11	6.81	6.98	
	$6a'8a'$				
$3^3A''$	$5a'2a''$	7.61	7.47	7.41	
$4^3A'$	$6a'7a'1a''2a''$	8.69			8.53 [9]
	$5a'7a'$				

*a:*Estimated from the perturbation in the $\tilde{A}$ state [5].

or isomeric HNC. The present calculation estimates the T_e for $1^3A' \rightarrow 4^3A'$ to be 33308 cm^{-1} which matches favorably well with the observed value 32844 cm^{-1}. In addition, our predicted CN stretching frequency (1001 cm^{-1}) for the $4^3A'$ state is also in accord with the experiment.

The geometries and vibrational frequencies obtained from the CASSCF calculation for the ground and excited states of HCN are displayed in Tables 5.2 and 5.3, respectively. To our knowledge, triplet state and high lying singlet geometries and

Table 5.2: *Comparison of experimental and theoretically computed ground and excited state geometries of HCN. Bond distances are given in angstroms and bond angles in degrees.*

State	r_{CH}			r_{CN}			∠HCN		
	Ref. [18]	Ref. [7]	Expt. [19]	Ref. [18]	Ref. [7]	Expt. [19]	Ref. [18]	Ref. [7]	Expt. [19]
$X^1\Sigma^+$	1.085	1.055	1.064	1.169	1.180	1.156	180.0	180.0	180.0
$1^1A''$	1.140	1.096	1.140	1.331	1.318	1.297	119.4	127.2	125.0
$2^1A'$	1.182	1.102		1.291	1.287		113.9	124.9	
$2^1A''$	1.105	1.076		1.332	1.316		143.6	164.4	
$3^1A'$	1.138	1.092	1.140	1.278	1.264		136.5	141.2	141.0
$3^1A''$	1.061	1.045		1.241	1.229		180.0	180.0	
$1^3A'$	1.125	1.081		1.313	1.294		121.9	128.6	
$1^3A''$	1.111	1.099		1.329	1.365		120.7	117.0	
$2^3A'$	1.098	1.063		1.331	1.320		147.4	160.0	
$3^3A'$	1.127	1.081		1.283	1.250		132.6	132.6	
$2^3A''$	1.107	1.061		1.329	1.314		143.7	157.4	
$3^3A''$	1.085	1.045		1.238	1.237		180.0	180.0	
$4^3A'$	1.109			1.571			121.0		
$4^3A''$	1.128			1.502			117.3		

the corresponding vibrational frequencies are not known experimentally. However, it is evident from Table 5.2 that our computed geometries are in agreement with those reported by Schwenzer *et al.*. The slight difference in the estimated bond lengths and bond angle between these two theoretical works arises mainly because of the choice of basis functions and the procedure adopted in minimizing the energy with respect to its internal coordinates, i.e., with respect to r_{CH}, r_{CN} and θ(HCN). Since our computed geometries and vibrational frequencies are reasonably close to the experiment, we feel that our predicted geometries and associated frequencies will also be reliable. While the calculated values for CN stretching and HCN bending frequencies are in accord with the experiment, the computed CH stretching frequencies for the $1^1A''$ and $3^1A''$ states differ appreciably from the experimental values. The reason for this deviation may be due to

Table 5.3: *Comparison of experimental and theoretically computed vibrational frequencies (in cm^{-1}) of HCN. Entrees within parentheses are experimental [9, 25, 19] vibrational frequencies.*

State	ω_1 [18] C-H Str.	ω_2 [18] C-N Str.	ω_3 [18] Bend
$X^1\Sigma^+$	3351 (3312)	2101 (2098)	702 (714)
$2^1A'$	1987	1433	499
$3^1A'$	2524 (2273)	1595 (1530)	760 (869)
$1^1A''$	2606 (3160)	1413 (1495)	948 (941)
$2^1A''$	3095	1414	935
$3^1A''$	3602 (2367)	1762 (1626)	1011 (1038)
$1^3A'$	2818	1525	981
$2^3A'$	3121	1452	875
$3^3A'$	2764	1814	1032
$4^3A'$	3038	1001 (1005)	866
$1^3A''$	2605	1413	948
$2^3A''$	3072	1439	966
$3^3A''$	3356	1759	893
$4^3A''$	2782	1462	1003

the strong vibrionic coupling of the CH stretching vibrations produced via intermediate $2^1A''$ state as has been pointed out by Bickel *et al.* [22], Lee [23] and Meenakhsi *et al.* [24].

5.2.2 Ionization potential of HCN

To our knowledge, only the first and second ionization potential of HCN are experimentally known so far. The electron impact experiment [26] estimates the first ionization potential of HCN to be 13.91 eV (89.1 nm). Later the vacuum ultraviolet (VUV) absorption spectrum of HCN between 62 and 148 nm was analyzed by Nuth and Glicker [25]. The VUV absorption spectra of HCN shows a weak vibrational structure that continues to the first adiabatic ionization potential (IP)

Table 5.4: *Vertical ionization potentials (in eV) of HCN.*

State	Peak type	Nayak *et al.* Ref. [18]	Experiment [25, 27]
$^2\Pi$	valence ($1\pi^{-1}$)	13.81	13.91
$^2\Sigma^+$	valence ($5\sigma^{-1}$)	13.94	14.01
$^2\Sigma^+$	valence ($4\sigma^{-1}$)	20.42	
$^2\Pi$	satellite	24.66	
$^2\Sigma^+$	satellite	26.56	
$^2\Sigma^+$	valence ($3\sigma^{-1}$)	29.24	

at 89.1 nm. It was also pointed out by Nuth and Glicker that a complex Rydberg series starting at 122 nm converges to the first ionization potential and the series beginning at about 116 nm converges to the second ionization potential. The adiabatic IP for $^2\Pi$ (13.60 eV) estimated by Turner *et al.* [27] was also in agreement with Nuth [25].

Table 5.4 reports the valence and satellite (shake-up) IPs of HCN obtained using the coupled cluster based linear response theory [17]. Both the first ($^2\Pi(1\pi^{-1})$) and second ($^2\Sigma^+(5\sigma^{-1})$) ionization potentials of HCN are in favorable agreement (off only by 0.1 eV or less) with the experiment. Since our computed IPs (the first and second) are in good agreement with the experiment, we strongly feel that our predicted third valence ionization potential ($^2\Sigma^+(4\sigma^{-1})$) and satellite IPs will also be quite accurate.

5.2.3 Dissociation energy of HCN

The HCN molecule can dissociate either into CH and N or CN and H species. Energy required to break HCN into CH and N is much higher than that needed to dissociate HCN into CN and H. Here, we compute the dissociation energy of HCN only for

$$\text{HCN}(^1\Sigma^+) \rightarrow CN(^2\Sigma^+) + H(^2S)$$

Table 5.5: *Spectroscopic constants of HCN ($^1\Sigma^+$) and CN ($^2\Sigma^+$).*

System	Spectroscopic constants	Nayak *et al.* Ref. [18]	Experiment [19, 28]
HCN			
	μ (in Debye)	3.28	
	D_e (in eV)	5.70	5.62
	B_0 (in cm^{-1})	1.44	1.48
CN			
	IP (in eV)	14.08	14.10
	r_{CN} (in Å)	1.20	1.17

channel using CC method. The dissociation energy is calculated in two steps. First, the HCN ($^1\Sigma^+$) ground state is computed using closed shell CC method. The ground state of CN($^2\Sigma^+$) is then calculated by adding an electron to the correlated closed shell ion CN^+ following the Fock-space scheme [16]

$$CN^+(^1\Sigma^+) + e \rightarrow CN(^2\Sigma^+).$$

Once the ground state energies of HCN($^1\Sigma^+$) and CN($^2\Sigma^+$) are known, the estimation of dissociation energy is trivial.

The dissociation energy (D_e) of HCN$\rightarrow CN(^2\Sigma^+) + H(^2S)$, dipole moment ($\mu$) and IP of CN are presented in Table 5.5. The accuracy of our estimated D_e, IP of CN and other properties of HCN (discussed above) clearly indicates the reliability of the method.

Bibliography

[1] R. Hanel *et al.*, Science **212**, 192 (1981).

[2] T. Ridgway, D. F. Carbon, and D. N. B. Hall, Astrophys. J. **225**, 138 (1978).

[3] L. E. Snyder and D. Buhl, Astrophys. J., **163**, L47 (1971); W. H. Huebner, L. E. Snyder and D. Buhl, Icarus **23**, 580 (1974).

[4] P. M. Solomon, K. B. Jeffers, A. A. Penzias and R. W. Wilson, Astrophys. J. **168**, L107 (1971); B. L. Ulich and E. K. Conking, Nature **248**, 121 (1974).

[5] G. Herzberg and K. K. Innes, Can. J. Phys. **35**, 842 (1957).

[6] A. D. Walsh, J. Chem. Soc. 2288 (1953).

[7] G. M. Schwenzer, Y. Yamaguchi, H. F. Schaefer, C. P. Baskin and C. F. Bender, J. Chem. Phys. **60**, 2787 (1974).

[8] G. M. Schwenzer, C. F. Bender, and H. F. Schaefer, Chem. Phys. Lett. **36**, 179 (1975).

[9] S. N. L. G. Krishnamachari and R. Venkatsubramanian, Scpectro. Lett. **19**, 55 (1986).

[10] W. D. Laidig, Y. Yamaguchi, and H. F. Schaefer, J. Chem. Phys. **80**, 3069 (1984).

[11] T. H. Dunning, J. Chem. Phys. **90**, 1007 (1989).

[12] D. E. Woon and T. H. Dunning, J. Chem. Phys. **103**, 4572 (1995).

[13] B. O. Roos, in *Advances in Chemical Physics*, edited by K. P. Lawley (Wiley Interscience, New York, 1987), Vol. 69, p. 339.

[14] J. Paldus, in *Methods in Computational Molecular Physics, NATO Study Institute, Series B: Physics*, edited by S. Wilson and G. Diercksen (Plenum, New York, 1992), Vol. 293, p. 99.

[15] R. Bartlett and J. Stanton, in *Reviews in Computational Chemistry*, edited by K. Lipkowitz and D.B.Boyd (VCH Publishers, New York, 1994), Vol. 5, p. 65.

[16] D. Mukherjee and S. Pal, Adv. Quantum Chem. **20**, 281 (1989).

[17] B. Datta, R. K. Chaudhuri and D. Mukherjee, J. Mol. Structure (Theochem) **361**, 21 (1996); R. K. Chaudhuri, B. Datta, K. Das and D. Mukherjee, Int. J Quantum Chem. **60**, 347 (1996) and references therein.

[18] M. K. Nayak, R. K. Chaudhuri, S. N. L. G. Krishnamachari, J. Chem. Phys. **122**, 184323 (2005).

[19] G. Herzberg, Electronic Spectra and Elctronic Strucure of Polyatomic Molecules, (Van Nostrand Reinhold Company, New York, 1966).

[20] A. Meenakshi, K. K. Innes, and G. A. Bickel, Mol. Phys. **68**, 1179 (1989).

[21] S. N. L. G. Krishnamachari and S. B. Kartha, Scpectro. Lett. **17**, 721 (1984).

[22] G. A. Bickel and K. K. Innes, Can. J. Phys. **62**, 1763 (1984).

[23] L. C. Lee, J. Chem. Phys. **72**, 6414 (1980).

[24] A. Meenakshi and K. K. Innes, J. Chem. Phys. **84**, 6550 (1986).

[25] J. A. Nuth and S. Glicker, J. Quant. Spectro. Radiat. Tranfer **28**, 223 (1982).

[26] J. D. Morrison and A. J. C. Nicholson, J. Chem. Phys. **20**, 1021 (1952).

[27] D. W. Turner, C. Baker, A. D. Baker and C. R. Brundle, in *Molecular Photoelectron spectroscopy*, Wiley New York (1970), p. 345.

[28] K. P. Huber and G. Herzberg, Constants of Diatomic Molecules, Vol. **4** (Van Nostrand Reinhold Company, New York, 1979).

Chapter 6

Conclusion and Future Plan

6.1 Summary of Results

In this concluding section, we will summaries the important results of our work, which are included in this thesis. It can be understood clearly that, this thesis highlights three aspects:

1. We have studied the effects of the violation of space inversion (P) and time-reversal (T) symmetry in heavy polar diatomics such as YbF and BaF molecules, which is arising from the intrinsic electric dipole moment of electrons d_e. As a result of this effects, these molecules can have permanent electric dipole moment: a signature of P, T-violation.

The ground to excited state transitions energies and some other related molecular properties of YbF are calculated in addition to the P, T-odd interaction constant $W_{\rm d}$ for the ground state of YbF molecule, using a fully-relativistic restricted active space (RAS) configuration interaction (CI) method. The present calculation estimates the P, T-odd interaction constant $W_{\rm d}$ to be -1.088$\times 10^{25}$ Hz/e-cm. We emphasize that the present estimate of $W_{\rm d}$ *lies in between* the values reported by Parpia [1] (-1.20$\times 10^{25}$Hz/e-cm) and Titov *et al.* [2] (-0.91$\times 10^{25}$Hz/e-cm), and

hence, appears to be quite consistent. Since our computed transitions energies and related molecular properties are in agreement with experiment, we strongly believe that our predicted $W_{\rm d}$ is quite reasonable. The present calculation clearly demonstrates that the correlation contribution to $W_{\rm d}$ (also to μ_e) from low lying unoccupied (at DF level) active orbitals is not significant. The fact that the contribution from low lying unoccupied active orbital is negligible, can be profitably used to reduce the computational costs by discarding these orbitals from the CI space.

The P,T-odd interaction constant $W_{\rm d}$ for the ground state of BaF molecule is also calculated using the fully-relativistic RASCI method. The present calculation estimates the P,T-odd interaction constant $W_{\rm d}$ to be -0.352$\times 10^{25}$ Hz/e-cm. We emphasize that the present estimate of $W_{\rm d}$ is in perfect agreement with the semi-empirical result of Kozlov and Labzowsky [3] as well as with the RASSCF-EO result of Kozlov *et al.* [4]. The present calculation further indicates that the semi-empirical estimate of $W_{\rm d}$ by Kozlov and Labzowsky is quite reliable. In addition to the reliable result of $W_{\rm d}$, our computed ground state dipole moment μ_e is also in agreement with experiment.

2. We have studied some properties of relativistic atoms and such as Sr, Yb, Ag, Hg and their positive ions. Since these systems are quite heavy, the relativistic effects are prominent in these systems.

Fully-relativistic valence universal multi-reference coupled cluster (VU-MRCC) method is applied to study the low lying states of the Sr and Yb atoms and to their positive ions. Satisfactory results are obtained for the transition energies, valence electron ionization potentials and other related properties such as nuclear magnetic dipole hyperfine constant A for the ground and excited states of Sr^+ and Yb^+, nuclear electric quadruple hyperfine constant B for the $^2D_{5/2}$ state of Sr^+. The present work clearly demonstrates that the accuracy of one-electron proper-

ties strongly depend upon the choice of basis set function. It further demonstrates that the contribution to the one-electron properties from orbital with higher angular momentum is non-negligible.

The core-valence extensive VU-MRCC method is also applied to study the ground state as well as the low lying excited states of Ag and Hg atoms and to their positive ions. For these systems also, we obtained reliable results for the transition energies and valence ionization potentials. In addition to that, we have also estimated satisfactory results for the nuclear magnetic hyperfine constant A and electric quadruple moment Θ of $^{199}Hg^{+}$. The present calculation estimates the electric quadruple moment Θ=-0.527 ea_0 for the $^2D_{5/2}$ of Hg^{+}, which is the most accurate estimate to our knowledge.

3. In addition to these above mentioned relativistic systems, we have also studied some non-relativistic molecular systems such as HCl, CuH and HCN. Because of their low Z values, the relativistic effects are not significant for these systems.

The core-extensive coupled cluster based linear response theory (CCLRT) is applied to study the ionization potentials of HCl and excitation energies of CuH. The vertical ionization potentials (valence as well as shake-up) of HCl are well reproduced in the present calculations. For example, the two main peaks $^2\Pi$ and $^2\Sigma$ at 12.8 and 16.6 eV are estimated to be at 12.54 and 16.61 eV, respectively, in our calculations. For CuH, estimated vertical transition energies are in agreement with experiment. The excitation energies of $1^1\Sigma$ and $1^3\Pi$ are off by 0.007 eV and 0.042 eV from experiment, respectively. The experimental transition energy for $X^1\Sigma \rightarrow \Delta$ is $\sim$ 3.53 eV. According to the present calculation this Δ state is probably the $1^1\Delta$ state, which is lying at 3.53 eV above the ground state. The ground state spectroscopic constants of CuH are not so good in our present calculations.

The ground and excited state properties (including geometries) of HCN are computed using the CASSCF and CC method. The computed transition energy and

CN stretching frequency strongly suggests that the transient band system in the region 2500-3050Åarises from $4^3A' \leftarrow 1^3A'$ transitions. The present study further suggests that the deviation of experimental bond angle from Walsh's prediction can be justified in terms of breakdown of single configuration picture. The first triplet-triplet transition of HCN, i.e., $1^3A'' \rightarrow 1^3A'$ occurs at 1.29μ, It would be possible to observe this transition in absorption spectrum for the photo-decomposition of the oxazoles or thiozole.

6.2 Future Plan

We would like to continue our work on the study of such effects in heavy polar diatomics. Until now, we have considered only one of the possible mechanism which can give rise to P,T-odd effects in atoms and molecules; the effects arising due to the intrinsic electric dipole moment (EDM) of electrons. Since, there are several other mechanisms (presented/described in the first chapter) which can violate P and T symmetry, we would like to study the effects of those mechanisms in future. In addition to that, we will also consider some interesting P-odd properties.

At present, we have made certain reasonable approximations in our calculations of the P,T-odd interaction constant $W_{\rm d}$ for the ground state of YbF and BaF molecules. However, those approximations can influence the accuracy of the result obtained for $W_{\rm d}$. For example, omission of the screening term $\mathbf{E}_{i,j}$ can overestimate the effective electric field and hence the result of $W_{\rm d}$. Similarly, the point charge approximation of the nuclei can also over estimate the P,T-odd constant. We would like to study these effects in future. Further more, we are also interested to analyze the influence of the mixing of ground state and low lying excited states of the systems.

It is practically impossible to include all electron correlation for such a heavy system via any of the correlated many-body methods and hence is quite difficult

to claim the accuracy of the calculations without any experimental result. That is why, it is absolutely necessary to study some other known (experimentaly) properties of the system which has also the similar kind of dependencies. For instance, the hyperfine structure constants A has also the similar structure as the P,T-odd interaction constant $W_{\rm d}$ has, and the experimental results of the constants A are well known for many systems. Therefore, we would like to study the hyperfine structure constants A also, in addition to the P,T-odd interaction constant $W_{\rm d}$, from which we can get an error estimate of the later depending on the error bar of former, to a certain extent. This kind of study will be useful for experimentalists to interpret their outcome.

We have used the method of configuration interaction (CI) in our calculations for the P,T-odd constant $W_{\rm d}$ and it is well known that, truncated CI does not preserves the size-extensivety, which is an important property of many electron system. On the other hand, the coupled cluster (CC) method has the main advantage of preserving the size-extensivety. Most of the many-body calculations are based on CC method now a days. We have planed to use the CC method for the study of P-odd and P,T-odd effects, in near future. Since, the experiments on YbF molecule are at the final stage and we can expect it's results by the end of this year, we are interested to study these effects in PbF and PbO, which are the prime experimental candidates and are being planed and prepared, respectively.

Bibliography

[1] F. A. Parpia, J. Phys. B **31**, 1409 (1998).

[2] A. V. Titov, N. S. Mosyagin, and V. F. Ezhov, Phys. Rev. Lett. **77**, 5346 (1996).

[3] M. G. Kozlov and L. N. Labzowsky, J. Phys. B **28**, 1933 (1995).

[4] M. G. Kozlov, A. V. Titov, N. S. Mosyagin and P. V. Souchkov, Phys. Rev. **A,56**, R3326, (1997).

Appendix A

Matrix elements of H_d using Cartesian Gaussian basis

A.1 Cartesian Gaussian spinor and basis function

In the first chapter, we discussed about the general form as well as the procedure for evaluating the matrix element of the P,T-odd interaction operator H_d using the Spherical Gaussian basis. As we have mentioned at the end of that chapter, there are some molecular codes which uses the Cartesian Gaussian basis. In that case, evaluating the matrix element of H_d is little bit complicated. Here, we will discuss one of the procedure for evaluating the spatial part of the matrix element. Further, we will consider only the atomic cases, where the Gaussian center coincides with the operator center. In terms of Cartesian Gaussian spinor, the basis functions can be defined as a linear combination of the following Gaussian spinors [1]

$$\phi_I = N_{k,\alpha} \prod_{i=1,3} (x_i - a_i)^{k_i} \exp\left[-\alpha(x_i - a_i)^2\right]\chi_{\pm} \tag{A.1}$$

where $N_{k,\alpha}$ is a normalization constant, $k = (k_1, k_2, k_3)$ and $\chi_{\pm}$ is two-component spinor (i.e. α or β spin function). The Gaussian is centered at a and the orbital angular momentum quantum number is defined as $L = \sum_i k_i$.

Assuming the Gaussian to be centered at the origin of our coordinate system, we can define the s, p and d type functions as

$$s = N_{k_{000},\alpha_s} \exp[-\alpha_s r^2]\chi_\pm$$

$$\begin{aligned} p_x &= N_{k_{100},\alpha_p}(x) \exp[-\alpha_p r^2]\chi_\pm \\ p_y &= N_{k_{010},\alpha_p}(y) \exp[-\alpha_p r^2]\chi_\pm \\ p_z &= N_{k_{001},\alpha_p}(z) \exp[-\alpha_p r^2]\chi_\pm \end{aligned}$$

$$\begin{aligned} d_{xy} &= N_{k_{110},\alpha_d}(xy) \exp[-\alpha_d r^2]\chi_\pm \\ d_{xz} &= N_{k_{101},\alpha_d}(xz) \exp[-\alpha_d r^2]\chi_\pm \\ d_{yz} &= N_{k_{011},\alpha_d}(yz) \exp[-\alpha_d r^2]\chi_\pm \\ d_{x^2} &= N_{k_{200},\alpha_d}(x^2) \exp[-\alpha_d r^2]\chi_\pm \\ d_{y^2} &= N_{k_{020},\alpha_d}(y^2) \exp[-\alpha_d r^2]\chi_\pm \\ d_{z^2} &= N_{k_{002},\alpha_d}(z^2) \exp[-\alpha_d r^2]\chi_\pm \end{aligned}$$

where we have used r^2 in place of $x^2 + y^2 + z^2$, the subscripts s, p and d denotes the different exponents for different kind of functions.

A.1.1 Difficulty in evaluating the matrix elements of H_d

If we use this form of Gaussian basis function to evaluate the matrix element of operator H_d, then we also need to write this operator using Cartesian coordinate system and then integrate over the whole volume.

As defined in first chapter, the P, T-odd interaction operator H_d is of the form

$$H_d \propto \frac{\hat{\sigma} \cdot \hat{r}}{r^2} \tag{A.2}$$

We can write $r^2 = x^2 + y^2 + z^2$ and $\hat{\sigma} \cdot \hat{r}$ as

$$\hat{\sigma} \cdot \hat{r} = \frac{\vec{\sigma} \cdot \vec{r}}{|\sigma||r|}$$

where, $|r| = (x^2 + y^2 + z^2)^{1/2}$ and $|\sigma| = ({\sigma_x}^2 + {\sigma_y}^2 + {\sigma_z}^2)^{1/2}$. Likewise, $\vec{\sigma} \cdot \vec{r}$ can be written as

$$\vec{\sigma} \cdot \vec{r} = \sigma_x x + \sigma_y y + \sigma_z z$$

which means,

$$H_d \propto \frac{\sigma_x x + \sigma_y y + \sigma_z z}{(x^2 + y^2 + z^2)^{3/2}} \tag{A.3}$$

Now, let us evaluate the matrix element of this above operator between s and p (p_z for example) type basis functions. Excluding the constant terms and the spin part, the integral involving spatial part looks like,

$$\int_{-\infty}^{+\infty} \int_{-\infty}^{+\infty} \int_{-\infty}^{+\infty} \frac{z^2 \exp[-(\alpha_s + \alpha_p)(x^2 + y^2 + z^2)]}{(x^2 + y^2 + z^2)^{3/2}} dxdydz \tag{A.4}$$

This integral is quite difficult to integrate and so, we have to think about some other alternative procedure.

A.2 Cartesian Gaussian basis using Spherical harmonics

The above mentioned problem of using the Cartesian Gaussian can be resolved by converting the Cartesian Gaussian into spherical polar coordinates and then expressing the angular parts, in terms of spherical harmonics Y_l^m. The necessity of expressing the angular part in terms of spherical harmonics is just to make it convenient for the integration of the angular part. Using this procedure, we can

express x, y, z and 1 as follows

$$\begin{aligned} x &= r\sin\theta\cos\phi = -r\sqrt{\frac{2\pi}{3}}(Y_1^1 - Y_1^{-1}) \\ y &= r\sin\theta\sin\phi = \frac{-r}{i}\sqrt{\frac{2\pi}{3}}(Y_1^1 + Y_1^{-1}) \\ z &= r\cos\theta = r\sqrt{\frac{4\pi}{3}}(Y_1^0) \\ 1 &= \sqrt{4\pi}(Y_0^0) \end{aligned}$$

where we have used the expressions for spherical harmonics defined as follows

$$\begin{aligned} Y_0^0 &= \frac{1}{\sqrt{4\pi}} \\ Y_1^0 &= \sqrt{\frac{3}{4\pi}}\cos\theta \\ Y_1^1 &= -\sqrt{\frac{3}{8\pi}}e^{i\phi}\sin\theta \\ Y_1^{-1} &= \sqrt{\frac{3}{8\pi}}e^{-i\phi}\sin\theta \end{aligned}$$

Some other higher order spherical harmonics are defined as

$$\begin{aligned} Y_2^0 &= \sqrt{\frac{5}{16\pi}}(3\cos^2\theta - 1) \\ Y_2^1 &= -\sqrt{\frac{15}{8\pi}}e^{i\phi}\sin\theta\cos\theta \\ Y_2^{-1} &= \sqrt{\frac{15}{8\pi}}e^{-i\phi}\sin\theta\cos\theta \\ Y_2^2 &= \sqrt{\frac{15}{32\pi}}e^{2i\phi}\sin^2\theta \\ Y_2^{-2} &= -\sqrt{\frac{15}{32\pi}}e^{-2i\phi}\sin^2\theta \end{aligned}$$

Using these expression and omitting the normalization constant as well as the spin part, we can write the spatial part of s, p and d type functions as

$$
\begin{aligned}
s &= \sqrt{4\pi}\exp(-\alpha_s r^2)[Y_0^0] \\
\\
p_x &= -r\sqrt{\frac{2\pi}{3}}\exp(-\alpha_p r^2)[Y_1^1 - Y_1^{-1}] \\
p_y &= \frac{-r}{i}\sqrt{\frac{2\pi}{3}}\exp(-\alpha_p r^2)[Y_1^1 + Y_1^{-1}] \\
p_z &= r\sqrt{\frac{4\pi}{3}}\exp(-\alpha_p r^2)[Y_1^0] \\
\\
d_{xy} &= \frac{r^2}{i}\sqrt{\frac{2\pi}{15}}\exp(-\alpha_d r^2)[Y_2^2 - Y_2^{-2}] \\
d_{xz} &= -r^2\sqrt{\frac{2\pi}{15}}\exp(-\alpha_d r^2)[Y_2^1 - Y_2^{-1}] \\
d_{yz} &= -\frac{r^2}{i}\sqrt{\frac{2\pi}{15}}\exp(-\alpha_d r^2)[Y_2^1 + Y_2^{-1}] \\
d_{x^2} &= r^2\sqrt{\frac{2\pi}{15}}\exp(-\alpha_d r^2)[Y_2^2 + Y_2^{-2} - Y_2^0 + \sqrt{5}Y_0^0] \\
d_{y^2} &= -r^2\sqrt{\frac{2\pi}{15}}\exp(-\alpha_d r^2)[Y_2^2 + Y_2^{-2} + Y_2^0 - \sqrt{5}Y_0^0] \\
d_{z^2} &= r^2\sqrt{\frac{16\pi}{45}}\exp(-\alpha_d r^2)[Y_2^0 + \sqrt{5/4}Y_0^0]
\end{aligned}
$$

In order to obtain these above expressions, we have used the following formulas for the products of two spherical harmonics given by Lindgren and Morrison [2].

$$
Y_k^q Y_{l'}^{m'} = \sqrt{\frac{2k+1}{4\pi}}\sum_{lm}(-1)^{l-m}\begin{pmatrix} l & k & l' \\ -m & q & m' \end{pmatrix}\langle l\|C^k\|l'\rangle Y_l^m \tag{A.5}
$$

where, the reduced matrix element $\langle l\|C^k\|l'\rangle$ is defined as

$$\langle l\|C^k\|l'\rangle = (-1)^l[(2l+1)(2l'+1)]^{1/2}\begin{pmatrix} l & k & l' \\ 0 & 0 & 0 \end{pmatrix} \tag{A.6}$$

It should be noted that, the $3-j$ symbol is non-zero, only when the angular momenta l, k, l' satisfy the triangular condition $|k-l'| \leq l \leq |k+l|$. Furthermore, the sum of the angular momenta, $l+k+l'$ must be even to have a non-zero value of the $3-j$ symbol.

A.2.1 The P,T-odd operator H_d in Spherical polar coordinates

Adopting the same procedure, we can also express the operator H_d in spherical polar coordinate. The first step is to write $\vec{\sigma}\cdot\vec{r}$ as

$$\vec{\sigma}\cdot\vec{r} = \sigma_x r\sin\theta\cos\phi + \sigma_y r\sin\theta\sin\phi + \sigma_z r\cos\theta \tag{A.7}$$

so that, the angular part of the operator H_d, $\hat{\sigma}\cdot\hat{r}$ can be written as

$$\hat{\sigma}\cdot\hat{r} = \frac{\vec{\sigma}\cdot\vec{r}}{|\sigma||r|} = \frac{\sigma_x\sin\theta\cos\phi + \sigma_y\sin\theta\sin\phi + \sigma_z\cos\theta}{|\sigma|} \tag{A.8}$$

where $|\sigma|$ is a constant quantity. The operators σ_x, σ_y and σ_z will act on the spin part of the basis functions. So, the spin dependent part can be separated from the spatial part of the integral. Here we will concentrate only on the spatial part of the integral, where the spatial part of the P,T-odd interaction operator H_d is of the form

$$H_d \propto \frac{\sin\theta\cos\phi + \sin\theta\sin\phi + \cos\theta}{r^2} \tag{A.9}$$

A.2.2 Matrix elements of the P,T-odd operator H_d

Let us first consider the s and p type functions. The only non-zero matrix element of the operator $\cos\theta/r^2$ (last term of the above expression) is between s and p_z. Matrix elements of H_d between functions of same parity is zero. Excluding the normalization constants and the spin dependent part, matrix element of the operator H_d between s and p_z looks like,

$$\langle s|\cos\theta/r^2|p_z\rangle = \frac{4\pi}{\sqrt{3}}\int_0^\infty r\exp[-(\alpha_s+\alpha_p)r^2]dr\int_\Omega Y_0^{0*}\cos\theta Y_1^0 d\Omega \qquad \text{(A.10)}$$

Similarly, the non-zero matrix elements of the same operator ($\cos\theta/r^2$) between p and d type functions can be obtained using the same procedure as

$$\begin{aligned}
\langle p_x|\cos\theta/r^2|d_{xz}\rangle &= \frac{2\pi}{3\sqrt{5}}\int_0^\infty R(r)dr\int_\Omega (Y_1^1-Y_1^{-1})^*\cos\theta(Y_2^1-Y_2^{-1})d\Omega\\
\langle p_y|\cos\theta/r^2|d_{yz}\rangle &= \frac{2\pi}{3\sqrt{5}}\int_0^\infty R(r)dr\int_\Omega (Y_1^1+Y_1^{-1})^*\cos\theta(Y_2^1+Y_2^{-1})d\Omega\\
\langle p_z|\cos\theta/r^2|d_{x^2}\rangle &= \frac{2\sqrt{2}\pi}{3\sqrt{5}}\int_0^\infty R(r)dr\int_\Omega Y_1^{0*}\cos\theta(Y_2^2+Y_2^{-2}-Y_2^0+\sqrt{5}Y_0^0)d\Omega\\
\langle p_z|\cos\theta/r^2|d_{y^2}\rangle &= -\frac{2\sqrt{2}\pi}{3\sqrt{5}}\int_0^\infty R(r)dr\int_\Omega Y_1^{0*}\cos\theta(Y_2^2+Y_2^{-2}+Y_2^0-\sqrt{5}Y_0^0)d\Omega\\
\langle p_z|\cos\theta/r^2|d_{z^2}\rangle &= \frac{8\pi}{3\sqrt{15}}\int_0^\infty R(r)dr\int_\Omega Y_1^{0*}\cos\theta(Y_2^0+\sqrt{5/4}Y_0^0)d\Omega \qquad \text{(A.11)}
\end{aligned}$$

Here, we have used the abbreviated form for the radial part of the integral as, $R(r)=r^3\exp[-(\alpha_p+\alpha_d)r^2]$. Here also, we have omitted the spin dependent term and the normalization constants.

Now, we can evaluate the radial and angular parts of the integrals separately. For evaluating the radial part, we can use the following standard formula for integrals.

$$\int_0^\infty r^{2n+1}e^{-ar^2}dr = \frac{n!}{2a^{n+1}}$$

where, n is a positive integer. For example, when the exponent of r is 1, the value

of the integral is $1/2a$, otherwise (for exponents 3,5,7...) we can obtain the result of the integral from the above formula, which is a remarkable simplification.

The next step is to evaluate the angular part of the integral. For this part also, we can use the following standard expression given by Arfken and Weber [3].

$$\begin{aligned}\int_{\Omega} Y_{L_1}^{M_1 *} \cos\theta Y_L^M d\Omega &= \left[\frac{(L-M+1)(L+M+1)}{(2L+1)(2L+3)}\right]^{1/2} \delta_{M_1,M}\delta_{L_1,L+1} \\ &+ \left[\frac{(L-M)(L+M)}{(2L-1)(2L+1)}\right]^{1/2} \delta_{M_1,M}\delta_{L_1,L-1} \qquad \text{(A.12)}\end{aligned}$$

Now, the problem of evaluating the matrix element is sorted out by using the spherical polar coordinates and above mentioned procedure. Using this method, we obtained the following results for the above integrals (i.e. final matrix elements of the operator $\cos\theta/r^2$).

$$\langle s|\cos\theta/r^2|p_z\rangle = \frac{2\pi}{3}\left(\frac{1}{\alpha_s+\alpha_p}\right) \qquad \text{(A.13)}$$

$$\langle p_x|\cos\theta/r^2|d_{xz}\rangle = \frac{2\pi}{15}\left(\frac{1}{\alpha_p+\alpha_d}\right)^2 \qquad \text{(A.14)}$$

$$\langle p_y|\cos\theta/r^2|d_{yz}\rangle = \frac{2\pi}{15}\left(\frac{1}{\alpha_p+\alpha_d}\right)^2 \qquad \text{(A.15)}$$

$$\langle p_z|\cos\theta/r^2|d_{x^2}\rangle = \frac{2\pi}{15}\left(\frac{1}{\alpha_p+\alpha_d}\right)^2 \qquad \text{(A.16)}$$

$$\langle p_z|\cos\theta/r^2|d_{y^2}\rangle = \frac{2\pi}{15}\left(\frac{1}{\alpha_p+\alpha_d}\right)^2 \qquad \text{(A.17)}$$

$$\langle p_z|\cos\theta/r^2|d_{z^2}\rangle = \frac{2\pi}{5}\left(\frac{1}{\alpha_p+\alpha_d}\right)^2 \qquad \text{(A.18)}$$

Further, we can adopt the same procedure to evaluate the matrix elements of the other terms in the expression of the P,T-odd interaction operator H_d (i.e. $\sin\theta\cos\phi/r^2$ and $\sin\theta\sin\phi/r^2$) as well as between other type of functions with higher l values (i.e. between d, f and f, g), and so on. There are some other methods which can be used to resolve the above mentioned problem. We discussed above one of them and are going to discuss one more simpler formulation below.

A.3 An alternative formulation to evaluate the matrix elements of H_d

After going through all these procedures mentioned in the previous sections, we found that the matrix elements of the P,T-odd operator H_d can also be evaluated without using the spherical harmonics (as discussed earlier), which seems to be a simpler formalism as discussed below.

Let us first write the s, p and d type basis functions (defined earlier) in terms of spherical polar coordinates without using the spherical harmonics. Neglecting normalization constants and the spin parts which can be written as

$$s = \exp\left[-\alpha_s r^2\right]$$

$$\begin{aligned} p_x &= r\exp\left[-\alpha_p r^2\right]\sin\theta\cos\phi \\ p_y &= r\exp\left[-\alpha_p r^2\right]\sin\theta\sin\phi \\ p_z &= r\exp\left[-\alpha_p r^2\right]\cos\theta \end{aligned}$$

$$\begin{aligned} d_{xy} &= r^2\exp\left[-\alpha_d r^2\right]\sin^2\theta\sin\phi\cos\phi \\ d_{xz} &= r^2\exp\left[-\alpha_d r^2\right]\sin\theta\cos\theta\cos\phi \\ d_{yz} &= r^2\exp\left[-\alpha_d r^2\right]\sin\theta\cos\theta\sin\phi \\ d_{x^2} &= r^2\exp\left[-\alpha_d r^2\right]\sin^2\theta\cos^2\phi \\ d_{y^2} &= r^2\exp\left[-\alpha_d r^2\right]\sin^2\theta\sin^2\phi \\ d_{z^2} &= r^2\exp\left[-\alpha_d r^2\right]\cos^2\theta \end{aligned}$$

Similarly, we can also write the infinitesimal volume element dv in terms of spherical polar coordinates as

$$dv = r^2 dr\sin\theta d\theta d\phi \tag{A.19}$$

In the next section, we will evaluate the matrix elements of H_d again, using this alternative formulation, where the limits of integration for r, θ and ϕ will be $(0-\infty)$, $(0-\pi)$ and $(0-2\pi)$, respectively.

A.3.1 Matrix elements of H_d using the alternative formulation

Using this formulation, matrix element of the operator $\cos\theta/r^2$ (last term of the expression for H_d) between s and p_z can be expressed as

$$\langle s|\cos\theta/r^2|p_z\rangle = \int_0^\infty r\exp[-(\alpha_s+\alpha_p)r^2]dr \int_0^\pi \sin\theta\cos^2\theta d\theta \int_0^{2\pi} d\phi$$

Similarly, other higher order non-zero matrix elements of the same operator $\cos\theta/r^2$ between p and d type functions can be written as

$$\begin{aligned}
\langle p_x|\cos\theta/r^2|d_{xz}\rangle &= \int_0^\infty R(r)dr \int_0^\pi \sin^3\theta\cos^2\theta d\theta \int_0^{2\pi} \cos^2\phi d\phi \\
\langle p_y|\cos\theta/r^2|d_{yz}\rangle &= \int_0^\infty R(r)dr \int_0^\pi \sin^3\theta\cos^2\theta d\theta \int_0^{2\pi} \sin^2\phi d\phi \\
\langle p_z|\cos\theta/r^2|d_{x^2}\rangle &= \int_0^\infty R(r)dr \int_0^\pi \sin^3\theta\cos^2\theta d\theta \int_0^{2\pi} \cos^2\phi d\phi \\
\langle p_z|\cos\theta/r^2|d_{y^2}\rangle &= \int_0^\infty R(r)dr \int_0^\pi \sin^3\theta\cos^2\theta d\theta \int_0^{2\pi} \sin^2\phi d\phi \\
\langle p_z|\cos\theta/r^2|d_{z^2}\rangle &= \int_0^\infty R(r)dr \int_0^\pi \sin\theta\cos^4\theta d\theta \int_0^{2\pi} d\phi
\end{aligned}$$

Here also, we have used the abbreviated form for the radial parts of the above integrals as, $R(r) = r^3\exp[-(\alpha_p+\alpha_d)r^2]$. Since the radial parts of these integrals are exactly same as earlier, we can use the same formula as given earlier to evaluate the radial integrals. Now, the angular parts of these integrals can be evaluated by using the following generalized formulas given by Spiegel *at al.* [5] as follows

$$\int \sin^n ax dx = \frac{-\sin^{n-1} ax\cos ax}{an} + \frac{n-1}{n}\int \sin^{n-2} ax dx \qquad \text{(A.20)}$$

for terms containing only powers of sin function, where $n \geq 1$.

$$\int \cos^n ax dx = \frac{\sin ax \cos^{n-1} ax}{an} + \frac{n-1}{n} \int \cos^{n-2} ax dx \tag{A.21}$$

for terms containing only powers of cos function, where $n \geq 1$.

$$\int \sin^m ax \cos^n ax = \frac{\sin^{m+1} ax \cos^{n-1} ax}{a(m+n)} + \frac{n-1}{m+n} \int \sin^m ax \cos^{n-2} ax dx \tag{A.22}$$

for terms containing both sin and cos functions, where $m, n \geq 1$.

Using these formulas for evaluating the angular part of the above integrals, we will obtain exactly the same results as earlier, for the matrix elements of the the operator $\cos\theta/r^2$. Similarly, we can evaluate other operators also (i.e. first and second terms of H_d). This formalism seems to be simpler for generalizing to evaluate the matrix elements of H_d between functions of with higher l values.

It should be noted that, both these formalisms described above are valid only when the center of the Gaussian and the center of the operator coincides such as atomic cases. For the case of molecules, both the centers can be different and these methods may be extended to valid for such multi-center cases with certain modifications (which is yet to be done). In this context, we would like to say that the method developed by McMurchie *et al.* [4] is valid for both atoms as well as molecules, which we have used in our molecular calculations implemented through DIRAC04 [6] code.

Bibliography

[1] P. J. C. Aerts and W. C. Nieuwpoort, Chem. Phys. Lett. **113**, 165 (1985).

[2] I. Lindgren and J. Morrison, *Atomic Many-Body Theory* (Springer-Verlag, New York, 1981), p. 45.

[3] G. B. Arfken and H. J. Weber, *Mathematical Methods for Physicists* (Elsevier, New Delhi, India, 2001), p. 804.

[4] L. E. McMurchie and E. R. Davidson, J. Comp. Phys. **26**, 218 (1978).

[5] M. R. Spigel and J. Liu, *Mathematical Handbook of Formulas and Tables* (McGraw Hill, Singapopore, 1999), p. 85.

[6] (see http://dirac.chem.sdu.dk/obtain/Dirac-site-license.shtml): *Dirac, a relativistic ab-initio electronic structure program, Release DIARC04 (2004)*, written by H. J. Aa. Jensen, T. Saue and L. Visscher with contributions from V. Bakken, E. Eliav, T. Enevoldsen, T. Fleig, O. Fossgaard, T. Helgaker, J. Laerdahl, C. V. Larsen, P. Norman, J. Olsen, M. Pernpointner, J. K. Pedersen, K. Ruud, P. Salek, J. N. P. Van Stralen, J. Thyssen, O. Visser, and T. Winther (http://dirac.chem.sdu.dk)

Appendix B

List of Publications

1. **Malaya K. Nayak** and Rajat K. Chaudhuri: "Ab initio calculation of P,T-odd effects in YbF molecule"; *Chemical Physics Letters* **419**, 191-194 (2006).

2. **Malaya K. Nayak** and Rajat K. Chaudhuri: "Ab *initio* calculation of P,T-odd interaction constant in BaF: a restricted active space configuration interaction approach"; *Journal of Physics B: At. Mol. Opt. Phys.* **39**, 1231-1235 (2006).

3. **Malaya K. Nayak** and Rajat K. Chaudhuri: "Relativistic coupled cluster method - Excitation and ionization energies of Sr and Yb atom"; *European Physical Journal D* **37**, 171-176 (2006).

4. **Malaya K. Nayak**, Rajat K. Chaudhuri and S. N. L. G. Krishnamachari: "Theoretical study on the excited states of HCN"; *Journal of Chemical Physics* **122**, 184323(1)-184323(4) (2005).

5. **Malaya K. Nayak**, Rajat K. Chaudhuri, S. Chattopadhyay and U. S. Mahapatra: "Applications of core-valence extensive multi-reference coupled cluster theory and core-extensive coupled cluster based linear response theory"; *Theochem* (submitted).